NACA RM E57G11



NACA

# RESEARCH MEMORANDUM

## ACCELERATIONS IN FIGHTER-AIRPLANE CRASHES

By Loren W. Acker, Dugald O. Black, and Jacob C. Moser

Lewis Flight Propulsion Laboratory
Cleveland, Ohio



NATIONAL ADVISORY COMMITTEE
FOR AERONAUTICS

WASHINGTON

November 4, 1957

NATIONAL ADVISORY COMMITTEE FOR AERONAUTICS

RESEARCH MEMORANDUM



# ACCELERATIONS IN FIGHTER-AIRPLANE CRASHES

By Loren W. Acker, Dugald O. Black, and Jacob C. Moser

## SUMMARY

An investigation was conducted on full-scale fighter airplanes to determine the magnitude, duration, and direction of accelerations imposed on the airplane structure and pilot during simulated crash landings.

Acclerations were measured on the airplane structure and on an anthropomorphic dummy which was installed in the cockpit of an FH-1 airplane. Five of these airplanes were crashed under circumstances approximating those observed in the military service. These crashes simulated three unflared landings, each at a different impact angle, a ground cart wheel, and a ground loop.

The maximum longitudinal acceleration measured at the center of gravity of the airplane increases rapidly with impact angle from a value of 8 g's for the $4^{\circ}$ angle of impact to a value of 60 g's for the $27^{\circ}$ angle of impact. The longitudinal accelerations measured on the cockpit floor during both the ground-loop and cart-wheel crashes are of about the same magnitude (less than 10 g's). Such accelerations can be easily tolerated by an adequately restrained pilot.

However, human tolerance to normal (vertical) accelerations was exceeded in all the unflared landing crashes.

## INTRODUCTION

Pilots involved in fighter-airplane crashes often receive severe injuries even though the cockpit remains uncrushed and the living space has not been encroached upon (refs. 1 and 2). To provide a basis for reducing these injuries, a series of airplanes were crashed experimentally to simulate the various types of crash landings encountered in the military service.

Severe injuries to the pilot may be caused by (1) being crushed if the cockpit collapses, (2) striking objects within the cockpit, or (3) experiencing longitudinal and normal (usually called vertical)

accelerations. In order to provide a basis for reducing these injuries through improved cockpit design and pilot equipment, the magnitude, duration, and direction of crash loads imposed on the airplane structure and the pilot must be determined. This report describes some measurements of these quantities obtained by crashing fighter aircraft under circumstances approximating those observed in service. These quantities were then compared with existing data on human tolerance to the sudden loads that occur in crashes to see whether the human tolerance had been exceeded.

The crashes that were conducted in this program included three simulated unflared landings, a ground cart wheel, and a ground loop.

The simulated unflared landing crashes were conducted with varying angles of impact. Increasing the angle of impact (angle between the tangent to the airplane's trajectory and the ground surface, at the point of impact) gave crashes of increasing intensity. In the crash at the greatest angle of impact, the cockpit collapsed completely. The two severest crashes thus bracketed the maximum longitudinal decelerating force that the airplane structure could transmit to the pilot without collapsing the cockpit. The jet fighter airplanes used were supplied by the Navy.

## APPARATUS

### Airplane

The airplanes used for this investigation were single-place, low-wing, twin-engine jet fighters of conventional structure (fig. 1). Both the front and rear spars of the center wing panel continued through the fuselage. The cockpit zone was formed by solid front and rear bulkheads connected by four rigid longerons which extended forward from the wing spars. The bulkhead, at the rear of the cockpit, was a solid, heavy aluminum plate which also served as armor plate. The cockpit floor ahead of the seat was a rather dense structure fastened to the two lower longerons. The floor under the pilot's seat was of light-gage sheet metal. The nose of the fuselage, ahead of the cockpit, was of low-density structure that collapses under low load. The belly of the fuselage, below the cockpit floor, was of a similar construction.

The pilot's seat (fig. 2) was an L-shaped bucket type mounted on two support tubes. The seat was free to slide vertically on the support tubes. Its vertical position could be adjusted by lock pins inserted in a series of holes drilled into each tube at 1/2-inch intervals. The support tubes slipped into sockets on the floor and were securely bolted at the top to the armor plate bulkhead at the rear of the cockpit. The lap belt and shoulder harness were fastened to the armor plate bulkhead instead of the seat. The seat supported the pilot only in the rearward and downward directions. Some lateral support was provided for the hips by the diagonal seat-pan braces.

During this investigation, all fuel tanks were removed and were replaced by data recording equipment. The airplane's gross weight and balance were adjusted by ballast to be equivalent to those of the airplane making a landing with minimum fuel.



## Dummy

An anthropomorphic dummy was used in all the crashes. This dummy had hinge points, weight distribution, center of gravity, and body contour to conform to that of a 200-pound average man.

The dummy was equipped with a Mae West, seat-pack parachute, and helmet. Figure 3 shows the dummy installed in the cockpit.

## Safety Harness

The various harnesses which restrained the dummy during the crashes are shown in figure 4. The straight-pull static tensile breaking strengths of the harness materials varied from 1500 to 8300 pounds. These values are tabulated in figure 4.

The harness for the unflared landing crash in which an $18^{\circ}$ ground impact angle existed was a standard military 3-inch nylon lap belt and a $1\frac{3}{4}$-inch cotton shoulder harness. The shoulder harness straps were fastened to the quick-release lap-belt buckle.

The harness used for the unflared landing crash at a $22^{\circ}$ contact angle and for the cart-wheel and ground-loop crashes was the same as that used in the $18^{\circ}$ crash except that the shoulder harness was made of dacron instead of cotton.

In the unflared landing crash at $27^{\circ}$, an experimental harness developed by Lt. Col. John Stapp, USAF, (ref. 3) was used. This harness consisted of two layers of 3-inch nylon webbing stitched together for the shoulder harness and the lap belt. In addition, two pieces of single-thickness 3-inch nylon webbing were used for thigh straps. These straps passed under the dummy's buttocks and came up the crotch and over the thighs as shown in figure 4. All straps were fastened together at the lap-belt buckle.

## CRASH PROCEDURE

The procedure used for conducting these experimental crashes is fully described in reference 4. Briefly, however, the crashes were

conducted in the following manner. The airplane was propelled by its own power along a 1700-foot runway to the crash area. When it reached the crash area, the airplane had attained a speed of about 112 miles per hour. The airplane was guided by a slipper substituted for the nose wheel. This slipper was slaved to a guide rail.

The crash barriers and crash area were arranged for each crash to produce the desired sequence of events. Except for the cart-wheel crash, the first barriers usually tore all or part of the landing gear off the airplane. The airplane then flew a short distance as a free-moving vehicle. In the unflared landing crashes, the difference between the experimental crashes and actual crashes is that the earth's slope, instead of the approach path, is at an angle with a horizontal plane. The accelerations measured in these experimental crashes are not seriously affected by this compromise.

To prevent a large crash fire, only enough fuel was provided to run the engines until the airplane reached the crash area. Then the fuel flow to the engines was stopped automatically.

## INSTRUMENTATION

Instruments and cameras were used to obtain a time history of the airplane's action during a crash, the movement of the dummy, the forces applied to the harness, and the accelerations of the airplane and the dummy. These data were recorded by one or more of the following methods:

(1) Cameras installed around the crash area

(2) Cameras installed on the airplane

(3) Telemeter system

(4) Magnetic tape recorders

### Photography

Motion-picture cameras located on the various camera platforms around the crash area and on the airplane recorded the action of the airplane and the dummy throughout the crash. The cameras on the airplane gave closeup motion pictures of the dummy's action. These cameras were installed on the wing and in front of and above the cockpit as shown in figures 5(a), (b), and (c), respectively. A section of the cockpit skin between two longerons was removed to expose the dummy's hip area to the wing-mounted camera. Sample frames of the film from these airplane cameras (fig. 6) show the area of interest covered by each camera.

A synchronizing system established a zero time for all motion-picture cameras and data recording instruments. Timing systems on both the cameras and data recorders established a continuous relation between the data. Thus, it was possible to correlate the data from all recording instruments and cameras.

## Telemeter System

The telemeter system provided a continuous record of the airplane and dummy accelerations and the harness forces during the crash. This system consisted of accelerometer and tensiometer transducers, a transmitter, and a receiving and recording station.

The accuracy of the system was ±2 percent of full scale up to oscillatory acceleration frequencies of 100 cycles per second. Further details of the telemetering system are provided in the appendix.

The general location of the telemeter transmitter in the airplane is shown in figure 7. The receiving and recording station located in the operations building (ref. 4) is shown in figure 8.

## Accelerometers

The accelerometers were mounted on machined steel blocks which were installed at various locations on the airplane and dummy. The specific location of each accelerometer as installed in the airplane and dummy is shown in figures 9 and 10 and is listed in the following table:

| Accelerometer location | Direction of acceleration | | | Figure |
|---|---|---|---|---|
| | Longi-tudinal | Ver-tical | Lat-eral | |
| Airplane floor (cockpit) | x | x | x | 9(a) |
| Airplane bulkhead | x | | x | 9(b) |
| Airplane center of gravity | x | x | x | 9(c) |
| Seat pan (cockpit) | | x | | |
| Dummy's head | x | x | x | 10(a) |
| Dummy's chest | x | x | x | 10(b) |
| Dummy's hips | x | x | x | 10(c) |

### Tensiometers

The forces exerted on the seat belt and shoulder harness by the dummy were measured by tensiometers and were recorded by the telemeter system. The tensiometers are described in the appendix. These tensiometers were installed at each attachment point of the restraining harness. Figure 11 shows the tensiometers installed on the shoulder harness and lap belt.

### Magnetic Tape Recorder

The magnetic tape recorder obtained time histories of the airplane and dummy acclerations not obtained by the telemeter system. The location of the recorders in the airplane is shown in figure 12. Each recorder converted the output of six acceleration transducers to a frequency-modulated signal and provided a seventh channel for tape speed compensation and time synchronization of records. In order to obtain the records in readable form, the magnetic tapes were run through a playback which converted the frequency-modulated signals to a graphic presentation of acceleration and time. Dynamically, the recorder produces graphic acceleration records with increasing error as the acceleration frequency increases. This error is not over $\pm 5$ percent of full scale at 100 cycles per second. At 0 cycle per second, the error is less than $\pm 2$ percent of full scale.

## RESULTS AND DISCUSSION

The accelerations were measured in the directions defined by the airframe coordinate system. Thus, aft accelerations along the longitudinal axis of the airplane decrease its speed. Normal accelerations, frequently called vertical, act perpendicular to the longitudinal axis of the airplane. An acceleration upward results from a pitching force that tends to increase the airplane's angle of attack.

### Longitudinal Accelerations

Description of unflared landing crashes. - In the three unflared landing crashes, both main landing-gear assemblies were ripped from the airplane by wheel abutments. The abutments that tore off the main landing-gear wheels and the abutment that tore off the nose-gear assembly are shown in figure 13. The latter abutment was set at an angle of $10^{\circ}$ to the longitudinal axis of the airplane to deflect the nose gear to one side and avoid impact with the underside of the airplane. In this way, damage to the dummy and the instrumentation by the nose gear was prevented. After the airplane passed through these barriers, it

became a free body which glided for approximately 85 feet before striking the sloping ground in the crash area. During this glide, the airplane pitched downward.

The airplanes struck the ground head-on with impact angles of 18°, 22°, and 27°. The airplanes in the 18° and 22° crashes bounced into the air after the initial impact and flew an additional 200 feet. A second impact occurred in these two crashes when the airplane slammed to the ground. In the 27° crash, a second impact did not occur as the airplane stopped within one airplane length from the point of initial impact with the ground.

Figure 14(a) shows a strip film from the motion pictures of the 18° unflared landing crash. In this crash, the longitudinal axis of the airplane and its flight path were parallel at the moment the nose hit the ground. The nose section crumpled first, then the cockpit section began to deform and deflect upward (fig. 14(a)). This cockpit deformation allowed the bulkhead, located at the rear of the cockpit, to dig into the ground. This digging action imposed a momentarily large acceleration. The airplane then pitched upward and slid up the slope.

In general, the same sequence of events occurred when the angle of impact was 22° (fig. 14(b)). In this crash, however, the longitudinal axis of the airplane tipped upward 9° with respect to the flight path at the moment of nose impact. Because of this airplane attitude, the bottom of the airplane was nearly parallel with the ground. The impact loads were therefore spread more uniformly over the bottom of the airplane. In this crash, the cockpit section did not deform and deflect upward as it did in the 18° crash. Instead, the whole airplane pitched upward when the cockpit section hit the ground (fig. 14(b)). The nose section of the airplane, however, crumpled in much the same manner as in the 18° crash.

When the impact angle was increased to 27° as shown in figure 14(c), the entire forestructure of the fuselage ahead of the wing collapsed. The airplane's path was essentially unchanged during the collapse of this fuselage forestructure. When the wing hit the ground, the airplane pitched upward and slid up the slope.

The data provided in this study by the unflared landing crashes show the relation between the strength of the airplane structure and the accelerations that occur. These accelerations should be the maximum values that the fuselage structure can transmit before collapsing because the airplane was crashed at the minimum flying weight. The strength of the airplane fuselage is simply an equal and opposite reaction to a given force which will begin the collapse of the structure. The maximum acceleration (in g's) which an airplane structure can transmit to the structure behind it before collapsing is the acceleration force applied to it divided by the weight of the airplane behind this structure.

Therefore, if the airplane's weight is at a minimum, the transmitted accelerations of the structure upon collapse should be the maximum obtainable.

The crushed structure, in these crashes, can be divided into three sections: (1) the nose section ahead of the cockpit (this structure is relatively weak and crushes readily), (2) the cockpit section which houses the pilot (this structure is somewhat stronger than the nose section but the belly structure below the floor is relatively weak), and (3) the wing structure. The wing structure, adjacent to the fuselage, is very strong and will resist high crash forces. The development of accelerations associated with the crashing of each section is discussed in the following paragraphs.

Accelerations transmitted by nose structure. - The acceleration data measured on the cockpit floor immediately behind the nose section of the airplane indicate the acceleration force that the nose section can transmit to the floor before the nose collapses.

During the time the nose structure was collapsing (the first 0.05 sec), the longitudinal acceleration in all three crashes gradually rose at approximately the same rate to a value of about 18 g's as shown in figure 15. This gradual rise indicates that progressively larger cross sections of the nose structure were involved as the nose collapsed. These data (fig. 15), therefore, show that the maximum acceleration the nose structure transmitted was about 18 g's. The nose structure then can withstand acceleration forces in the order of magnitude of 18 times the airplane weight.

The values from figure 15 and subsequent acceleration curves were obtained by fairing these curves to disregard the high-frequency components. It is felt that these components represent vibration of the structure that supports the accelerometer mounting brackets. Since these high-frequency components have little effect on human beings, they should be disregarded.

The records for the cockpit floor (fig. 15) show accelerations greater than the 18 g's just discussed.

In all three crashes, after the nose section had collapsed, the stronger cockpit structure hit the ground. This stronger structure produced a further increase in the accelerations measured on the cockpit floor. In the 18° crash, these accelerations rose to about 20 g's at 0.06 second (fig. 15(a)). At this time, the cockpit structure failed in bending, and the cockpit deflected upward. Because of this deformation, the ground plowing of the forward part of the airplane decreased. Consequently, the deceleration of this portion of the airplane decreased.

In the 22° crash after the fuselage nose crumpled, the cockpit structure dug into the ground harder than in the 18° crash because the cockpit structure did not deflect upward. This resulted in an acceleration peak of 30 g's between 0.06 and 0.07 second (fig. 15(b)).

In the 27° crash, after the nose structure collapsed, the acceleration of the cockpit floor (fig. 15(c)) rose rapidly because the cockpit floor also collapsed and the accelerometer itself hit the ground. The acceleration of 140 g's produced by ground contact indicated at this time (0.065 sec) should not be compared with other acceleration data.

CT-2

Accelerations transmitted by cockpit structure. - The acceleration data measured on the bulkhead at the rear of the cockpit indicated the acceleration that the cockpit structure transmitted.

The acceleration data measured on the bulkhead at the rear of the cockpit are shown for all three of the unflared landing crashes in figure 16. This bulkhead is used as the anchoring structure for the dummy's restraining harness. The accelerations imposed on this bulkhead therefore would be transmitted to the dummy's restraining harness.

In the 18° crash, the bulkhead acceleration rose to about 20 g's at 0.06 second (fig. 16(a)). The acceleration then dropped to zero when the cockpit structure deflected upward at 0.065 second. When this happened, the bulkhead itself dug into the ground. This plowing increased the acceleration at the bulkhead to 35 g's at 0.1 second. This loading, however, was applied directly to the bulkhead when the structure itself struck the ground. Since this load was not transferred through the cockpit structure, no appreciation for the crushing strength of the cockpit structure can be obtained from this crash.

In the 22° crash, the cockpit structure was near collapse as indicated by the wrinkles in the fuselage skin (fig. 17). The acceleration at the bulkhead during this crash rose to a peak value of about 35 g's at 0.085 second (fig. 16(b)). The normal component of this accelerating force crushed the belly structure and allowed the bulkhead itself to dig into the ground. A short peak of 50 g's at 0.095 second resulted. Although exposed to longitudinal accelerations between 30 and 35 g's for 0.03 second, the cockpit was not crushed as shown in figure 18. At the time the 35-g peak was attained, all the airplane accelerating force was transmitted through the cockpit structure since airplane components aft of the cockpit were not yet in contact with the ground. Since the beginning of the cockpit collapse occurred at 35 g's, it is assumed that the collapse strength of the cockpit is equivalent to an acceleration load of 35 times the weight of the airplane behind the cockpit.

An accelerating force that caused complete collapse of the cockpit structure was obtained in the 27° crash. The acceleration history

(fig. 16(c)) shows that the acceleration increased gradually as the nose structure collapsed. The acceleration continued to build up while the cockpit collapsed. An acceleration of about 40 g's was recorded while the cockpit structure was collapsing, as indicated by the data between 0.07 and 0.08 second. After the cockpit structure had collapsed, the bulkhead accelerometer itself hit the ground. When this happened, a large acceleration was indicated. This acceleration is similar to the acceleration that occurred when the accelerometer on the cockpit floor hit the ground and was suddenly stopped. Therefore, this acceleration also should not be compared with other acceleration data.

From the preceding data, it can be seen that incipient failure of the cockpit occurred at a longitudinal acceleration of 35 g's, and complete failure occurred at 40 g's. Since this cockpit structure was able to withstand loads up to 40 g's, the military services' decision to design their fighter-pilot's restraining equipment for 40 g's is realistic in this instance.

The gross relation between airplane structural strength and maximum acceleration observed in this fighter-airplane study was also observed in the study of light-airplane crashes (ref. 5). The maximum acceleration in the light-airplane crashes was also limited by the strength of the structure in the forepart of the airplane although the airplane structure and crash circumstances were different from the fighter-airplane crashes. The light-airplane structure consisted of fabric-covered tubular steel members, while the fighter airplane had an aluminum monocoque-type structure. In the light-airplane crashes, the airplanes struck a mound of earth at an angle of 55° at speeds between 42 and 60 miles per hour. By comparison, the fighter airplanes crashed into the ground at angles between 4° and 27° with a speed of 112 miles per hour.

The fighter- and light-airplane crash data demonstrated the obvious point that the strength of the uncrushed structure ahead of the pilot and the weight of the airplane behind him determine the maximum acceleration he will receive.

Accelerations of center-section wing panel structure. - Some appreciation for the strength of the center-section wing panel structure can be obtained from the acceleration data measured at the center of gravity of the airplane. The center of gravity is located approximately 6 feet behind the bulkhead at the rear of the cockpit. The wing roots are fairly thick since they house the engines. The airplane structural strength in this zone is correspondingly high. The longitudinal accelerations measured at the airplane's center of gravity for the 18°, 22°, and 27° unflared landing crashes are shown in figure 19. The maximum acceleration recorded at the center of gravity of the airplane was 60 g's during the 27° crash. In this crash, when the acceleration at the center of gravity rose to a maximum of 60 g's at 0.12 second (fig. 19(c)), the

center-section wing panel structure struck the ground. The amount of damage to this structure was minor as shown in figure 20. The only parts that received serious damage in this area were the engine air inlet ducts. It appears then that this structure can transmit large longitudinal accelerations before it fails.

Longitudinal accelerations in ground-loop and cart-wheel crashes. - During a ground-loop crash (fig. 21) the airplane rotates about a vertical axis while the airplane is in a nearly horizontal attitude. Such an accident was simulated by ripping off only the left main landing gear with an abutment similar to those used in previous crashes. The left wing tip then dropped to the ground. After the airplane had moved about 50 feet into the crash area, the left wing tip struck an earthen bank (fig. 22) which rotated the airplane rapidly until the opposite (right) wing tip struck the mound. At this point, both the nose and right wheel struts collapsed and the airplane stopped rotating. It then slid tail first until it struck a second earthen bank located across the crash area centerline (fig. 22). While the airplane was sliding rearward, (2.3 sec after impact), it gouged a hole in the top of the second mound and bounced into the air tail first. It then slammed down on its belly and came to rest some 50 feet behind this second bank (fig. 21).

The longitudinal acceleration of the cockpit floor measured in the ground-loop crash is shown in figure 23. Because the angle of initial impact with the ground was small, the initial longitudinal acceleration rose to only 4 g's. Following the initial impact, the airplane slid along the ground for approximately 2.3 seconds. During this time the acceleration was generally less than 3 g's. By the time the airplane struck the second mound of earth going rearward, its velocity was reduced to 60 miles per hour. Upon striking the mound at this reduced velocity, the airplane rose over it without significant damage to the airplane structure. As a consequence, the longitudinal component of the cockpit floor acceleration (fig. 23(a)) had a peak of only 9 g's (2.33 sec) which lasted for 0.1 second. This was the maximum longitudinal acceleration encountered in the ground-loop crash.

The lateral acceleration of the cockpit floor, as shown in figure 23(b), is of the same order of magnitude as the longitudinal cockpit floor acceleration.

The cart-wheel crash was created by rolling the airplane into a left-wing-down attitude before it left the guide rail. This was done by running the airplane along a twisted ramp 85 feet long at the crash end of the runway (fig. 24). This ramp rolled the airplane with uniform rotational acceleration until the wing was at a 30° angle with the horizontal as shown in the strip film from motion pictures in figure 25. Upon reaching this 30° position, the left wing struck an earthen bank

CT-2 back

(fig. 24), located approximately 10 feet beyond the end of the ramp, which cartwheeled the airplane. As the airplane tumbled, it struck the ground nose first (fig. 25). With the nose acting as a pivot, the airplane turned until the left wheel again struck the ground (fig. 25). This impact destroyed the left landing gear. The airplane then landed on its belly and slid to a stop.

The longitudinal accelerations encountered in the cart-wheel crash (fig. 26(a)) were less than 10 g's. Peaks up to 9 g's occurred when the wing tip and fuselage nose dug into the ground. Because of the wheel-like motion of the airplane, the bearing point shifted from one place on the airplane to another, and the accelerations in the cockpit were small. The lateral accelerations on the cockpit floor in this crash were also low as shown in figure 26(b).

The accelerations on the cockpit floor are of about the same magnitude in both the ground-loop and cart-wheel crashes. Such accelerations can be easily tolerated by an adequately restrained pilot.

Variation of maximum longitudinal acceleration with impact angle at center of gravity of airplane. - The previous discussion has indicated that the angle of impact influences the severity of a crash. An indication of the magnitude of this influence can be obtained by comparing the maximum longitudinal accelerations at the center of gravity for various impact angles. Such a comparison is shown for four of the crashes in figure 27. The center-of-gravity acceleration is chosen for this comparison because the data were not obscured by local failures of this region in all four crashes.

The data shown in figure 27 were obtained from the longitudinal acceleration data at the airplane center of gravity for the 18°, 22°, and 27° unflared landing crashes (fig. 19) and the data for the initial impact of the ground-loop crash (fig. 28) whose initial angle of impact was 4°. It can be seen from figure 27 that the acceleration increases rapidly with angle of impact from a value of 8 g's for the 4° angle of impact to a value of 60 g's for a 27° angle of impact.

Longitudinal acceleration received by dummy. - The acceleration of the pilot is determined by the acceleration of the structure to which he is attached, the load elongation characteristics of his restraining harness, and the resiliency of his own body and clothing.

Body resiliency acts like a harness stretch in permitting body movement relative to the airplane. The effective stretch in the man - restraining-harness combination is the sum of the harness stretch and the body deformation. If the pilot's harness stretches under load, that part of his body restrained by the harness acquires a velocity relative

to the airplane. When the airplane deceleration endures until the harness has become taut and the pilot still has velocity relative to the airplane, the pilot's body will experience a deceleration equal to that of the airplane plus the additional deceleration required to bring the pilot's body back to the speed of the airplane. If the airplane deceleration declines while the harness is still stretching, his peak deceleration may not attain the peak airplane deceleration. Otherwise, the pilot's deceleration may exceed that of the airplane. If the pilot is attached rigidly to the structure, he will undergo the same deceleration as the structure to which he is attached.



The anthropomorphic dummy used in this study could not be expected to duplicate exactly the resiliency of a human; therefore, the response of the dummy to accelerations may be somewhat different from that of a human. However, the data obtained with this dummy should give some indication of the accelerations a human might experience.

The restraining harness used in this study was attached directly to the bulkhead at the rear of the cockpit. The seat, therefore, was not involved in the support of the dummy in the longitudinal direction.

The similarity of the accelerations measured on the dummy's hips with those of the bulkhead at the rear of the cockpit can be seen for the 18° unflared landing crash in figure 29. It is evident that the standard military 3-inch nylon lap belt used in this crash was sufficiently rigid to keep the dummy's hips from exceeding the bulkhead acceleration. The harness and the dummy's sponge-rubber flesh filtered out the high-frequency components of the bulkhead acceleration and delayed the acceleration of the dummy's hips by approximately 0.02 second. Both accelerations attained a peak of about 35 g's. High-frequency components of the bulkhead acceleration rose to 45 g's. It is evident that these high-frequency components have little effect on the acceleration response of the pilot.

The $1\frac{3}{4}$-inch cotton shoulder harness with the nylon lap belt used in the 18° crash, however, did not restrain the dummy's chest sufficiently, and amplification of the acceleration occurred. The pictures of the crash (fig. 14(a)) show the marked forward displacement of the dummy's shoulders permitted by the excessive harness stretch. This stretching allowed the dummy's chest to attain relative velocity with respect to the airplane. When the harness finally became taut, the acceleration of the dummy's chest (fig. 30(a)) exceeded that of the airplane structure (fig. 30(b)). The maximum chest acceleration was about 45 g's as compared with 35 g's for the maximum acceleration of the airplane.

Similar results were obtained in the light-airplane crash tests (ref. 5). Higher accelerations were measured on the dummy's chest than on the airplane structure to which he was restrained.

By comparing these accelerations with the accelerations which human beings have tolerated, it is possible to determine whether a pilot can tolerate the maximum accelerations that can be transmitted to him before the cockpit collapses. References 3 and 6 indicate that human subjects have been voluntarily subjected to decelerations of 45 g's for intervals up to 0.06 second without injury when properly restrained. The harness used in these tolerance studies consisted of a lap belt, thigh straps, a shoulder harness, and a chest strap. It was pointed out in the section "Accelerations transmitted by cockpit structure" that incipient cockpit failure occurred with a load of 35 g's, and complete collapse occurred at a load of 40 g's. Therefore, if a pilot is properly restrained in this type of airplane, he would survive the maximum longitudinal accelerations this airplane can transmit before the cockpit collapses.

Longitudinal accelerations resulting from tearing out complete landing gear. - The accelerations associated with tearing all landing gear assemblies from the airplane at the same time (impact with wheel abutment) were felt by the dummy only as a series of weak jolts. The longitudinal accelerations of the cockpit floor, bulkhead, and dummy's hips measured in the 18° crash during this action (fig. 31) show this result. The cockpit floor and bulkhead at the rear of the cockpit both show high-frequency acceleration patterns. This high-frequency shuddering is damped out, and the peak acceleration transmitted to the dummy's hips is about 8 g's. This pulse continued for about 0.05 second. Data from the other crashes show the same results.

These data show that the accelerations associated with tearing out the landing gear are not an important survival hazard because of their low magnitude and short duration.

## Restraining-Harness Loads

The loads on the restraining harness are derived largely from longitudinal accelerations. The normal acceleration component is supported largely by the seat. For this reason the harness loads are compared to the longitudinal component of the acceleration in this discussion.

The data from the 18° unflared landing crash indicate that the harness loads are somewhat below those that might be expected from the acceleration records. The shoulder-strap loads totaled 1800 pounds at the instant (0.12 sec) the left strap broke as shown in figures 32(a) and (b). At the same instant (0.12 sec) the left-lap-belt load was 900 pounds (fig. 32(c)). The right end of the lap-belt tension was not obtained. If the total lap-belt load is assumed to be double that of the left-belt value, the total lap-belt load would be 1800 pounds. The sum of the harness loads would be 3600 pounds. Since the dummy weighed

200 pounds, this 3600-pound load corresponds to a deceleration of 18 g's. At the same instant, the longitudinal acceleration of the dummy's chest was 45 g's (fig. 30(a)). This difference may be the result of friction between the buttocks and seat plus the legs being restrained by the rudder pedals. The acceleration calculated from the restraining-harness loads, then, is less than half the acceleration measured on the dummy's chest. These results do not mean, however, that the restraining harness can be designed for half the acceleration load.

## Normal Accelerations

In the previous discussion, it was shown that a properly supported pilot can survive greater accelerations in the longitudinal direction than the airplanes used in this investigation are capable of transmitting to him through the fuselage nose and cockpit structure. These structures would collapse and crush the pilot before exceeding the tolerance level of a human to accelerations in the longitudinal direction.

The tolerance level of humans to accelerations in a normal direction (parallel to and compressing the spine when in normal seated position) is much lower than those for the longitudinal direction (ref. 7). The maximum design acceleration for upward ejection seats for the U.S. Navy and Air Force is 20 g's. Swedish experience with upward ejection seats designed for a maximum acceleration of 25 g's has resulted in occasional spine injuries. It may be concluded that the maximum normal acceleration tolerable without injury is about 20 to 25 g's in contrast to 40 g's for the longitudinal direction (perpendicular to the spine).

Variation of maximum normal acceleration with impact angle at center of gravity. - The normal accelerations of the airplane center of gravity, associated with the initial impact of the airplane during a crash, vary with angle of impact much in the same manner as the longitudinal acceleration. Accelerations for the initial impact in the $4^{\circ}$ ground-loop crash and the $22^{\circ}$ crash are shown in figure 33. Data were not obtained at the airplane center of gravity in the $18^{\circ}$ and $27^{\circ}$ unflared landing crashes. As the impact angle became steeper, the velocity component of the airplane normal to the slope increased. As a consequence, the area under the acceleration-time curve grew with this increased vertical velocity component. For the $4^{\circ}$ angle of impact, a peak vertical acceleration of 8 g's occurred. At an impact angle of $22^{\circ}$, the peak normal acceleration rose to about 42 g's. These maximum normal accelerations of the airplane at the center of gravity have been plotted against impact angle in figure 34.

The cockpit was not crushed in the $22^{\circ}$ crash. The normal acceleration during this crash, however, was 42 g's. This acceleration is well beyond presently accepted human tolerance limits for blows parallel to and compressing the spine.

Normal accelerations from striking ground after stall. - In the 22° unflared landing crash, the airplane bounced into the air following its first impact with the ground. After flying 200 feet, the airplane struck the ground tail first as shown in the strip film from motion pictures in figure 35. In this event, the cockpit section of the airplane fell about 20 feet, and the normal velocity was about equal to the forward velocity. The magnitude of the normal accelerations of the cockpit floor during this second impact is shown in figure 36. In this stall and slamming-down period, between 2.86 to 2.91 second after impact (fig. 36), the maximum normal acceleration on the cockpit floor was about 55 g's as compared with about 30 g's that occurred in the first impact (fig. 37). The base duration of this 55-g pulse was about 0.05 second.

Normal accelerations in cart-wheel crash. - The normal accelerations in the cart-wheel crash were relatively small. During the entire cart-wheel crash, the maximum normal acceleration of the cockpit floor was about 15 g's at 2.2 seconds with several short pulses of about 10 g's as shown in figure 38. A similar result was obtained for accelerations in the longitudinal direction.

Normal accelerations transmitted to dummy. - The normal accelerations transmitted to a pilot during a crash may or may not be of the same magnitude as those on the floor under him. If the structural tie between a pilot and the floor is sufficiently rigid, the two accelerations should be essentially the same. On the other hand, if a pilot is sitting on compressible material (cushion or a seat pack parachute), or if the seat fails, the blow may be either attenuated or amplified.

Two instances in which the normal acceleration of the dummy was greater than that of the cockpit floor occurred during the 22° unflared landing crash. The first instance occurred when the airplane struck the inclined slope. It is believed that during this impact the seat adjusting mechanism failed in a normal direction. The pins sheared through the holes in the support tubes (fig. 39). This failure allowed the dummy to move downward and to acquire velocity relative to the cockpit floor. When the dummy bottomed against the cockpit floor, the hip acceleration exceeded the maximum floor acceleration. The peak normal acceleration on the dummy's hips (fig. 40(a)) was about 60 g's as compared with an acceleration on the cockpit floor of 35 g's (fig. 40(b)). The second instance occurred when the airplane again struck the ground after it flew into the air following the first impact (fig. 35). During this second impact, the dummy was free to move because of the seat failure that occurred in the first impact. Again the acceleration of the dummy's hips exceeded those of the cockpit floor. The peak normal acceleration of the dummy's hips (fig. 41(a)) was more than twice the acceleration of the cockpit floor (fig. 41(b)).

Normal blows such as these just described would have injured a pilot. For example, the second blow on the dummy's hips was several times larger than the 20-g acceleration accepted as the maximum for upward ejection seat design. It is apparent, then, that means of reducing the overshoot and attenuating the normal blows would provide worthwhile gains in crash survival.



In contrast to the blows just described, normal blows that could be considered tolerable for an adequately restrained pilot occurred during the ground-loop crash. The normal acceleration on the dummy's hips, as the airplane slid over a bank, was only 5 g's as shown in figure 42(a). Larger normal acceleration of the dummy's hips occurred after the airplane slid over the bank and fell approximately 5 to 6 feet. During this action, the normal acceleration on the dummy's hips was 18 g's (fig. 42(b)).

It may be concluded from the foregoing discussion that normal accelerations that exceed human tolerance may occur in a crash that is otherwise survivable. If maximum crash impact in which a pilot may survive is to be obtained, means for attenuating these normal accelerations should be investigated. Several means of attenuating these accelerations are discussed in reference 8.

## CONCLUSIONS

From the information obtained with five experimental crashes with FH-1 fighter airplanes, three of which were unflared landing crashes at $18^{\circ}$, $22^{\circ}$, and $27^{\circ}$ angles of impact, a cart-wheel and a ground-loop crash, the following conclusions can be made:

1. An adequately restrained pilot can withstand greater longitudinal accelerations than the cockpit structure of this airplane can transmit to him before it collapses.

2. Human tolerance to normal acceleration was exceeded in all the unflared landing crashes.

3. Incipient failure of the cockpit structure occurred at a longitudinal acceleration of 35 g's. Complete failure occurred at 40 g's.

4. The longitudinal accelerations of the bulkhead and the dummy's hips were similar which indicates that the lap-belt restraint used in this study was sufficiently rigid to prevent dynamic overshoot.

5. The longitudinal chest accelerations exceeded those of the airplane structure which showed that the standard shoulder harness allowed the dummy's chest to attain excessive relative velocity with respect to the airplane.

6. In some crashes, the normal accelerations measured on the dummy's hips were as much as twice those measured on the cockpit floor.

Lewis Flight Propulsion Laboratory
National Advisory Committee for Aeronautics
Cleveland, Ohio, July 15, 1957

## APPENDIX - DESCRIPTION OF TELEMETERING DATA RECORDING SYSTEM

The telemetering system consisted essentially of transducers for converting the accelerations or belt forces to electrical pulses. These pulses were fed into a radio transmitter carried in the airplane. The transmitter converted the information to radio waves that were transmitted to the receiving station. The receiving station then reconverted the radio signals to electrical pulses that were fed to recording galvanometers. The galvanometers in turn recorded the data on photographic paper.

The accelerometers were of the variable-inductance, suspended-slug type and had a measured undamped natural frequency of approximately 300 cycles per second. They were filled with silicone damping fluid and individually checked for a damping ratio of 0.60 to 0.64. This damping ratio resulted in a flat response within 5 percent, up to 85 percent of the undamped natural frequency. As a result, the accelerometer response was flat within ±5 percent to 250 cycles per second.

The tensiometers were also in the variable-inductance category of transducers. They consisted of two rigidly interconnected beams that held a powdered-iron slug in proper alinement within a coil. Tension applied to the lap belt or shoulder harness caused the beams to deflect and resulted in a relative displacement between the slug and coil. This produced a change in the apparent inductance at the terminals. The tensiometers had a calculated undamped natural frequency (first mode) of 1920 cycles per second; and, since an undamped system has a flat response within 5 percent up to 22 percent of the undamped natural frequency, this system did not require damping, and the response was flat within 5 percent up to 420 cycles per second.

The telemeter system, exclusive of transducers and recorders, had an accuracy ±2 percent of full-scale amplitude, and a frequency response flat within ±2 percent from steady-state conditions to 200 cycles per second. The nature of frequency-modulation discriminators is such that an increase in amplitude lowers the limit of flat frequency response. This system faithfully reproduces nonoscillatory conditions to full-scale amplitude, but at 200 cycles per second the amplitude must be held within ±20 percent of full scale from the center of the range in order to have within ±2 percent flat frequency response.

Galvanometers which had a response that was flat within 5 percent to 300 cycles per second were used for recording the three components of airplane acceleration. The galvanometers used to record the belt tensions and dummy accelerations were flat within 5 percent to 100 cycles per second.

## REFERENCES

1. Jones, Walton L.: Typical Impacts of Jet Aircraft Land Crashes. Jour. Aviation Medicine, vol. 24, no. 6, Dec. 1953, pp. 474-482.

2. Charles, John P.: Fractured Vertebrae in U.S. Navy Aircraft Accidents. Jour. Aviation Medicine, vol. 24, no. 6, Dec. 1953, pp. 483-490.

3. Stapp. John Paul: Human Exposures to Linear Deceleration. Pt. 2. The Forward-Facing Position and the Development of a Crash Harness. AF Tech. Rep. No. 5915, Pt. 2, U.S. Air Force, Wright-Patterson Air Force Base, Dayton (Ohio), Dec. 1951.

4. Black, Dugald O.: Facilities and Methods Used in Full-Scale Airplane Crash-Fire Investigation. NACA RM E51L06, 1952.

5. Eiband, A. Martin, Simpkinson, Scott H., and Black, Dugald O.: Accelerations and Passenger Harness Loads Measured in Full-Scale Light-Airplane Crashes. NACA TN 2991, 1953.

6. Pesman, Gerard J., and Eiband, A. Martin: Crash Injury. NACA TN 3775, 1956.

7. Frost, Richard H.: Escape from High-Speed Aircraft. Aero. Eng. Rev., vol. 14, no. 9, Sept. 1955, pp. 35-45.

8. Pinkel, I. Irving, and Rosenberg, Edmund G.: Seat Design for Crash Worthiness. NACA TN 3777, 1956.


Figure 1. - Airplane used in jet fighter crashes.

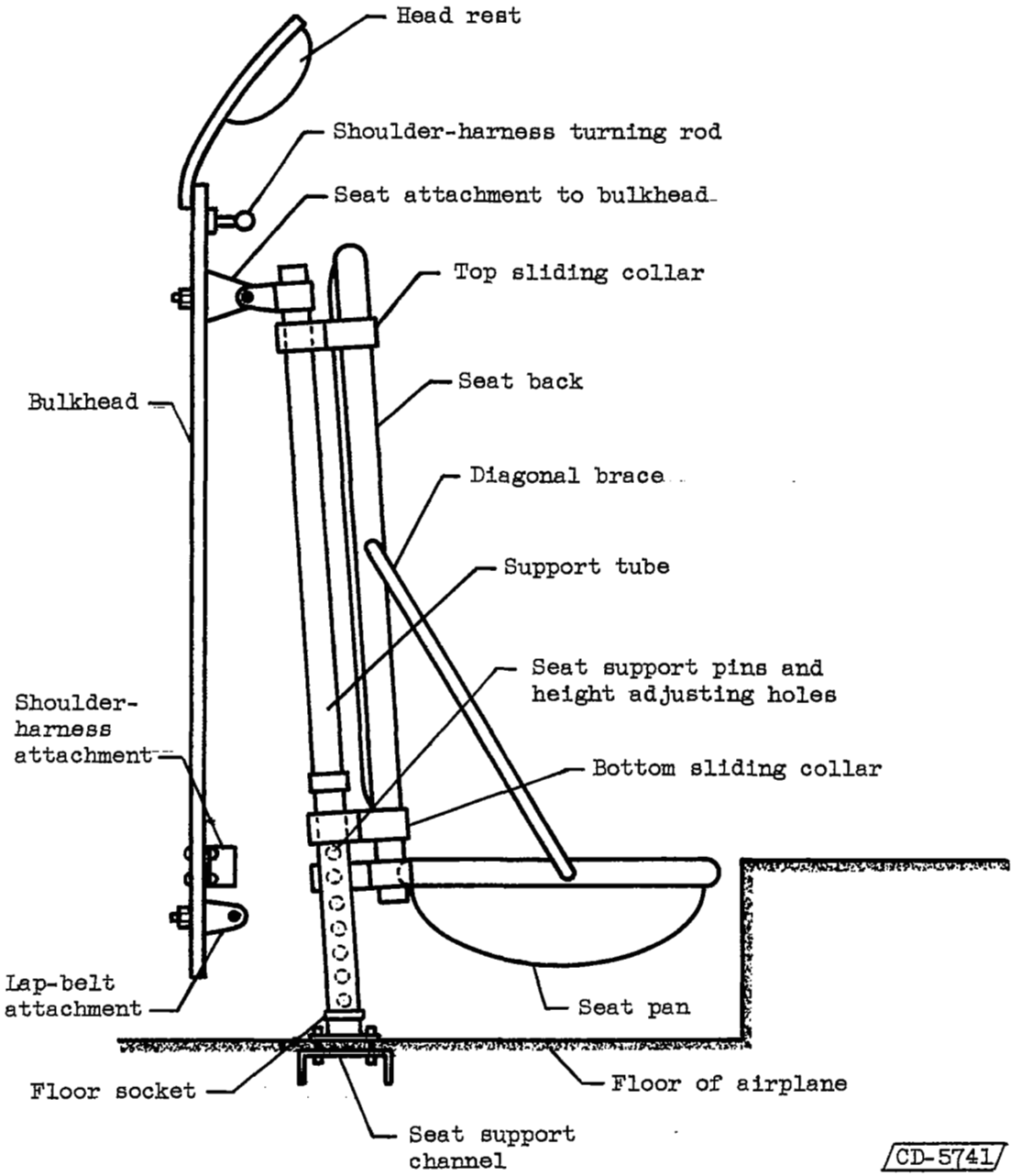


Figure 2. - Bucket-type pilot's seat as installed in fighter airplane.

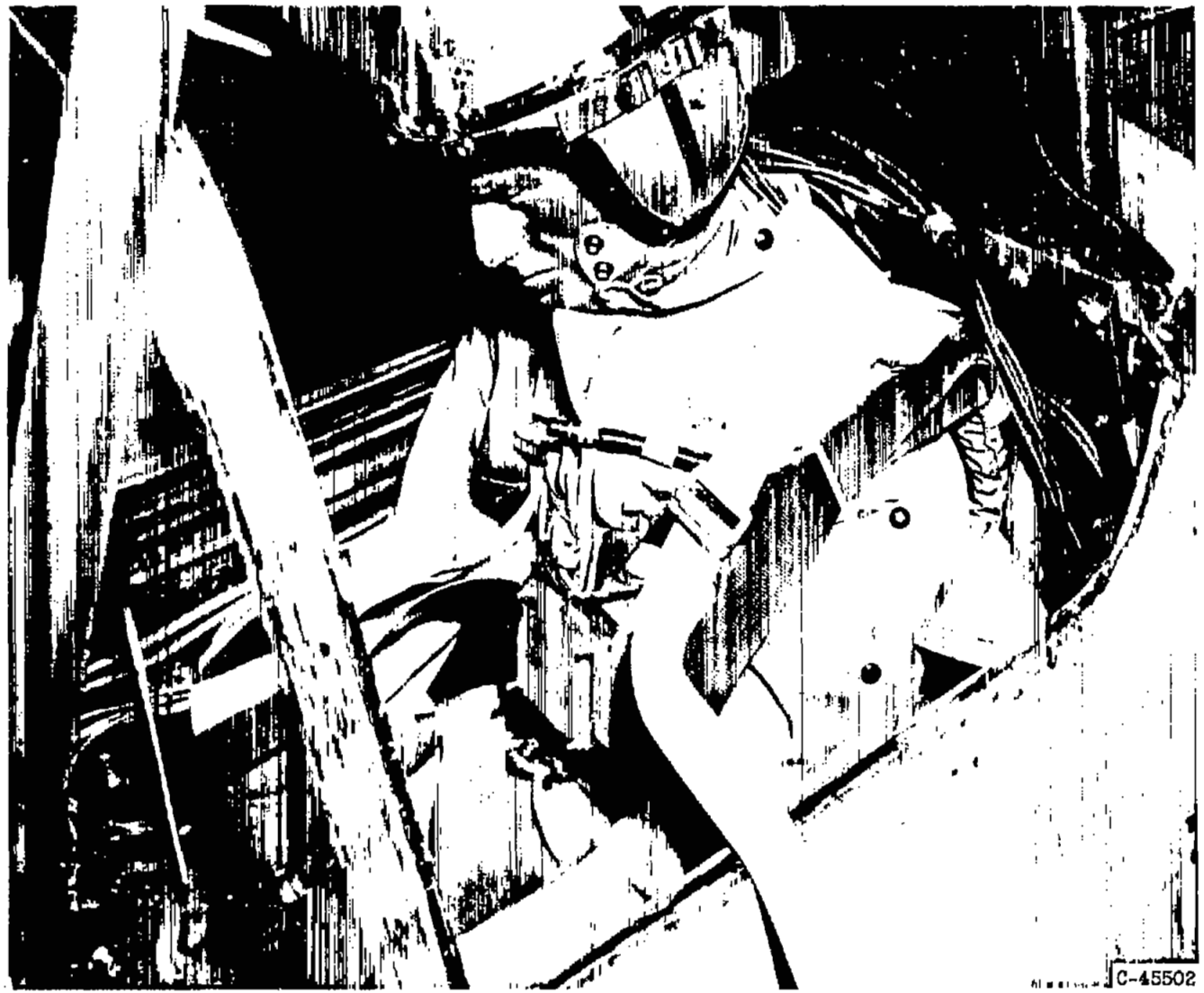


Figure 3. - Anthropomorphic dummy installed in cockpit of fighter airplane.

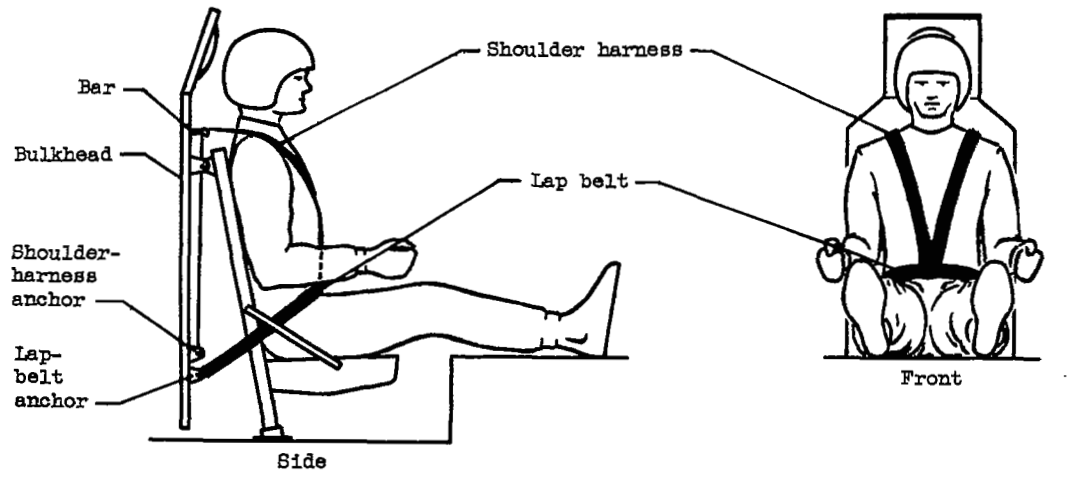


(a) Unflared landing (18° and 22°), cart-wheel, and ground-loop crashes.

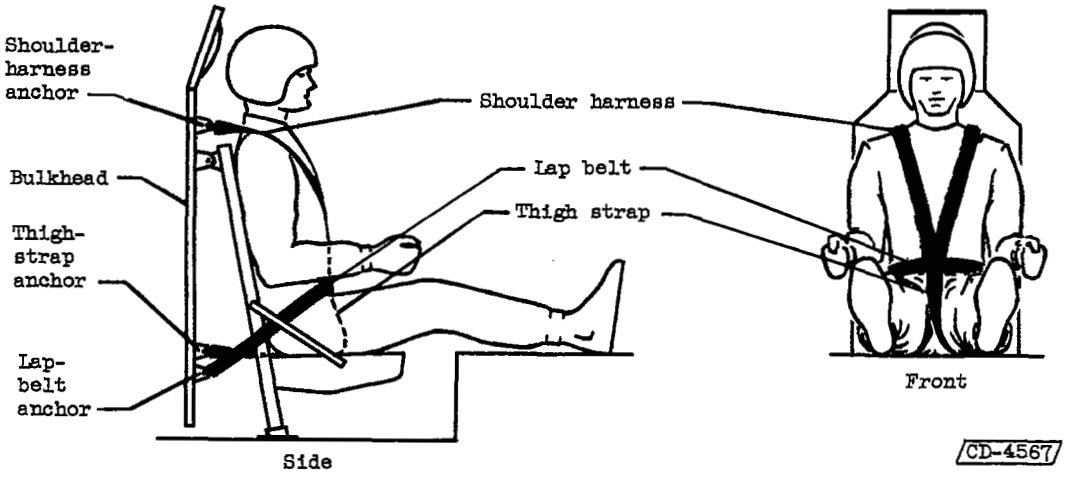


(b) 27° Unflared landing crash.

| Crash | Shoulder harness | | Lap belt | | Thigh Strap | |
|---|---|---|---|---|---|---|
| | Material | Strength, lb | Material | Strength, lb | Material | Strength, lb |
| 18° | 1-3/4" Cotton | 1500 | 3" Nylon (standard military) | 3000 | -- | -- |
| 22° Cart wheel and ground loop | 1-3/4" Dacron | 5000 | 3" Nylon (standard military) | 3000 | -- | -- |
| 27° | 3" Nylon | 8300 | 3" Nylon | 8300 | 3" Nylon | 4150 |

Figure 4. - Sketch of harnesses which restrained anthropomorphic dummy in seat during crash.

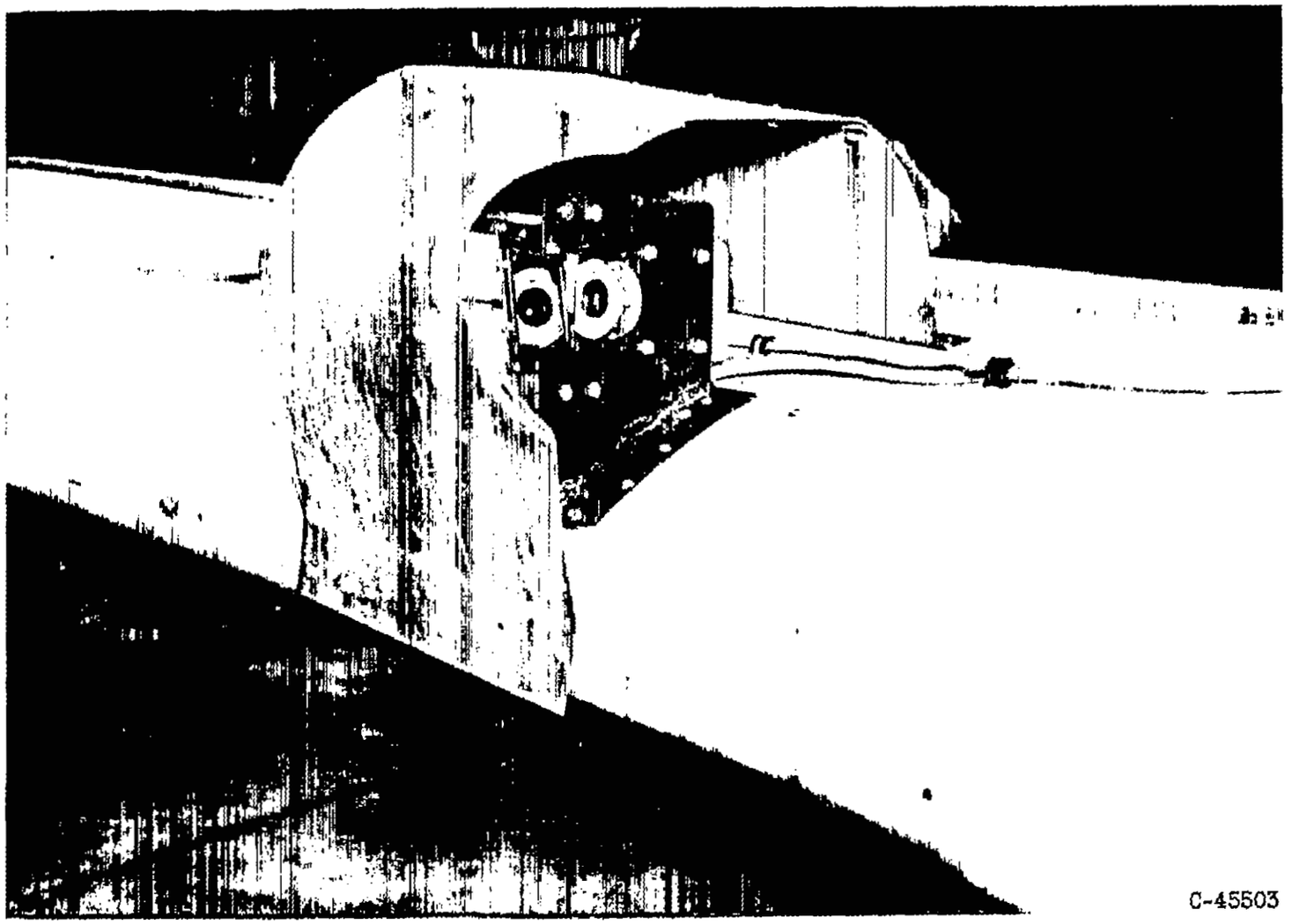


(a) Right wing.

Figure 5. - Location of cameras installed on airplane to photograph dummy's action during crash.

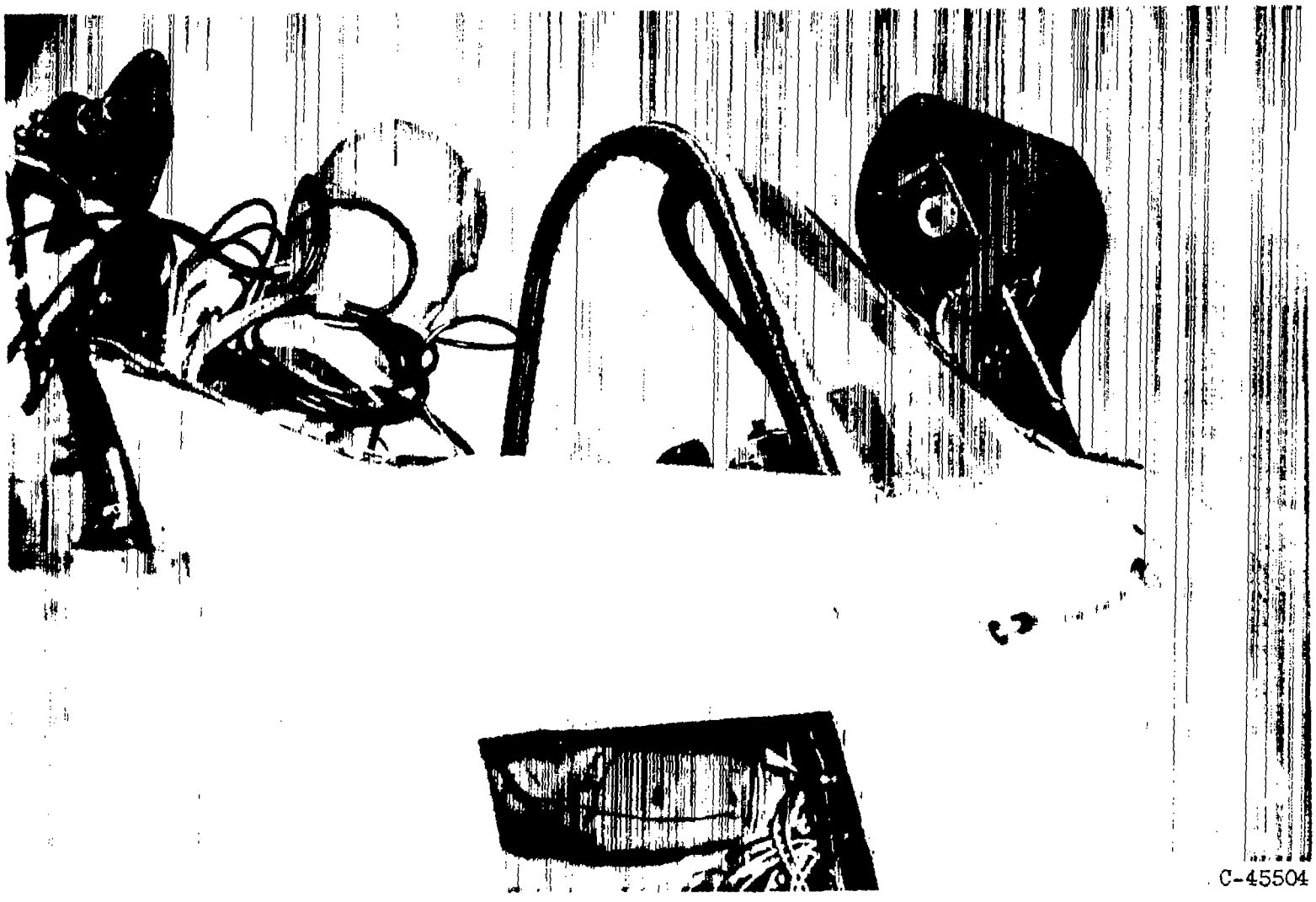


(b) In front of cockpit.

Figure 5. - Continued. Location of cameras installed on airplane to photograph dummy's action during crash.

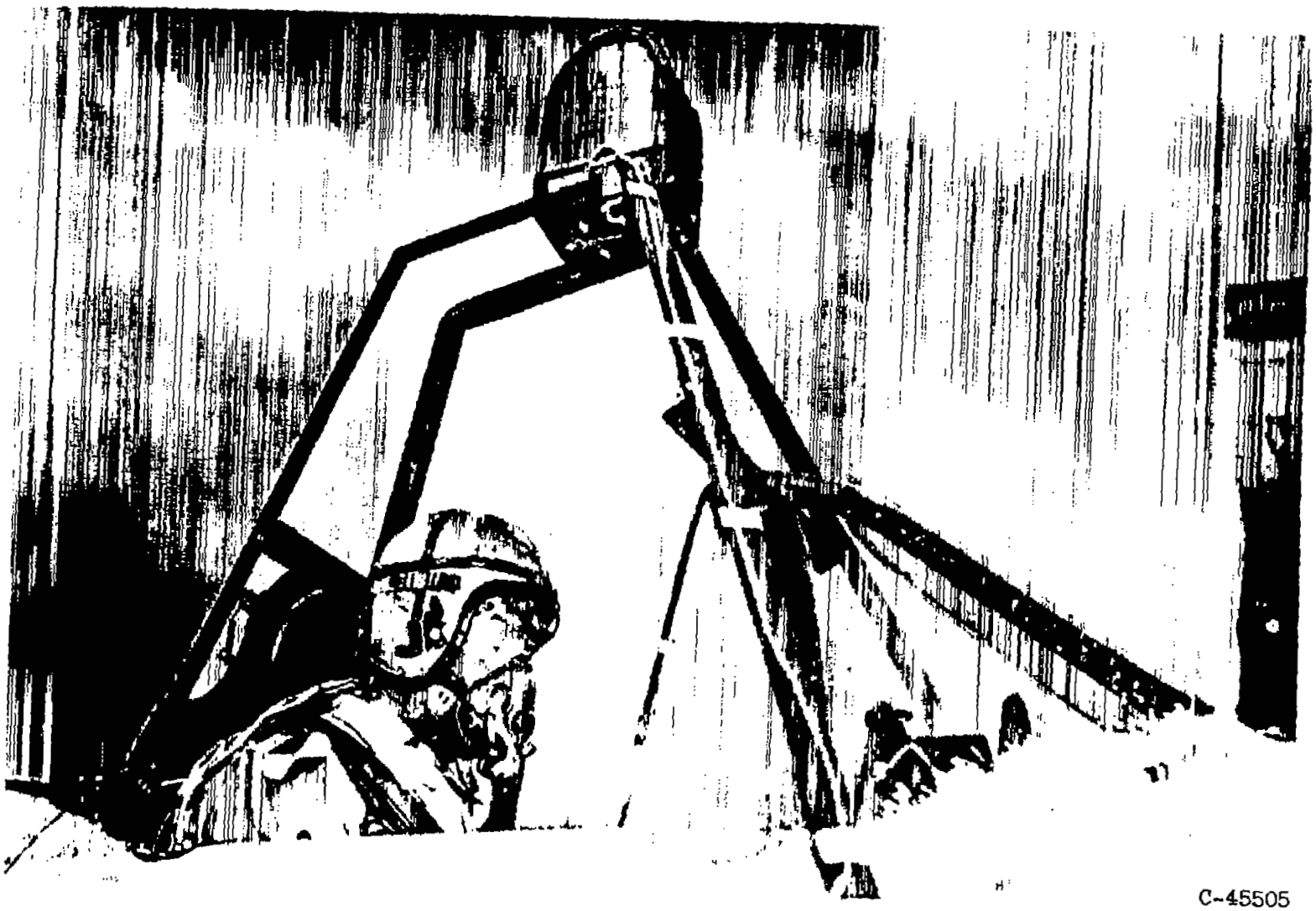


(c) Above cockpit.

Figure 5. - Concluded. Location of cameras installed on airplane to photograph dummy's action during crash.

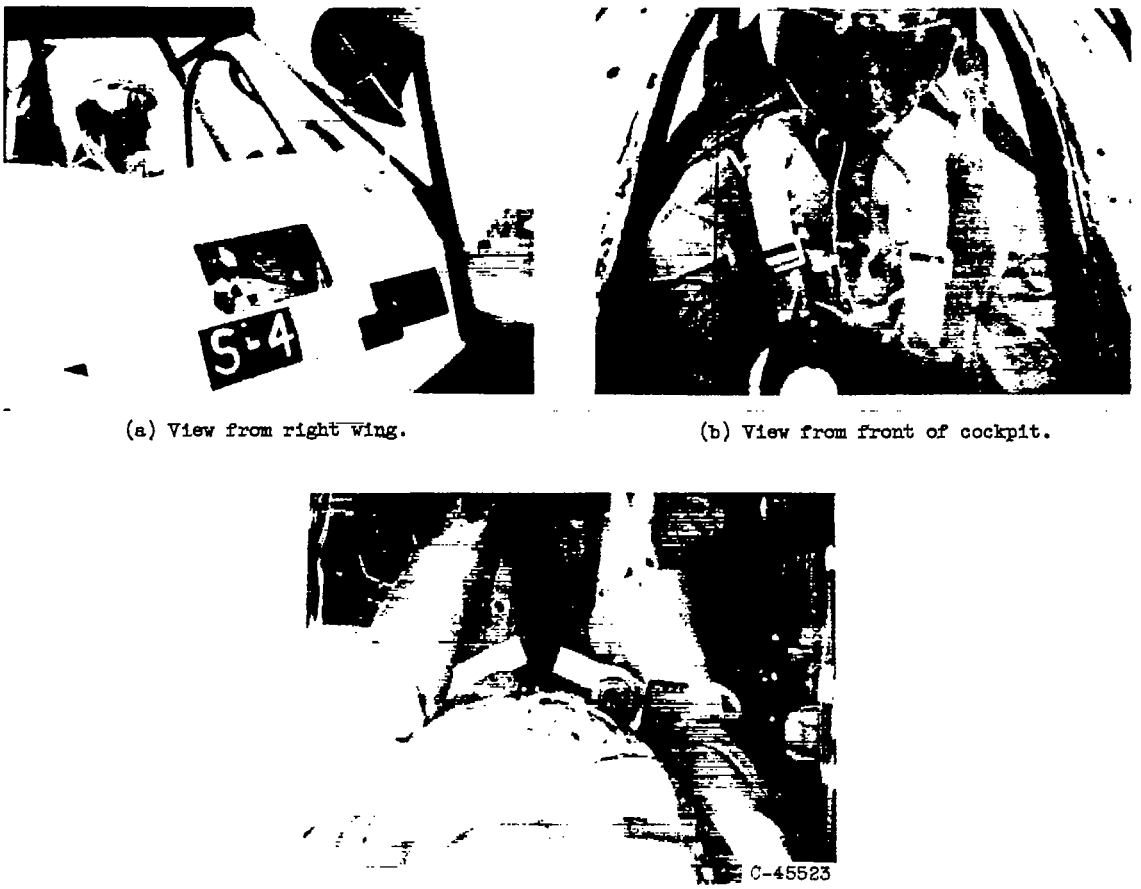


(a) View from right wing.

(b) View from front of cockpit.

(c) View from above cockpit.

Figure 6. - Sample photographs from airplane cameras of dummy in airplane.

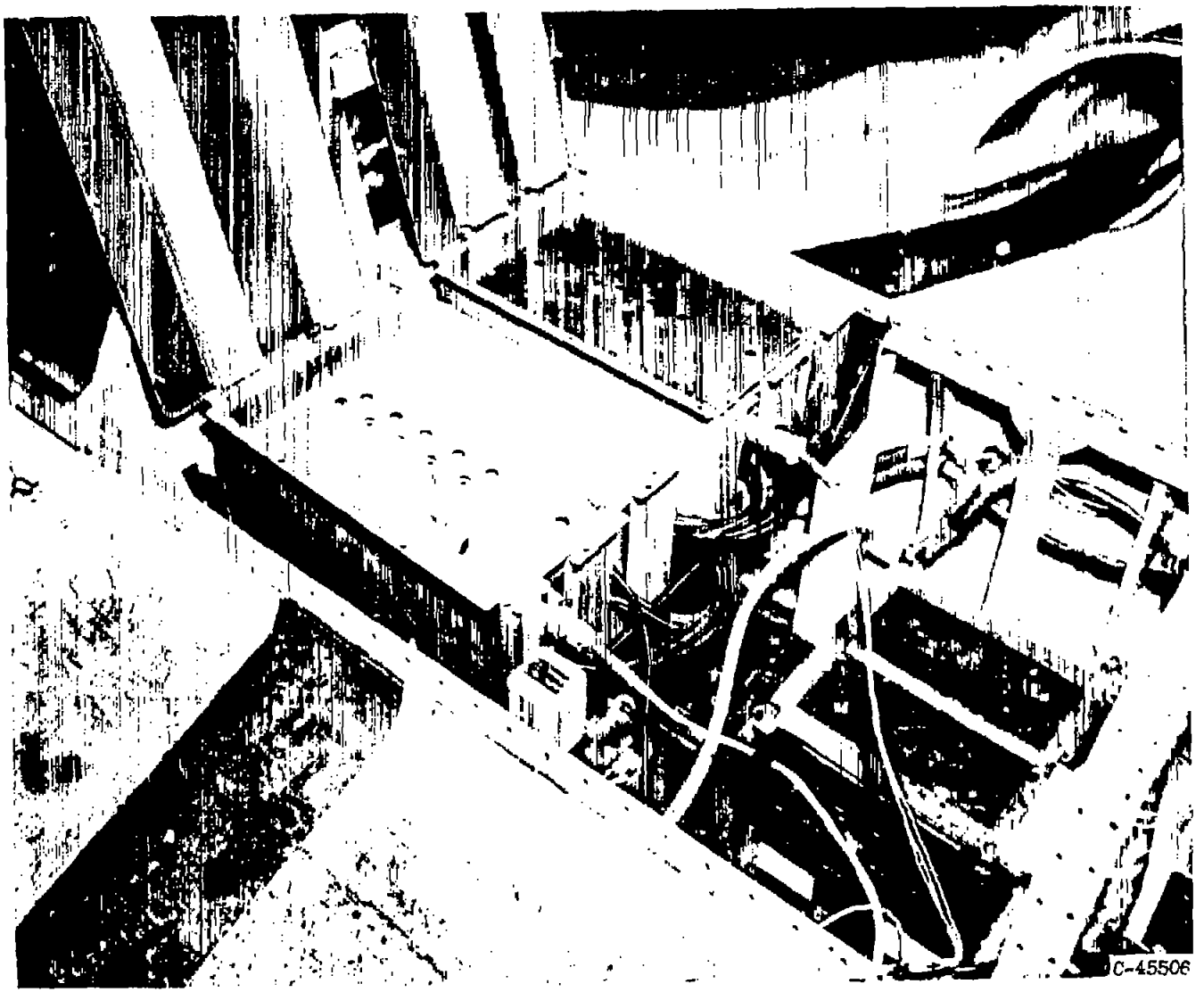


Figure 7. - Telemeter transmitter installed in airplane.

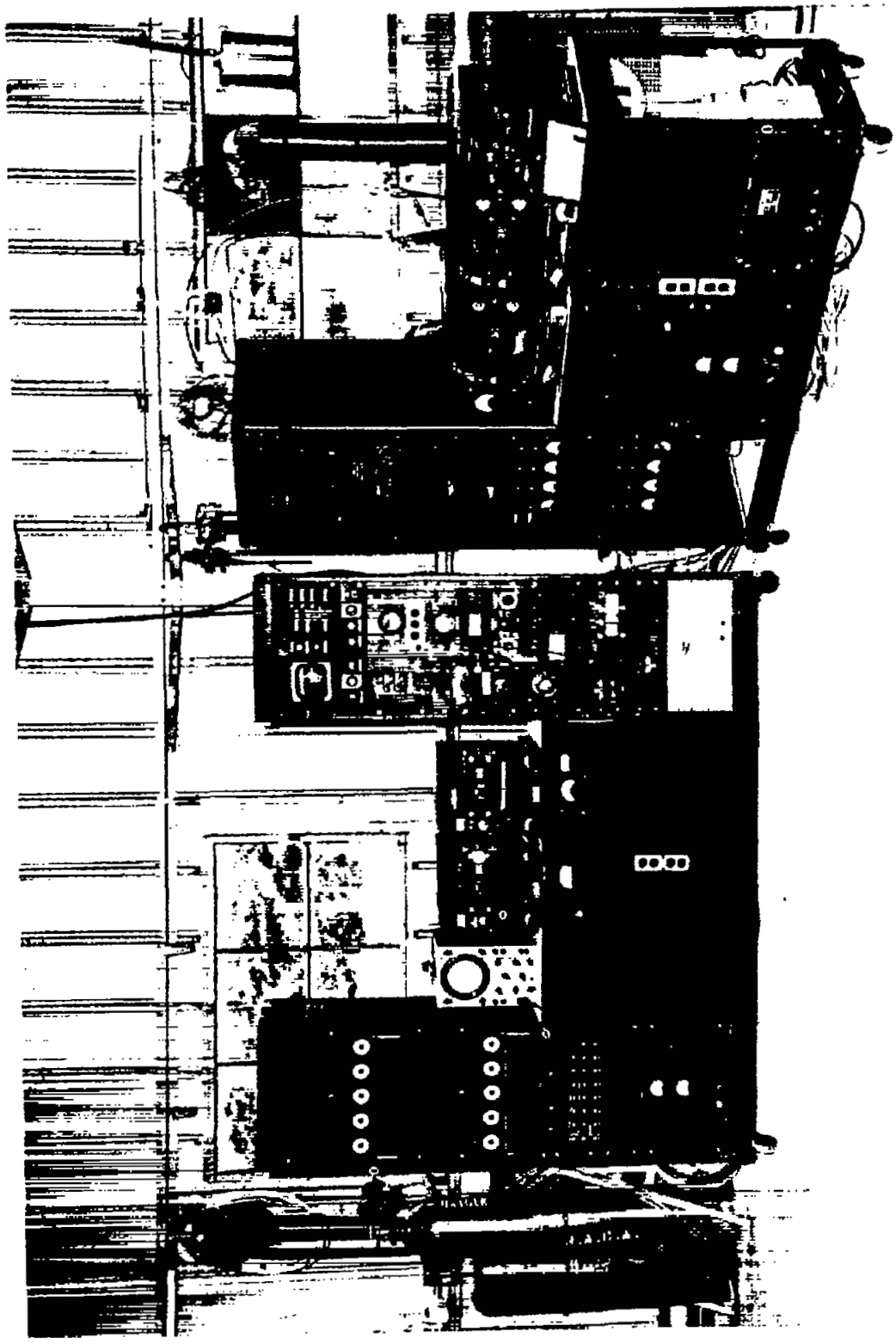

C-45507

Figure 8. - Receiving and recording telemeter station in operations building.

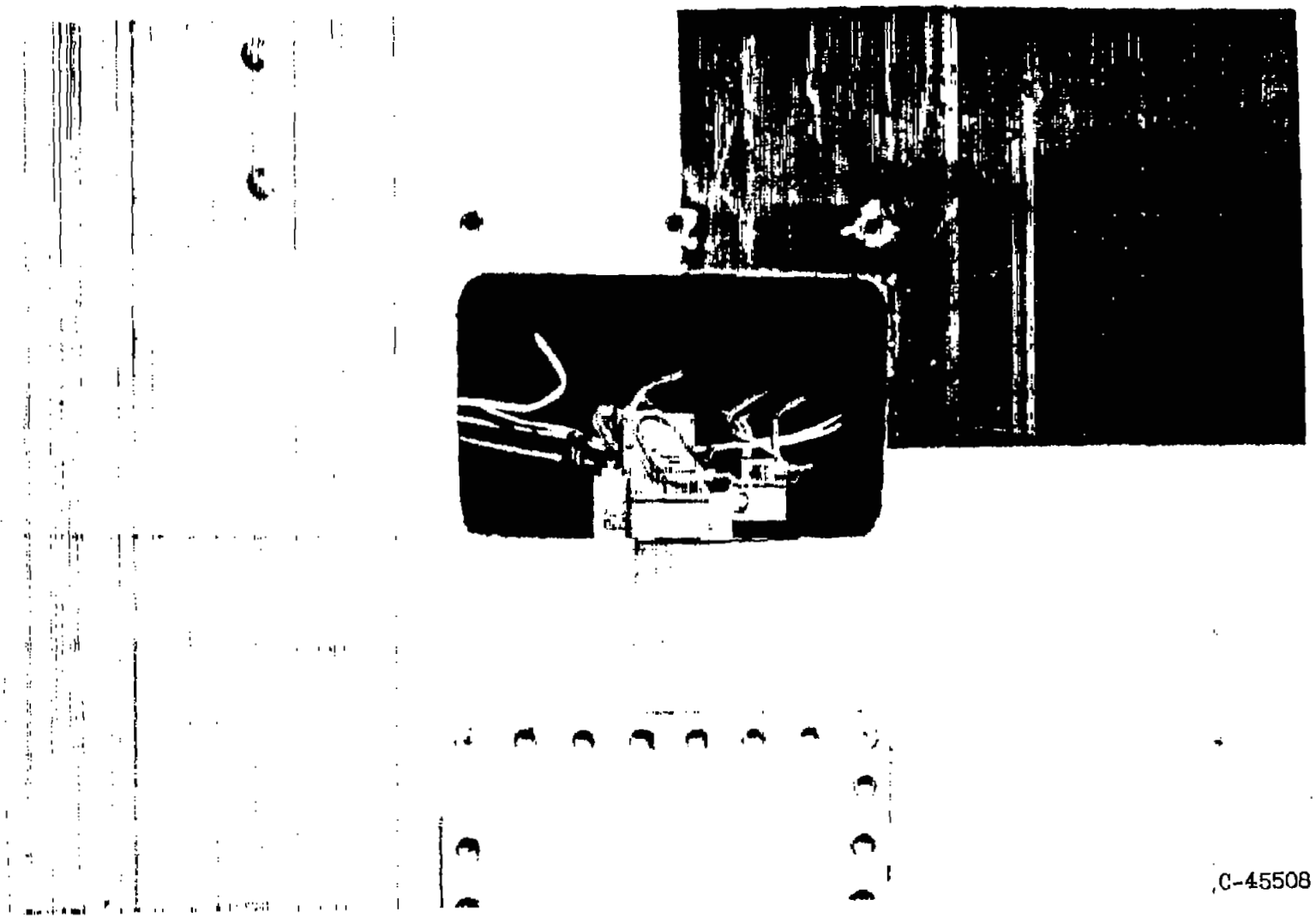

C-45508

(a) Cockpit floor.

Figure 9. - Accelerometers installed in fighter airplane.

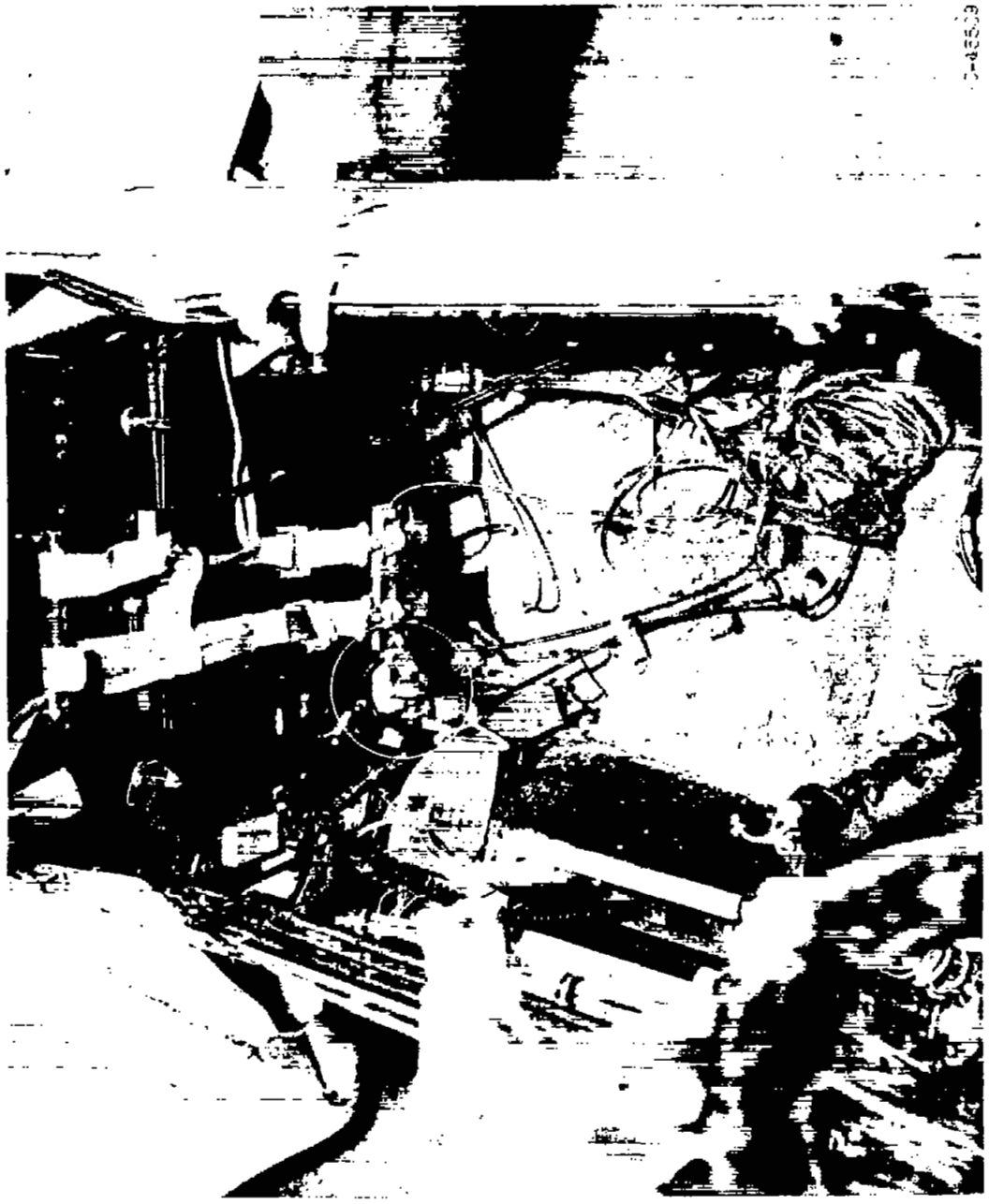

(b) Bulkhead.

Figure 9. - Continued. Accelerometers installed in fighter airplane.

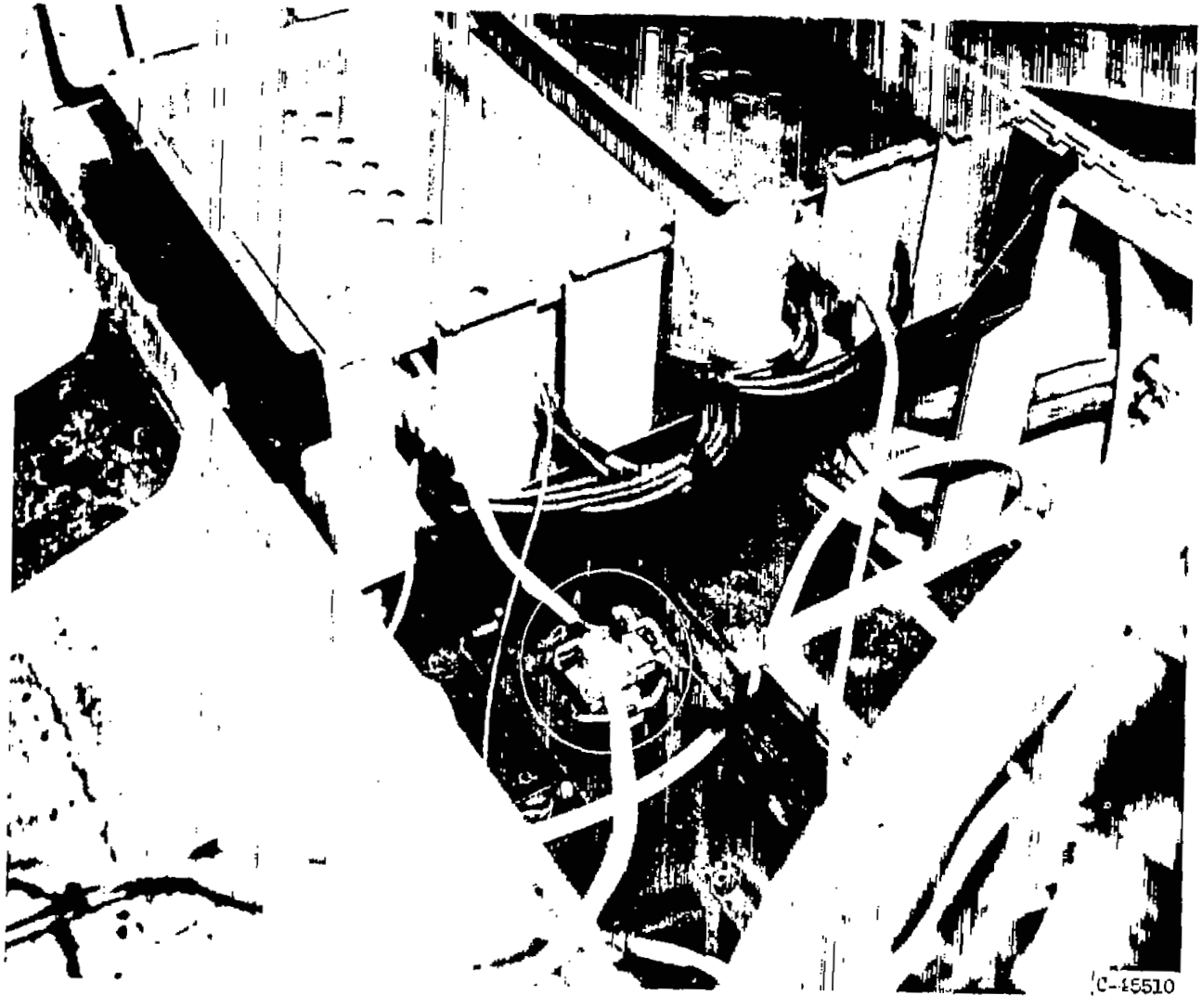


(c) Center of gravity.

Figure 9. - Concluded. Accelerometers installed in fighter airplane.


(a) Head.

Figure 10. - Accelerometers installed in anthropomorphic dummy.

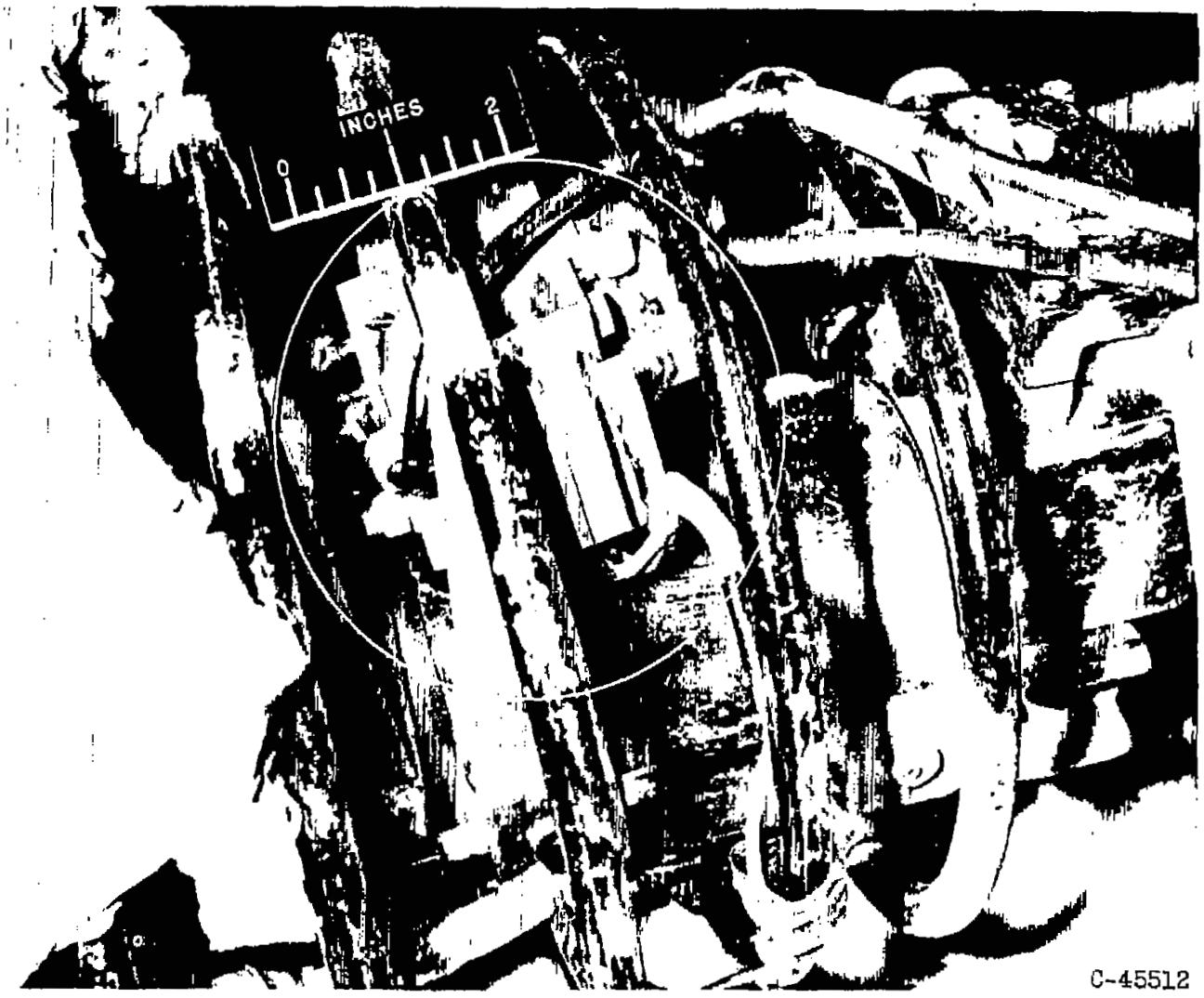


(b) Chest.

Figure 10. - Continued. Accelerometers installed in anthropomorphic dummy.

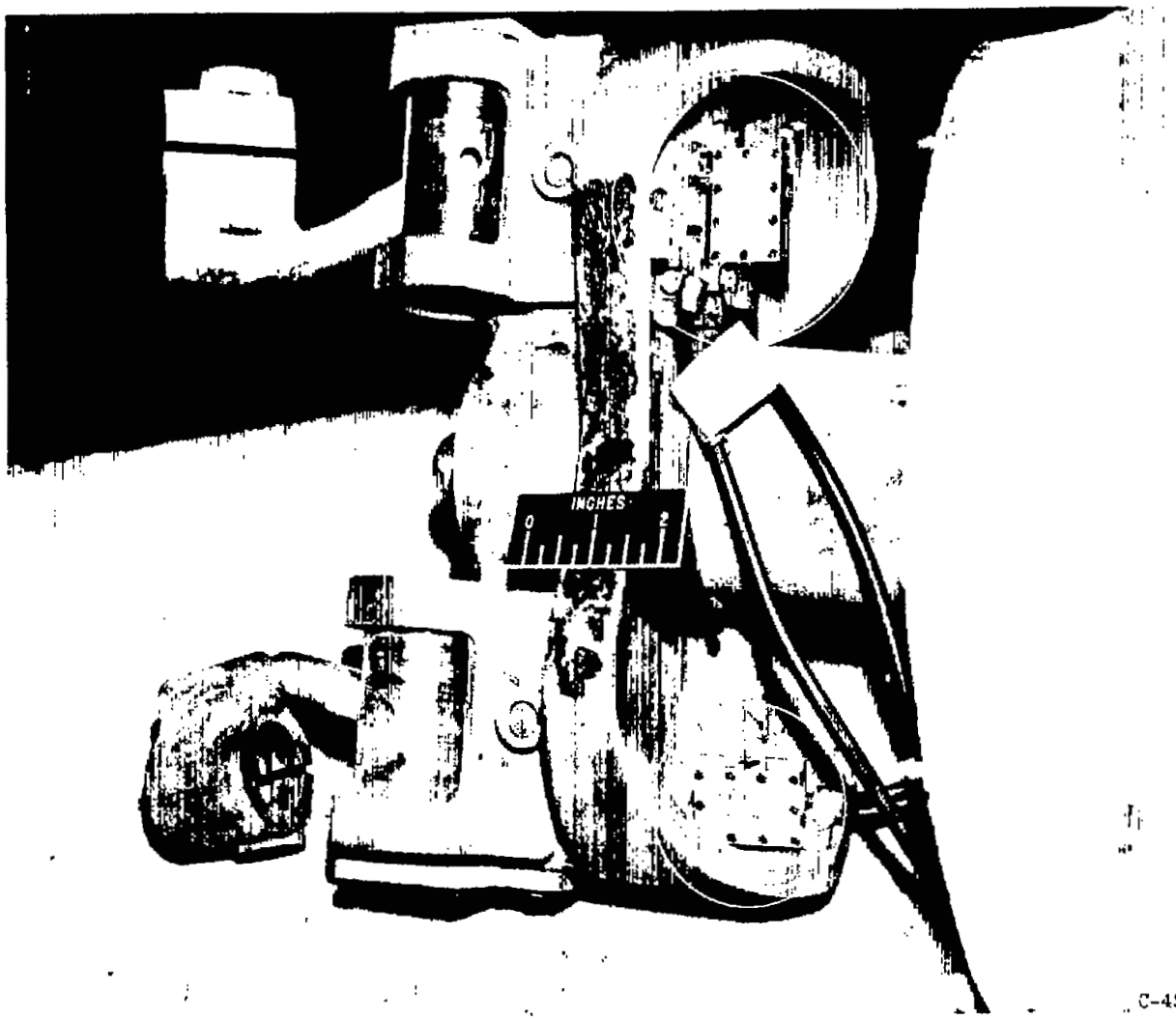


(c) Hips.

Figure 10. - Concluded. Accelerometers installed in anthropomorphic dummy.

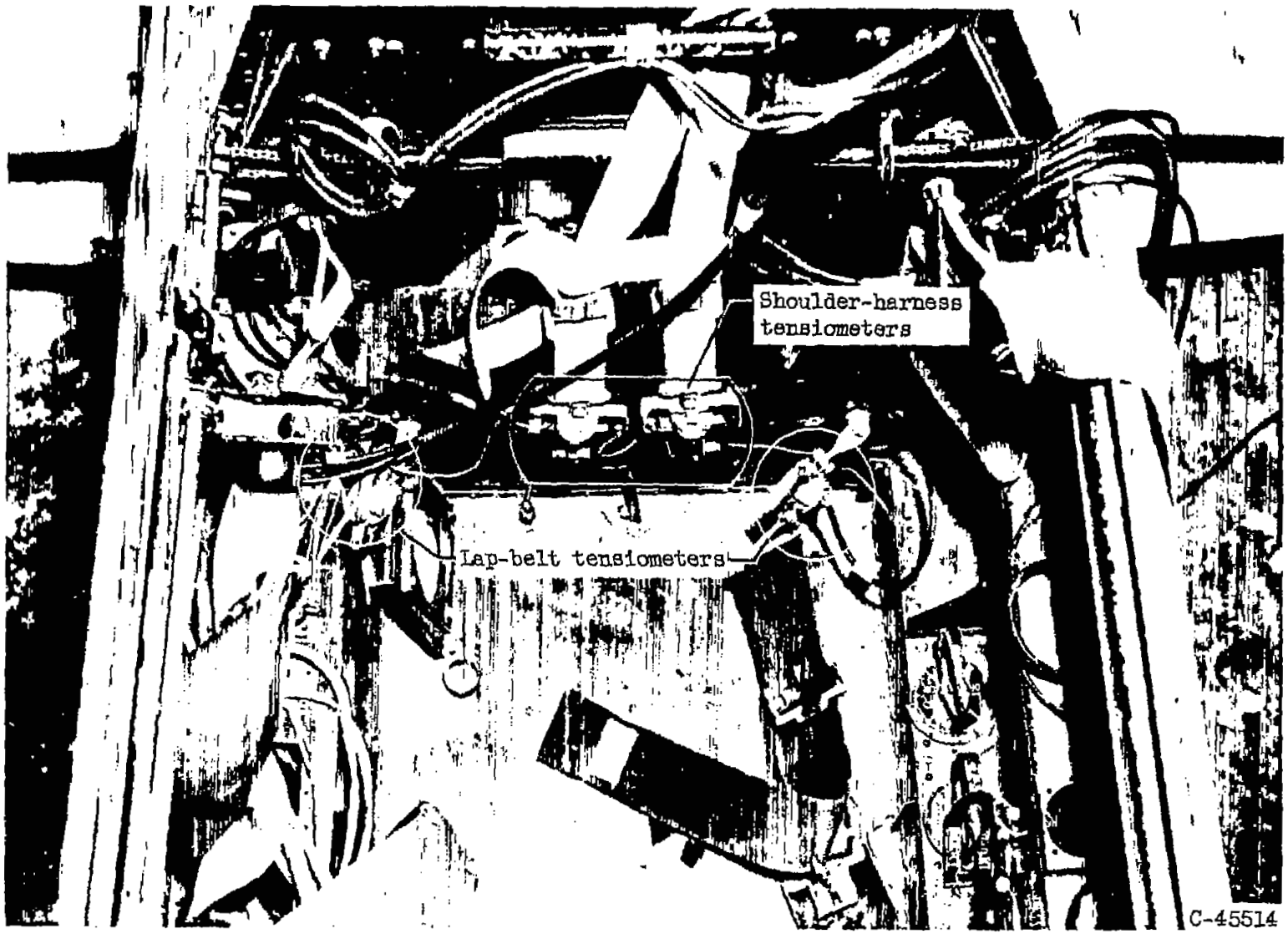


Figure 11. - Tensiometers installed on shoulder harness and lap belt.

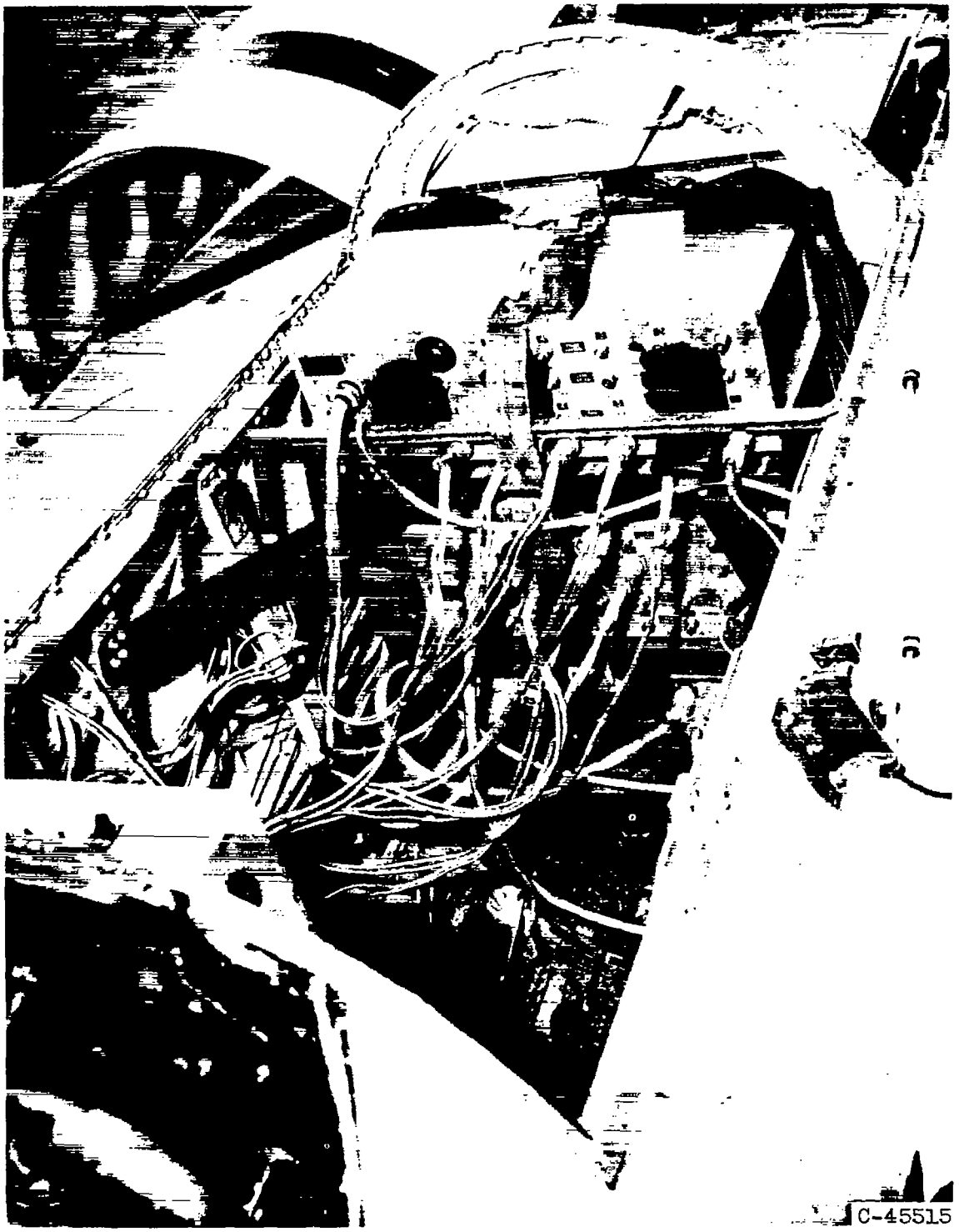


Figure 12. - Magnetic tape recorders installed in fighter airplane.

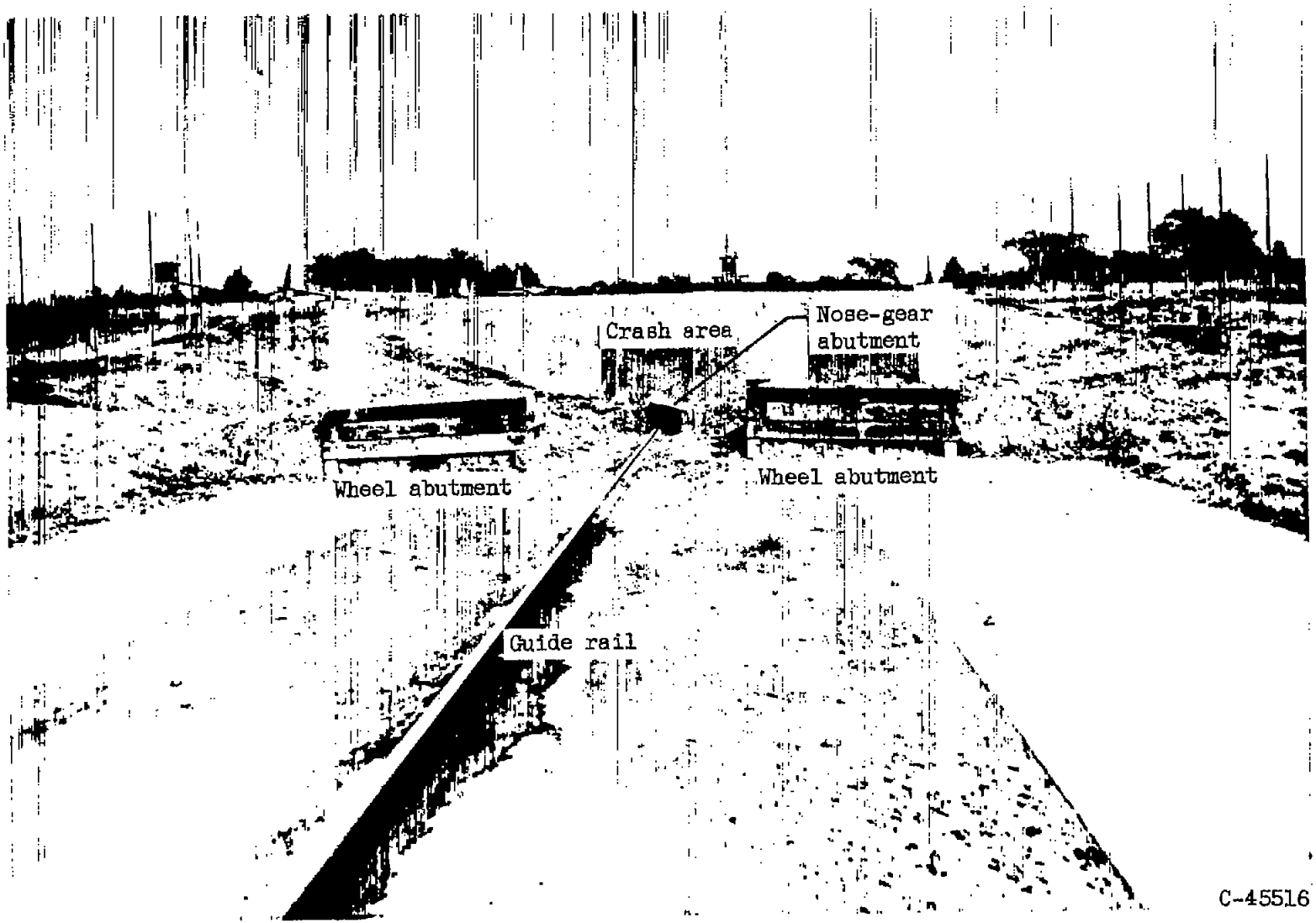


Figure 13. - Crash area used for unflared landing crashes showing wheel and nose-gear abutments.

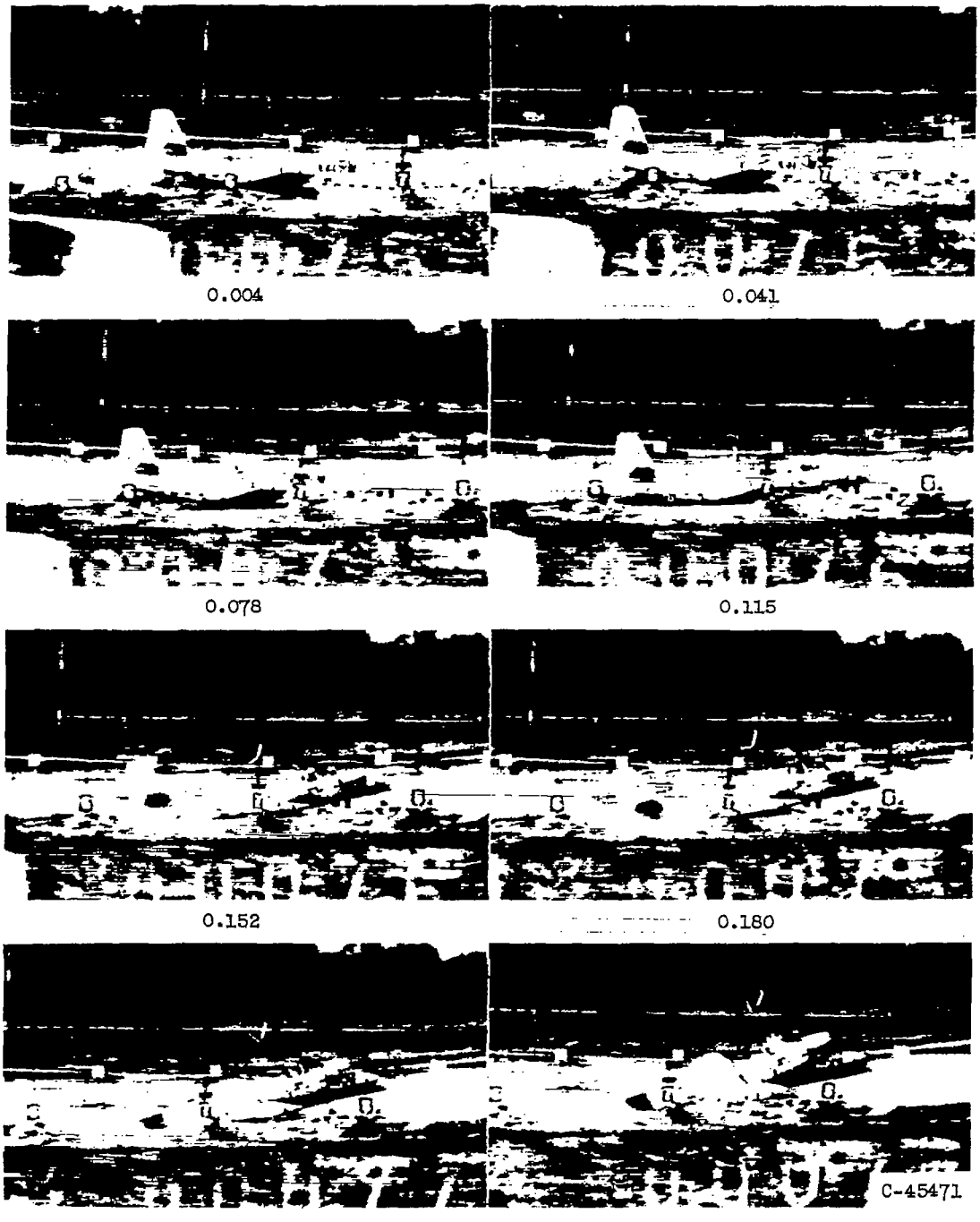


Time after nose impact with ground, sec

(a) 18°.

Figure 14. - Strip film from motion pictures of 18°, 22°, and 27° unflared landing crashes.

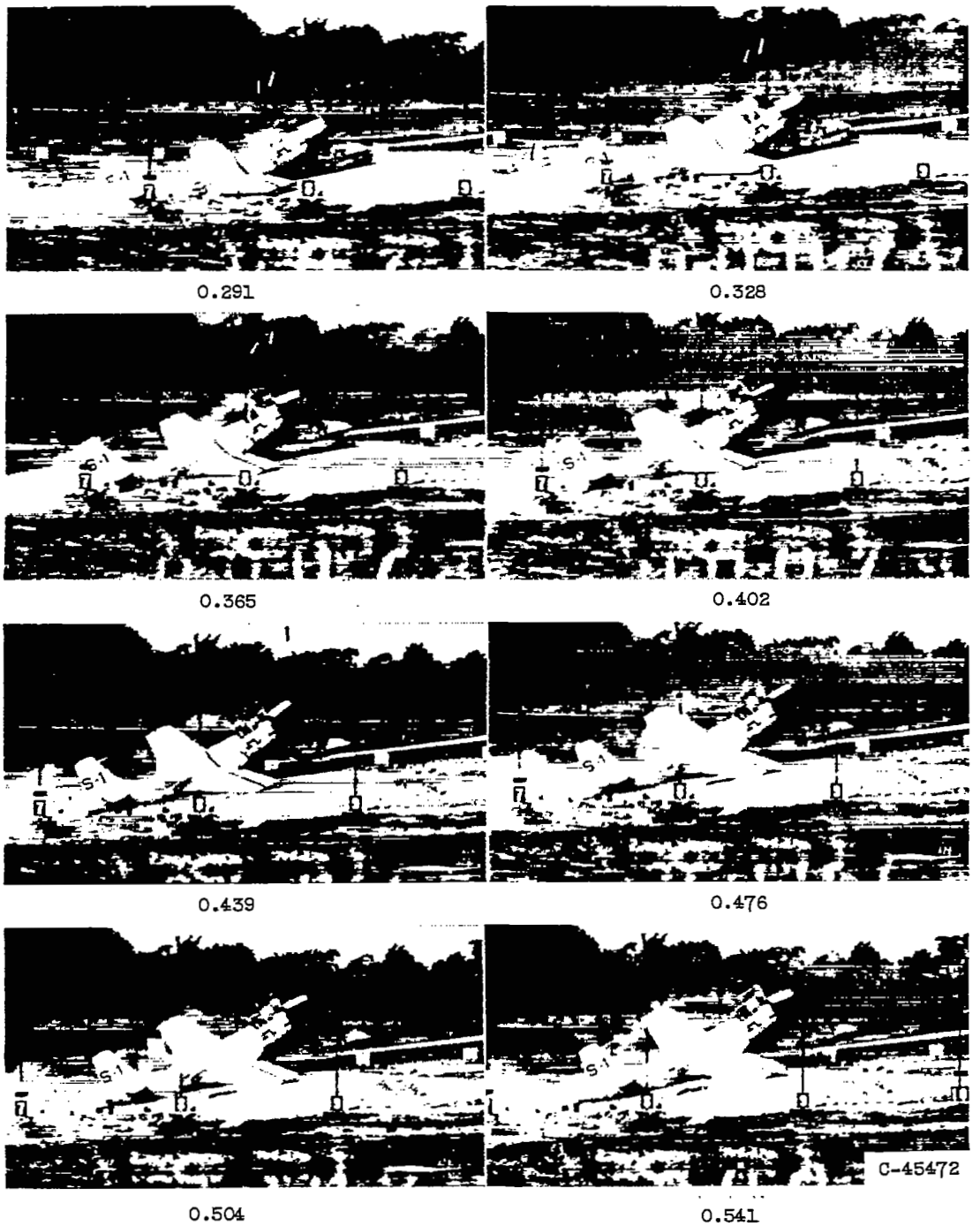


Time after nose impact with ground, sec

(a) Concluded. 18°.

Figure 14. - Continued. Strip film from motion pictures of 18°, 22°, and 27° unflared landing crashes.

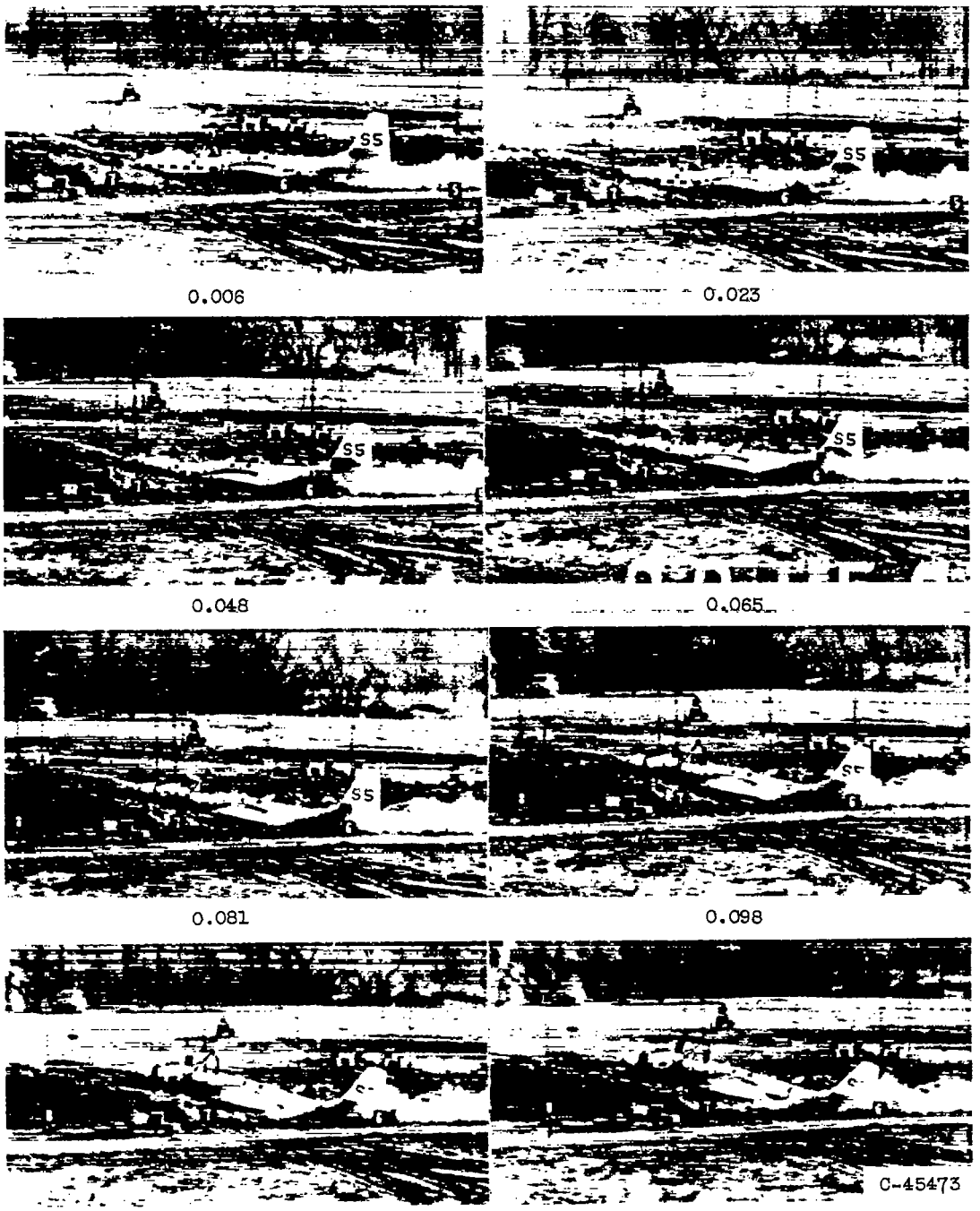


Time after nose impact with ground, sec

(b) 22°.

Figure 14. - Continued. Strip film from motion pictures of 18°, 22°, and 27° unflared landing crashes.

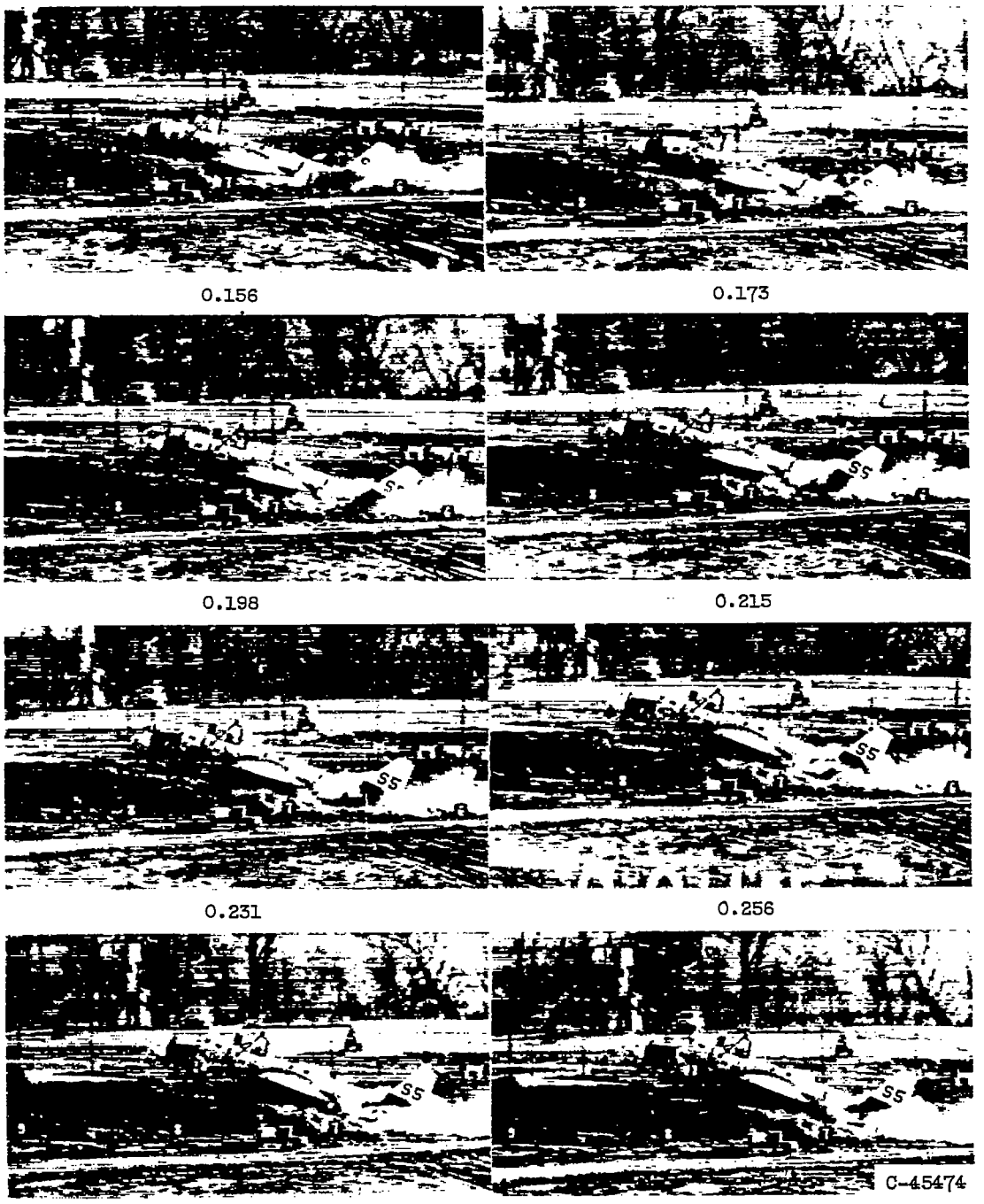


Time after nose impact with ground, sec

(b) Concluded. 22°.

Figure 14. - Continued. Strip film from motion pictures of 18°, 22°, and 27° unflared landing crashes.

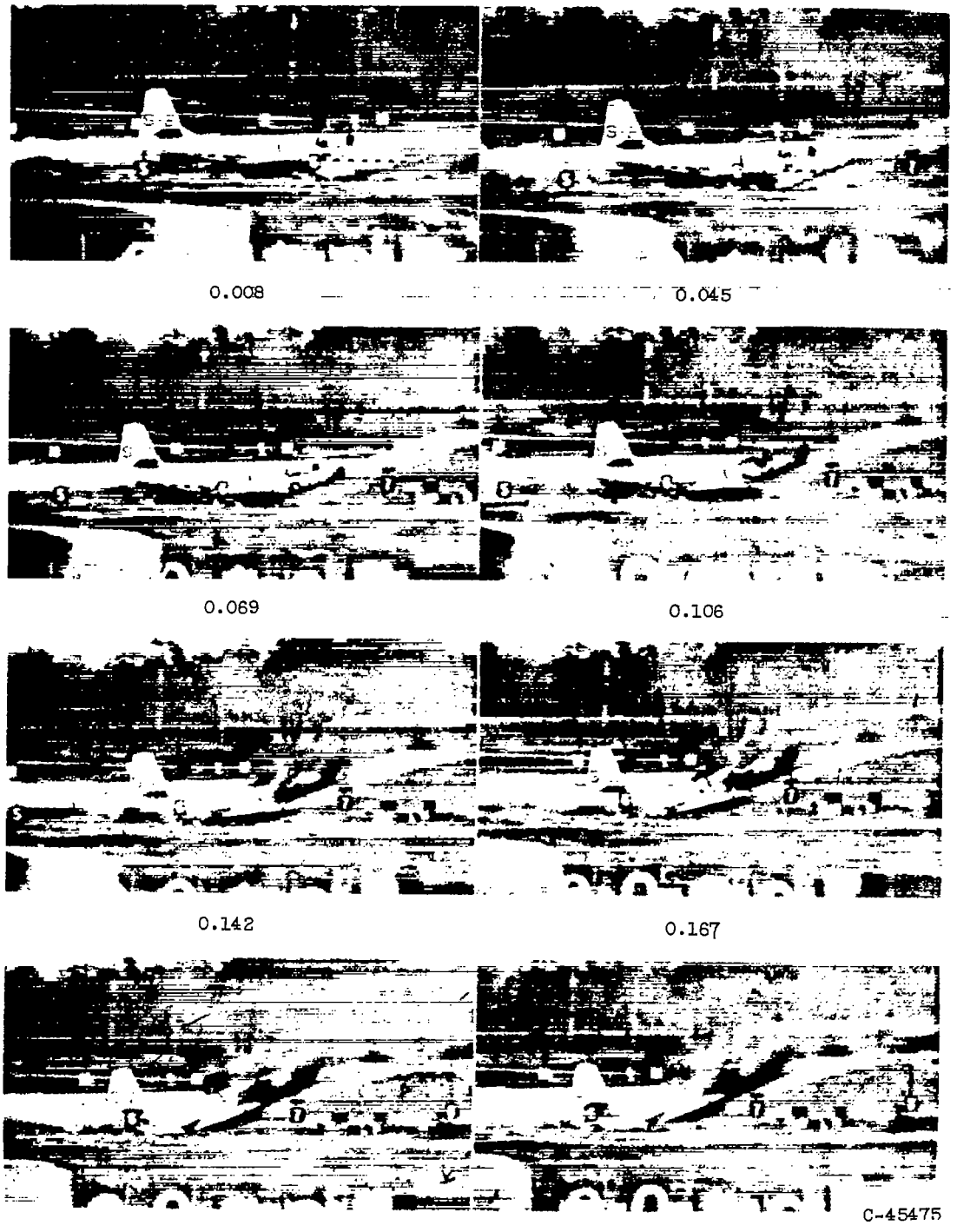


Time after nose impact with ground, sec

(c) 27°.

Figure 14. - Continued. Strip film from motion pictures of 18°, 22°, and 27° unflared landing crashes.

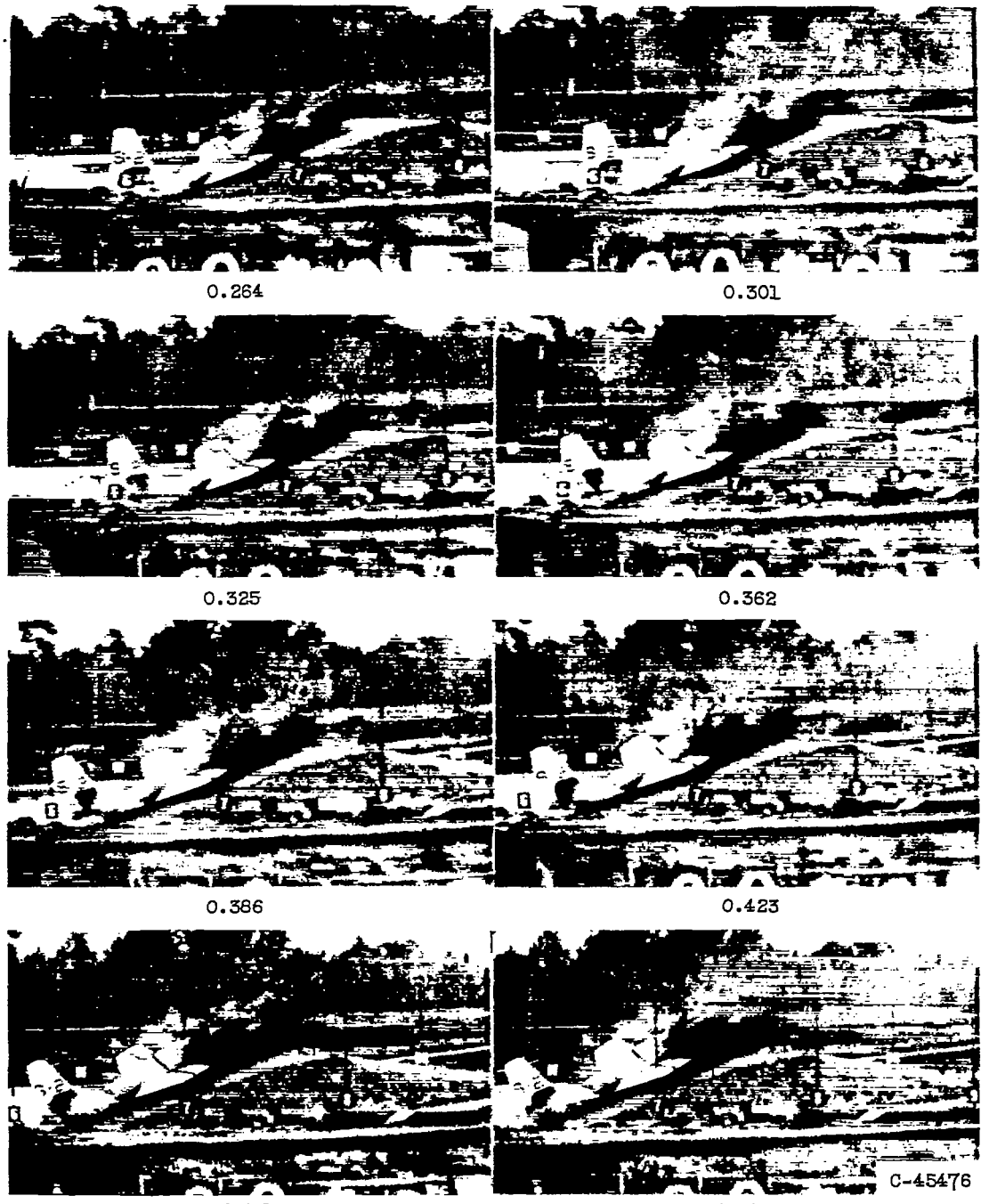


Time after nose impact with ground, sec

(c) Concluded. 27°.

Figure 14. - Concluded. Strip film from motion pictures of 18°, 22°, and 27° unflared landing crashes.

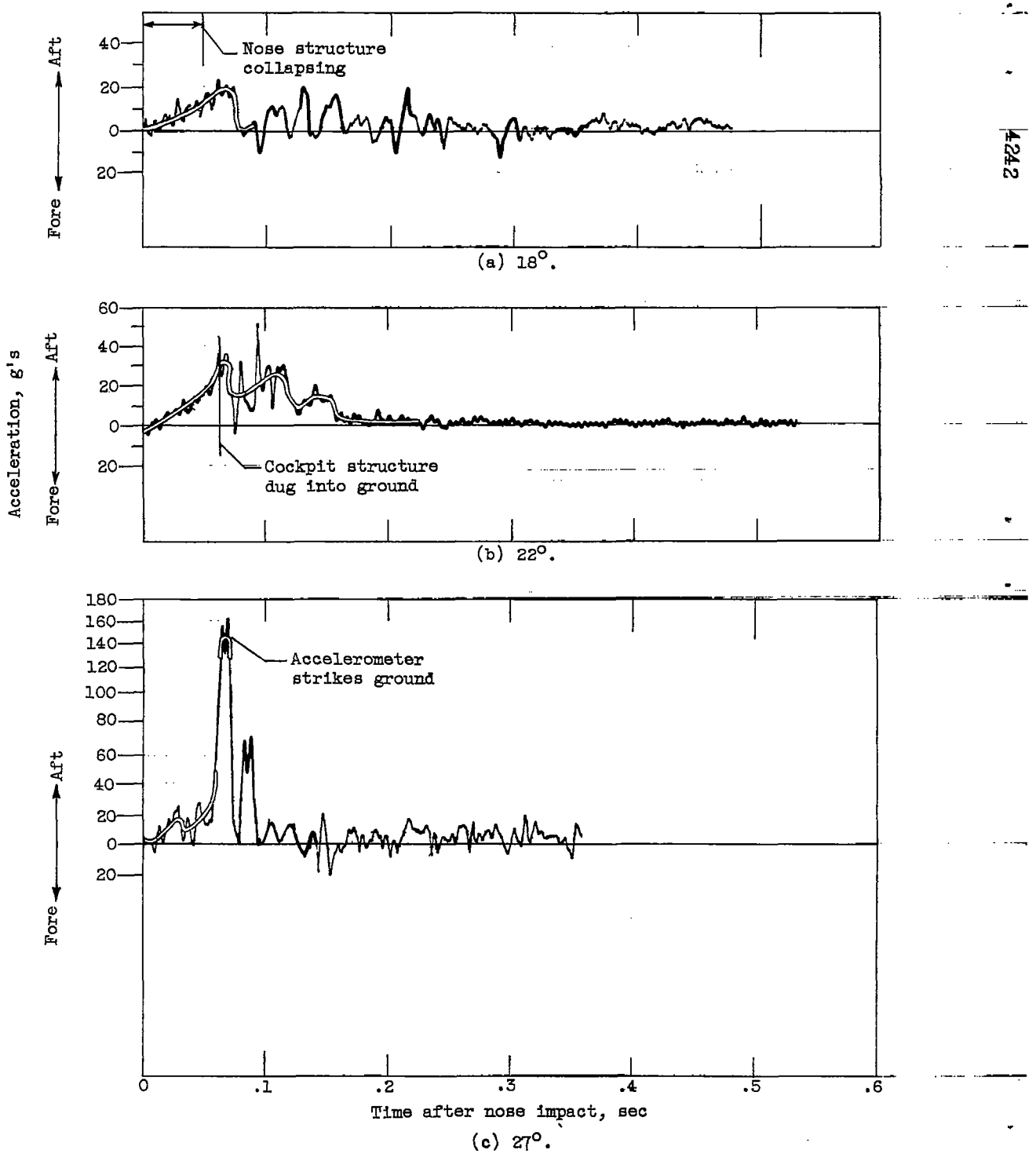


Figure 15. - Longitudinal acceleration of cockpit floor in unflared landing crashes of fighter airplane.

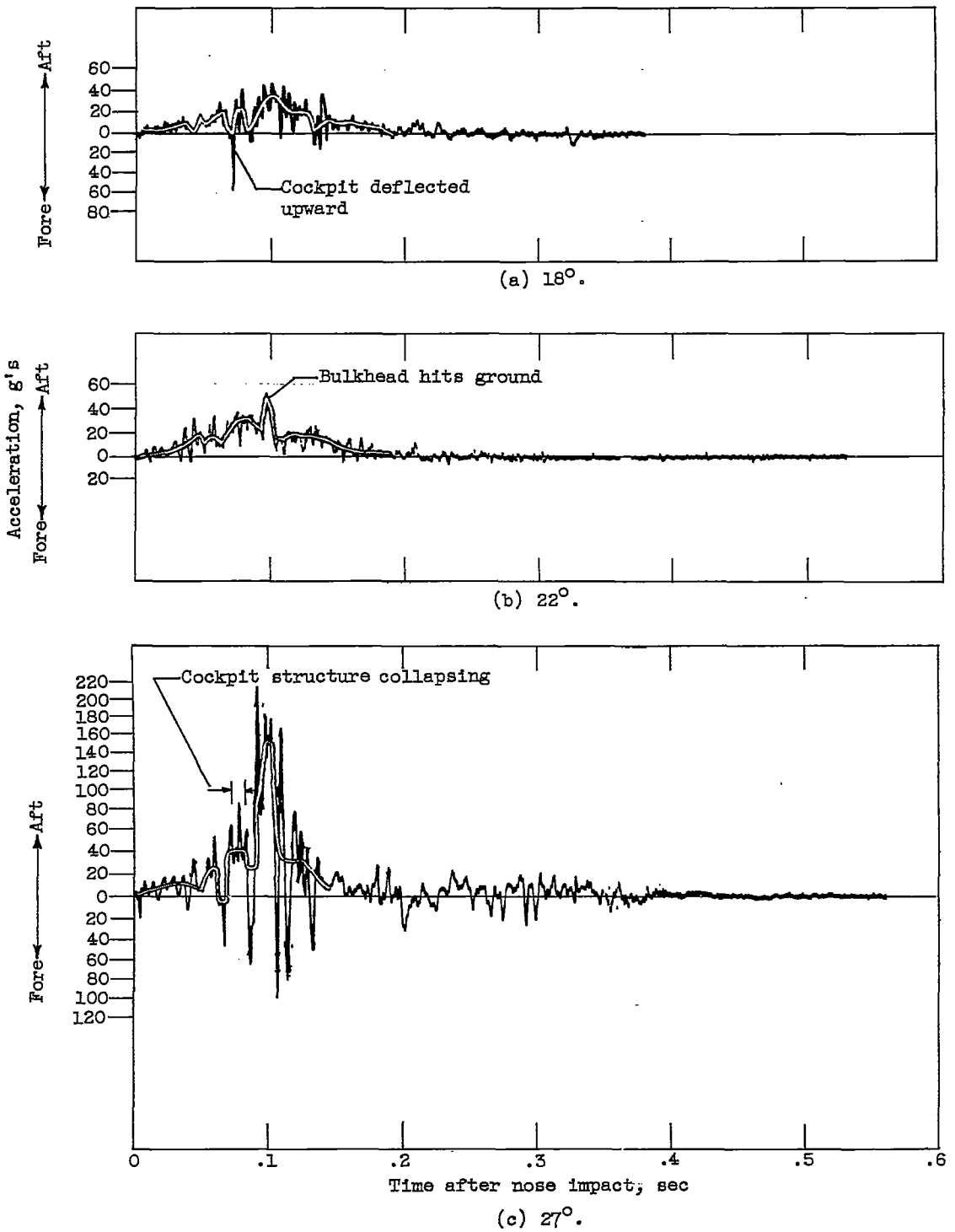


Figure 16. - Longtudinal acceleration of bulkhead at rear of cockpit in unflared landing crashes of fighter airplane.

Figure 17. - Extent of damage to structure and skin in cockpit area after 22° unflared landing crash.


Figure 18. - Cockpit of jet fighter after 22° unflared landing crash.

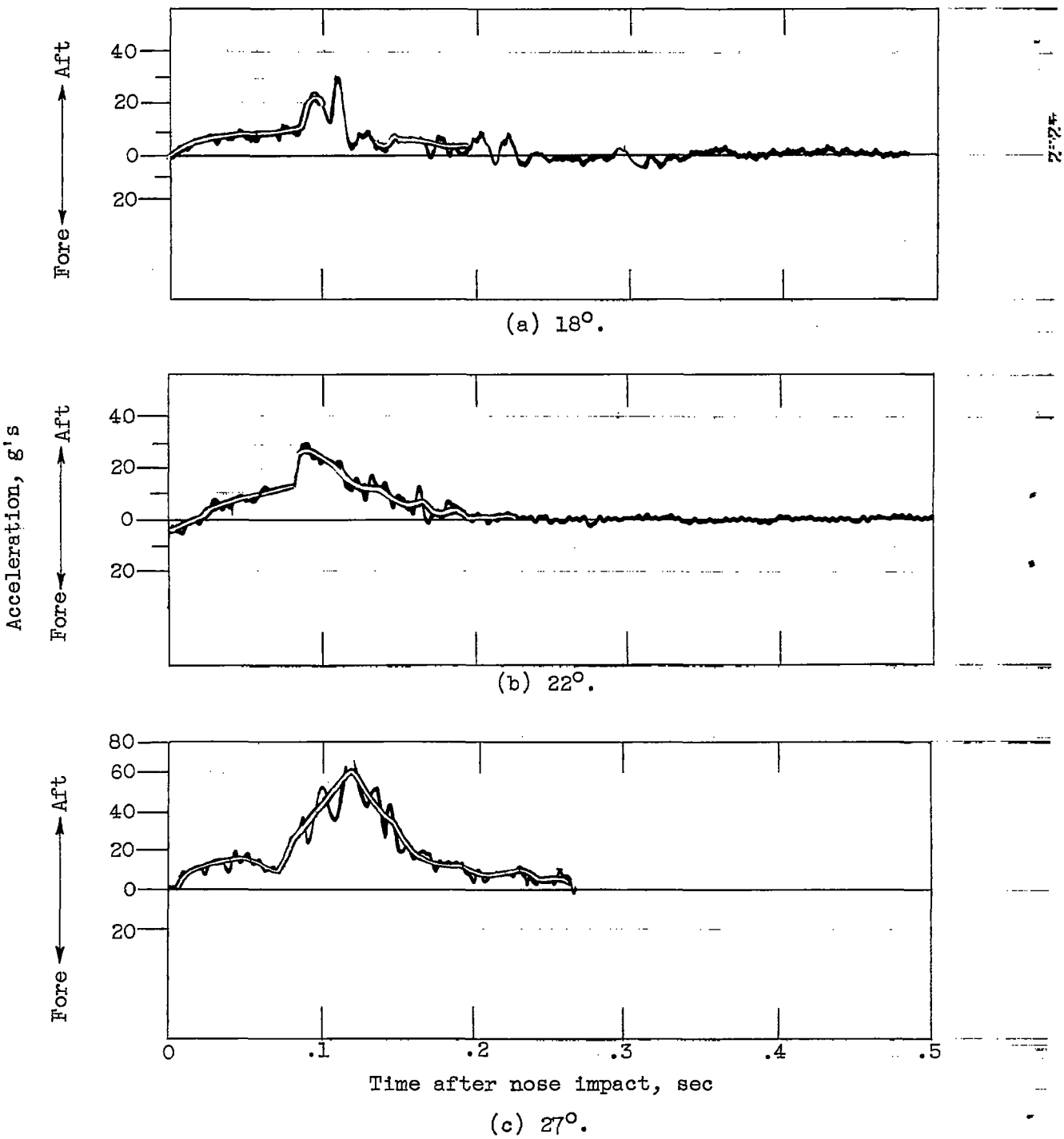


Figure 19. - Longitudinal acceleration of airplane center of gravity in unflared landing crashes of fighter airplane.

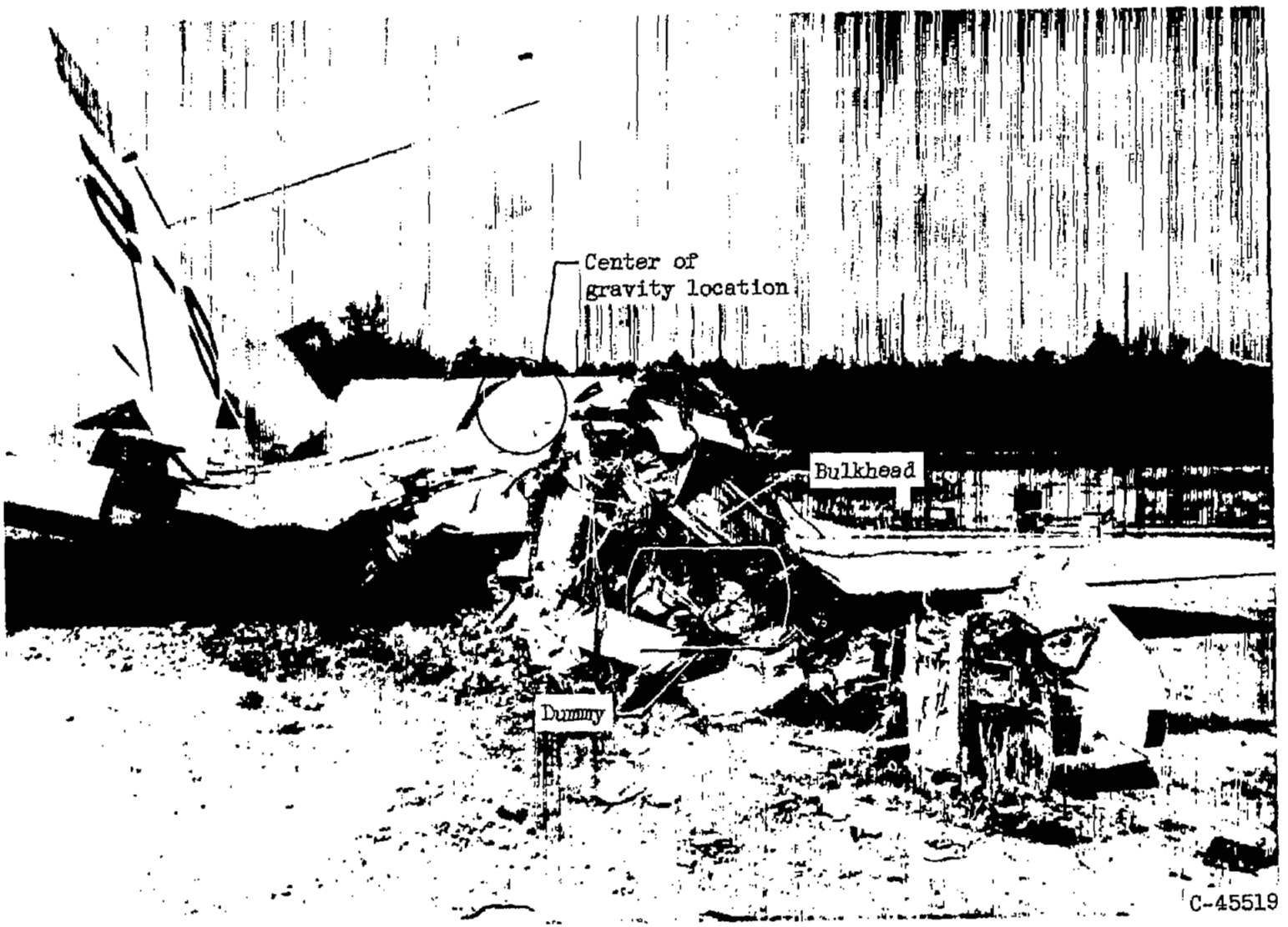


Figure 20. - Extent of damage to fighter airplane after 27° unflared landing crash.

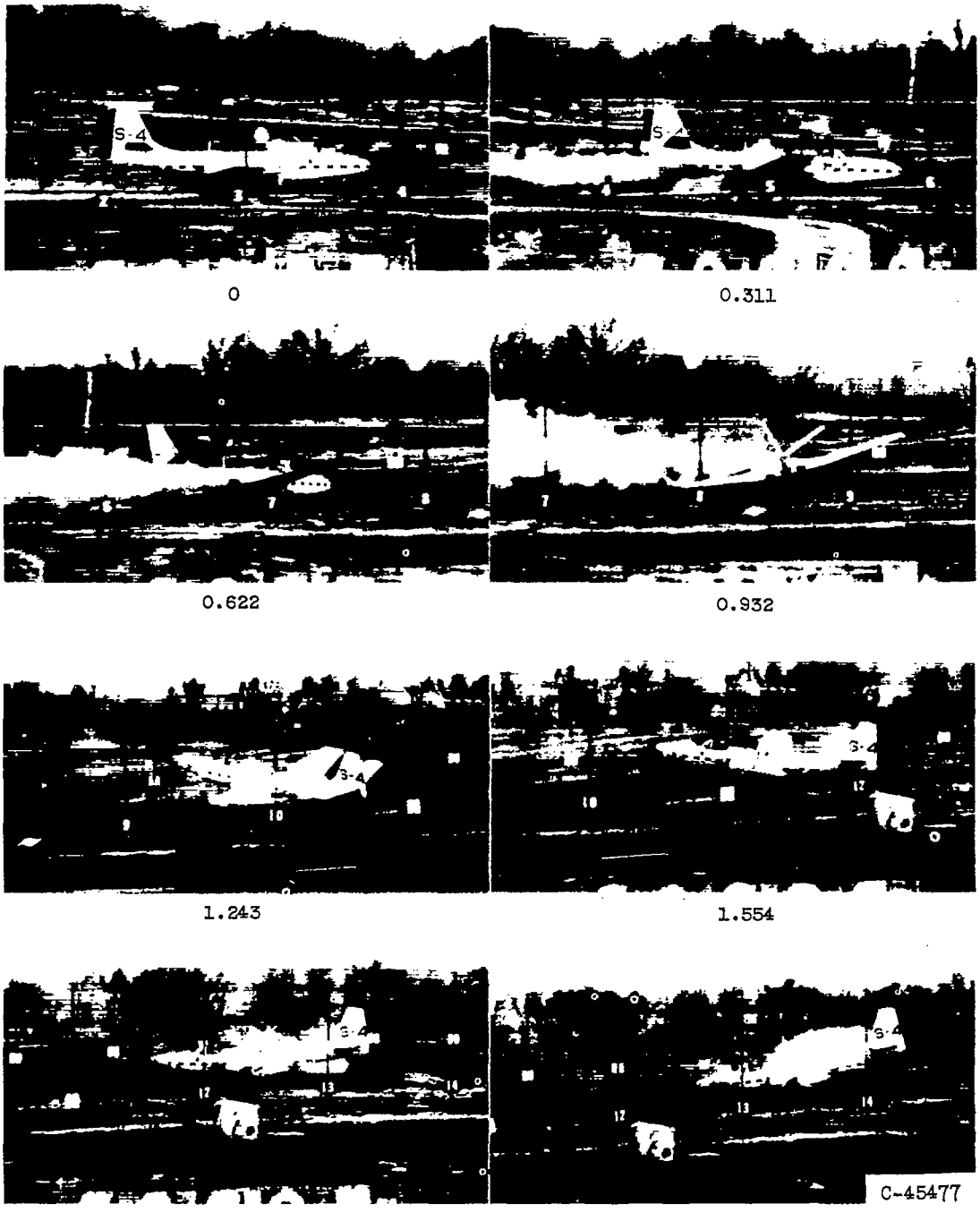


Time after wheel abutment impact, sec

(a) 0 to 2.165 seconds.

Figure 21. - Strip film from motion pictures of ground-loop crash.

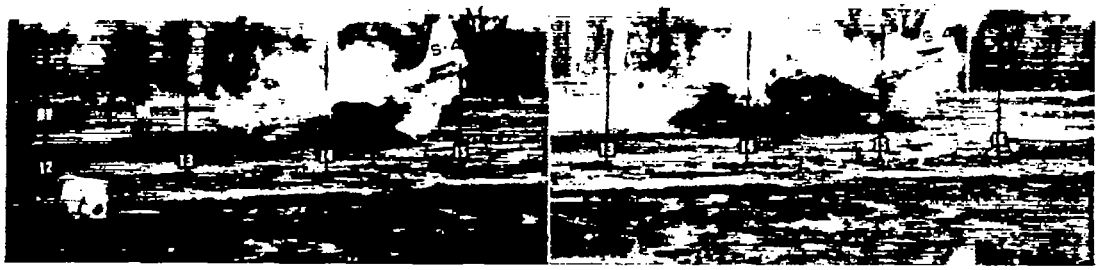

2.475 2.786

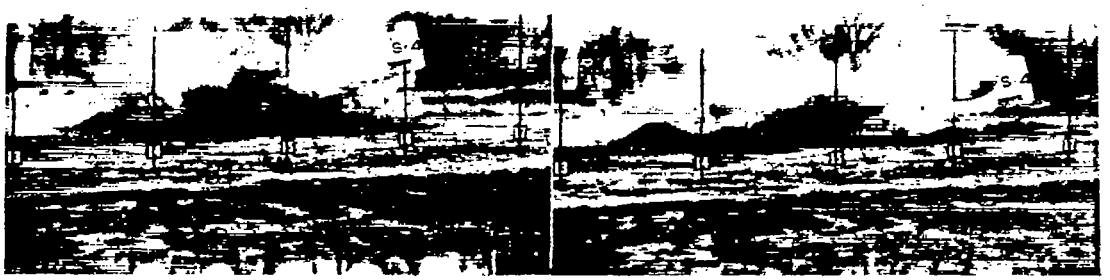

3.097 3.408

3.719 4.029


4.340 4.651

Time after wheel abutment impact, sec

(b) 2.475 to 4.651 seconds.

Figure 21. - Concluded. Strip film from motion pictures of ground-loop crash.

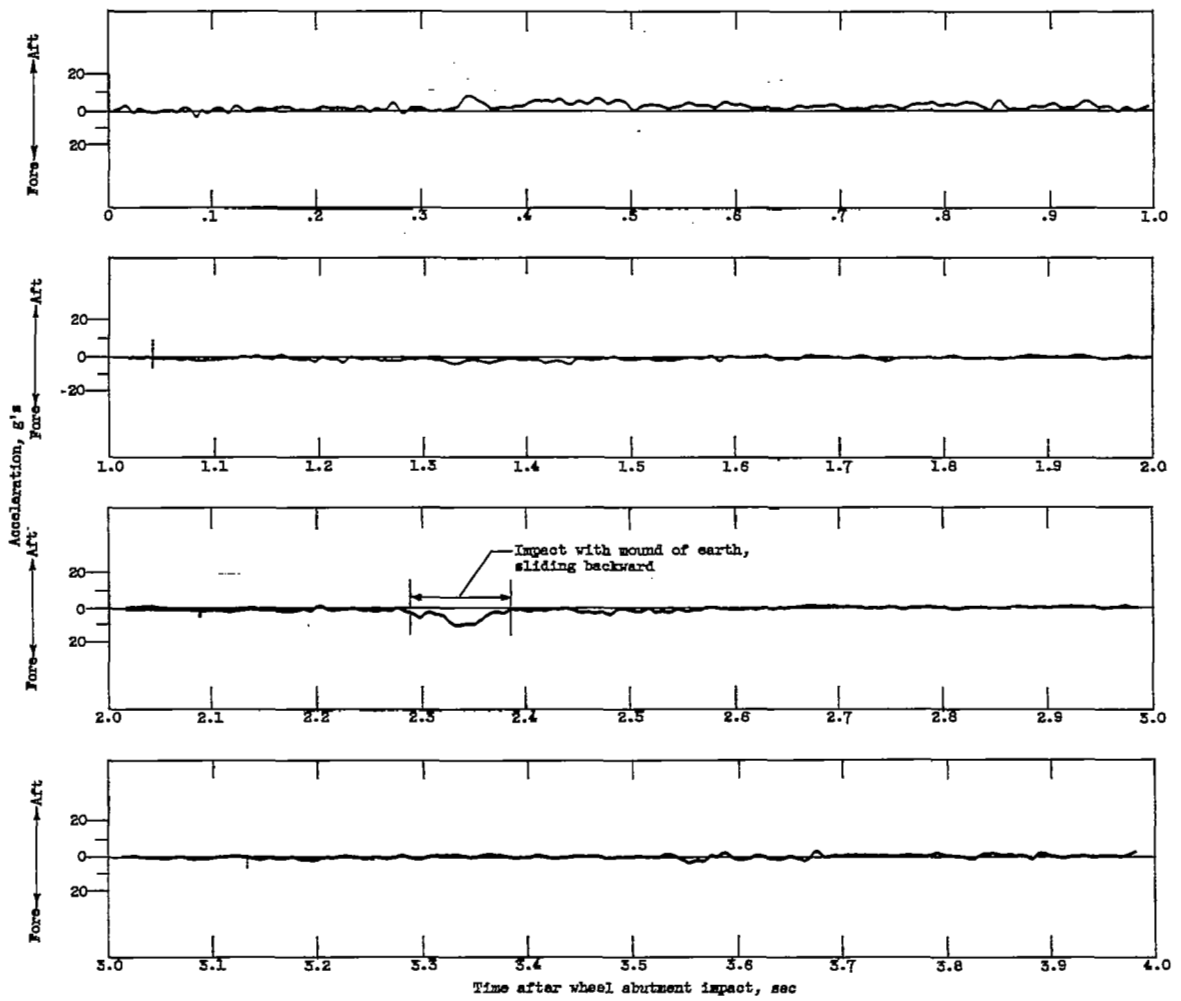


(a) Longitudinal.

Figure 23. - Acceleration of cockpit floor during ground-loop crash of fighter airplane.

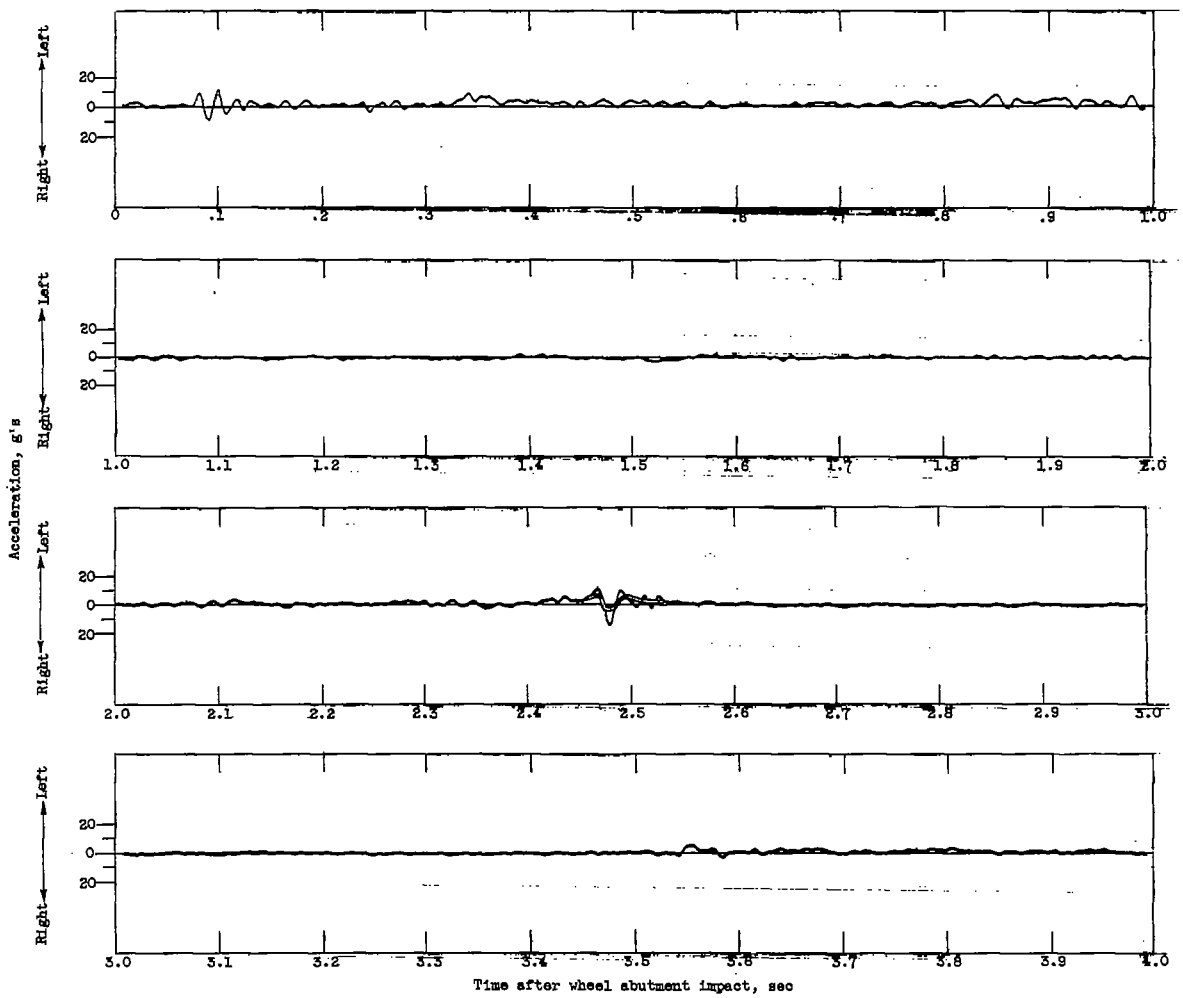


(b) Lateral.

Figure 23. - Concluded. Acceleration of cockpit floor during ground-loop crash of fighter airplane.

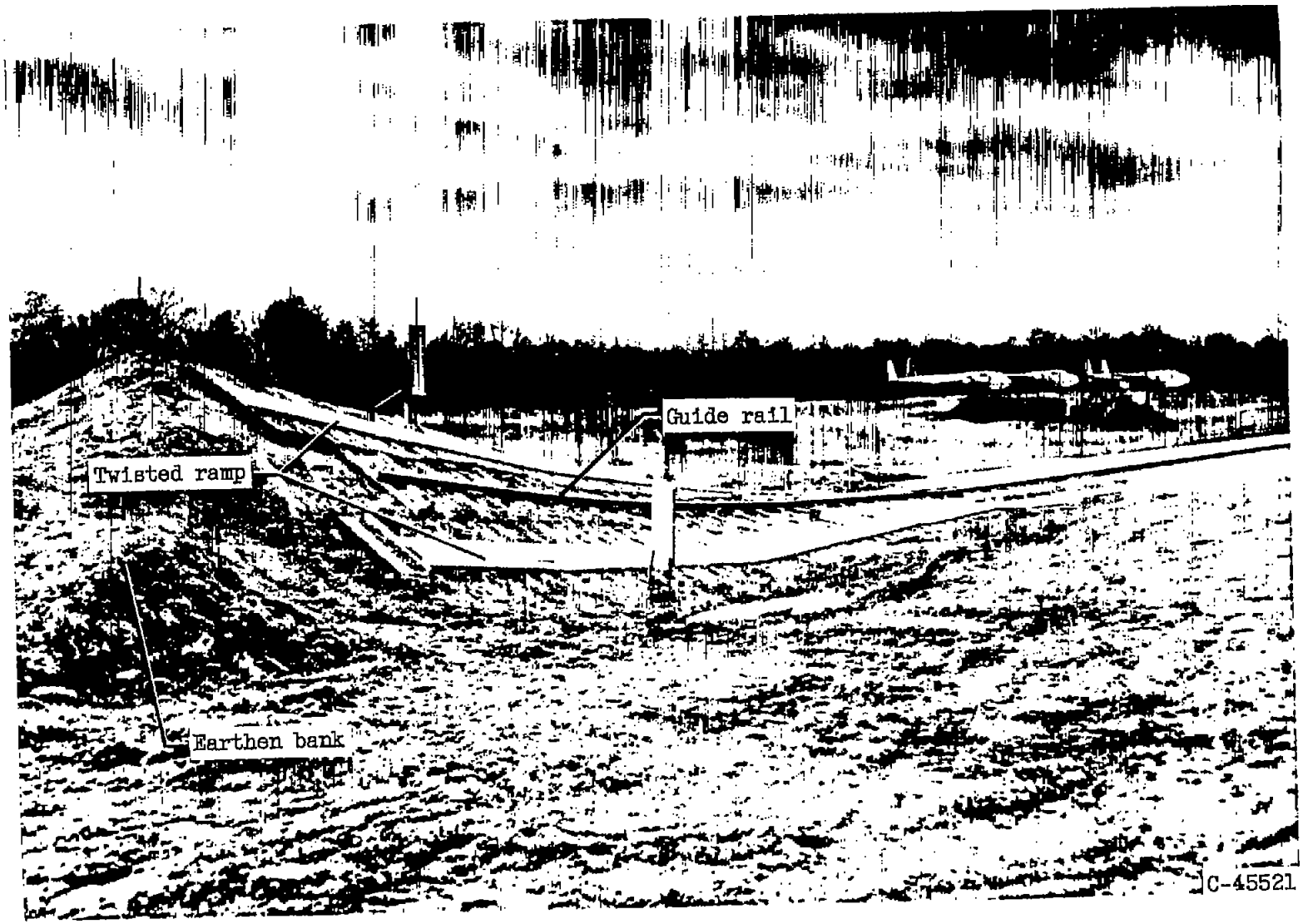


Figure 24. - Ramp designed to cart-wheel airplane entering crash area.

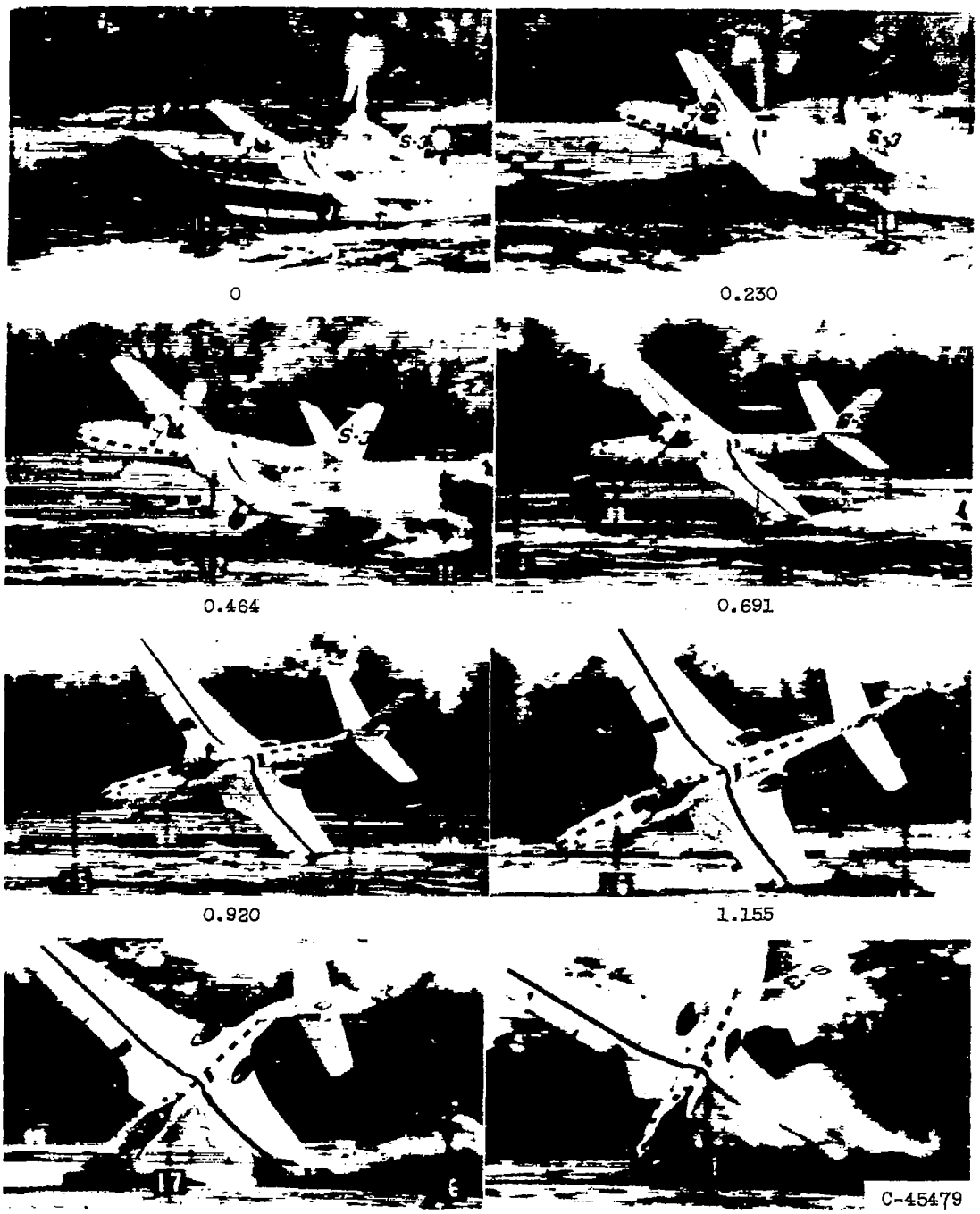


Time after nose gear left guide rail, sec

(a) 0 to 1.618 seconds.

Figure 25. - Strip film from motion pictures of cart-wheel crash of fighter airplane.

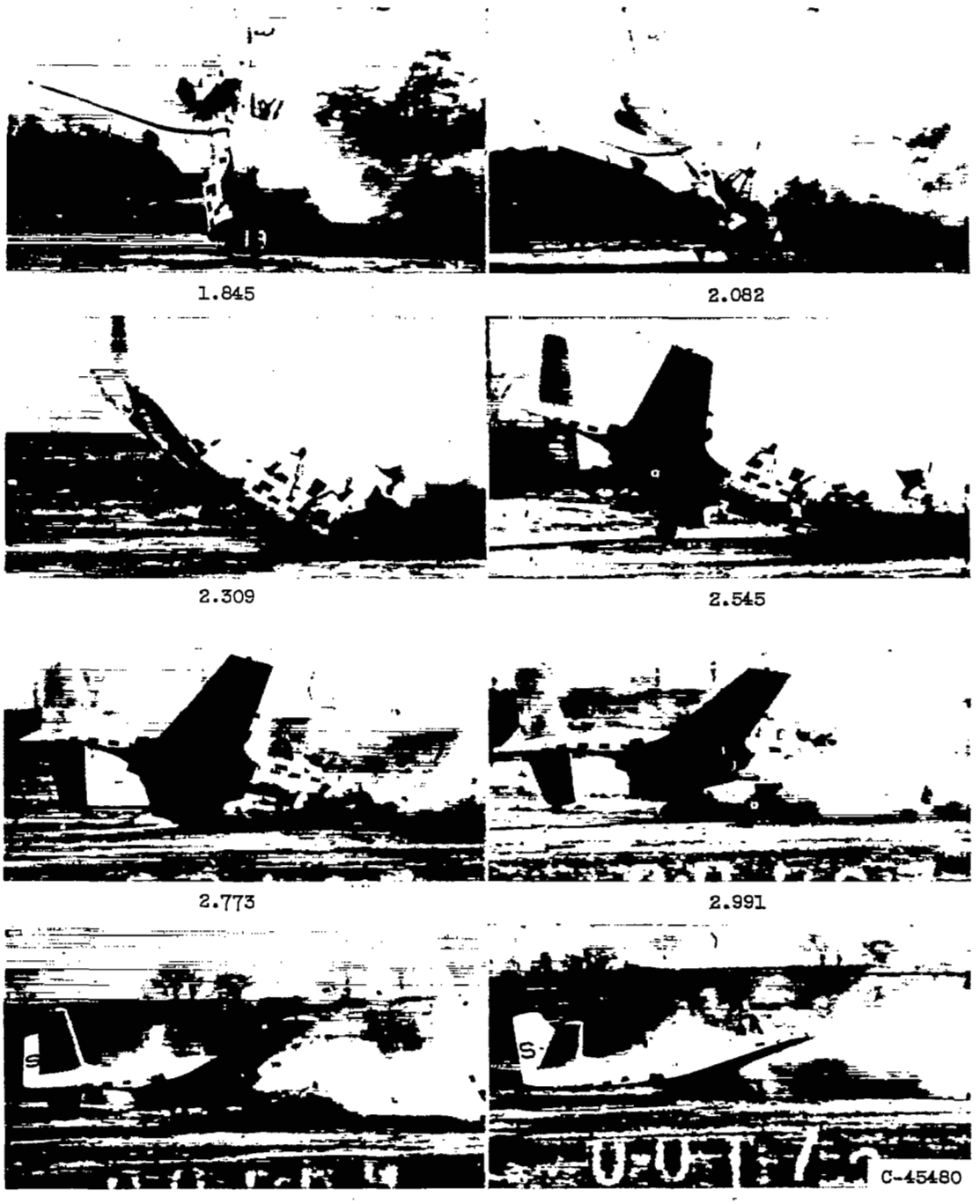


Time after nose gear left guide rail, sec

(b) 1.845 to 3.460 seconds.

Figure 25. - Concluded. Strip film from motion pictures of cart-wheel crash of fighter airplane.

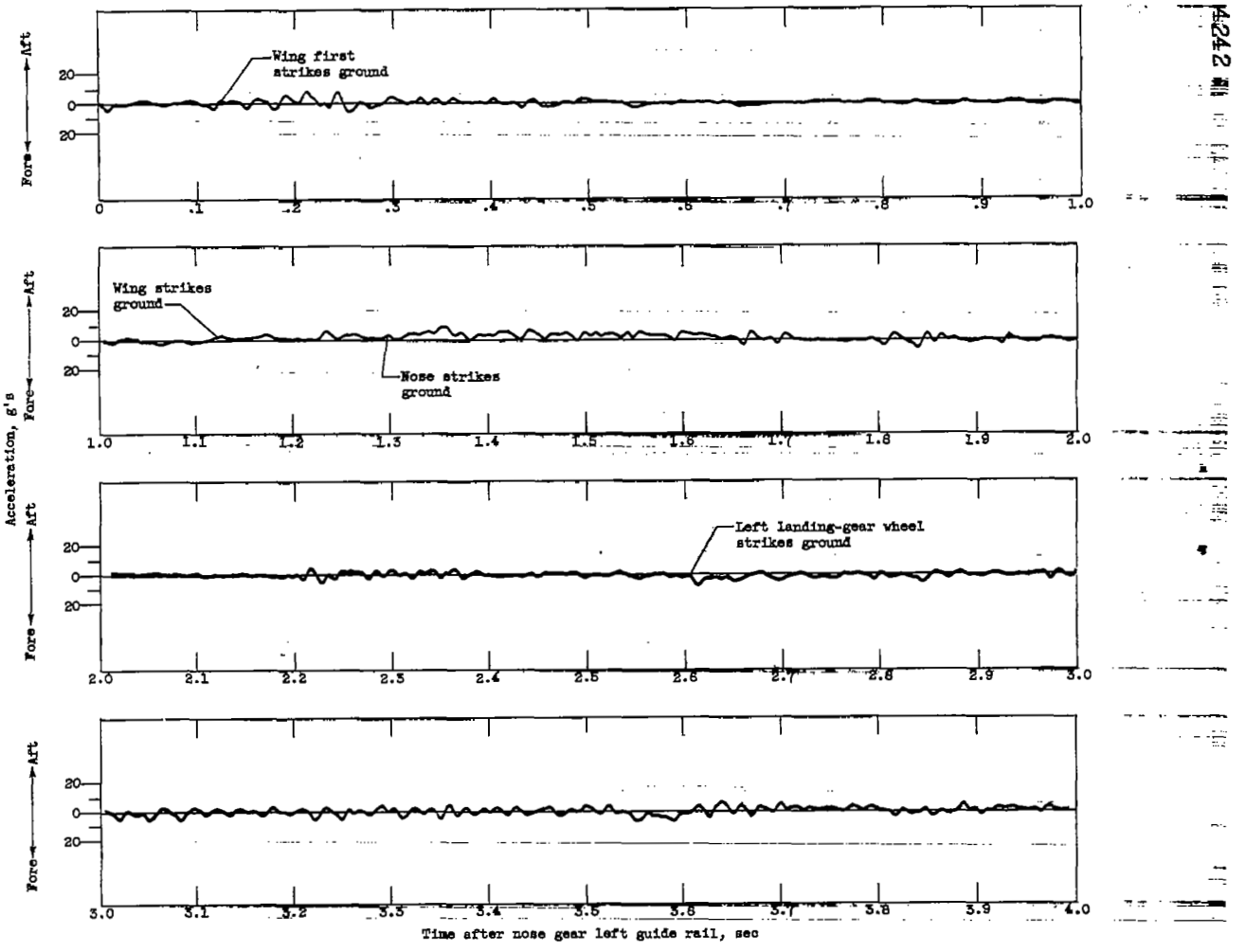


(a) Longitudinal.

Figure 26. - Acceleration of cockpit floor during cart-wheel crash of fighter airplane.

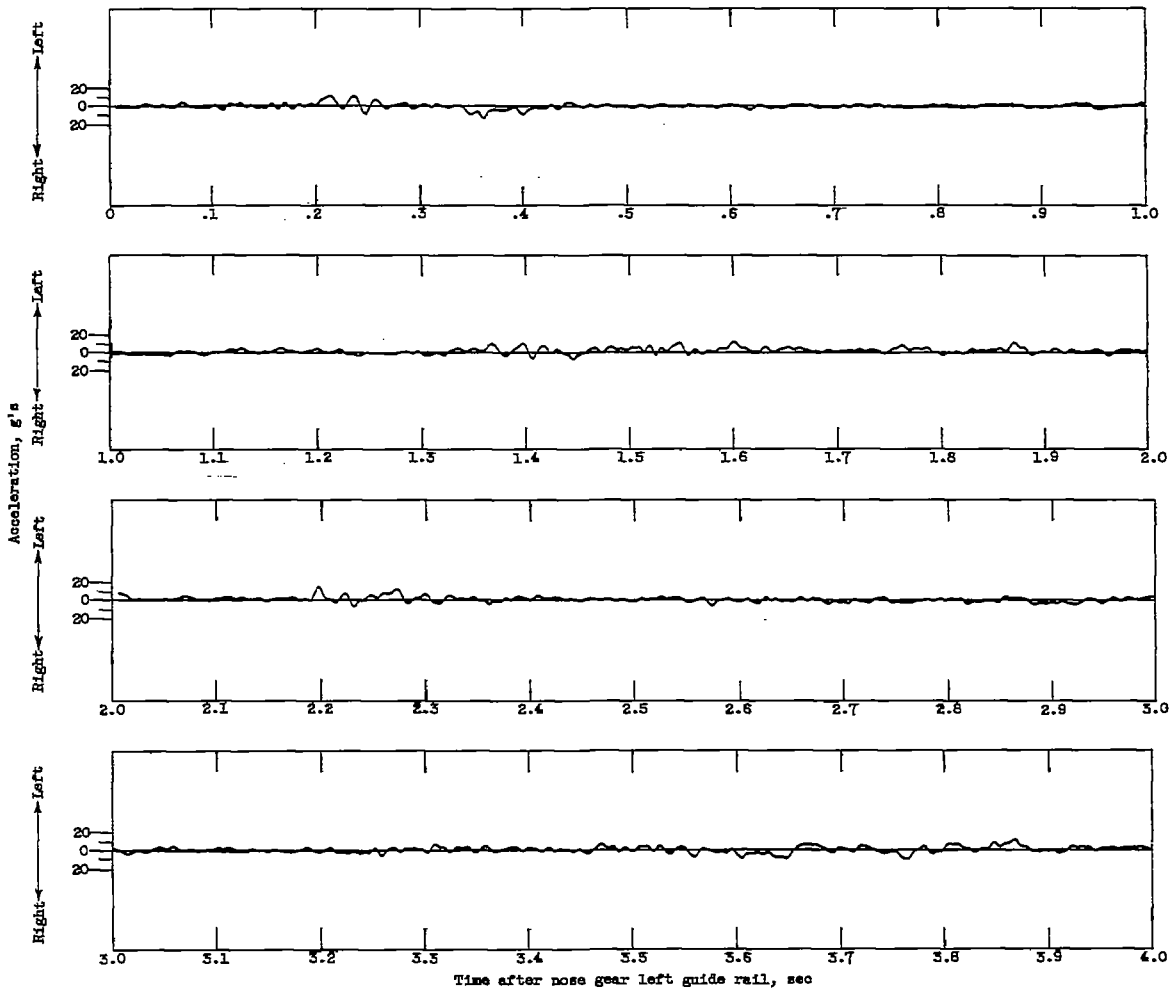


(b) Lateral.

Figure 26. - Concluded. Acceleration of cockpit floor during cart-wheel crash of fighter airplane.

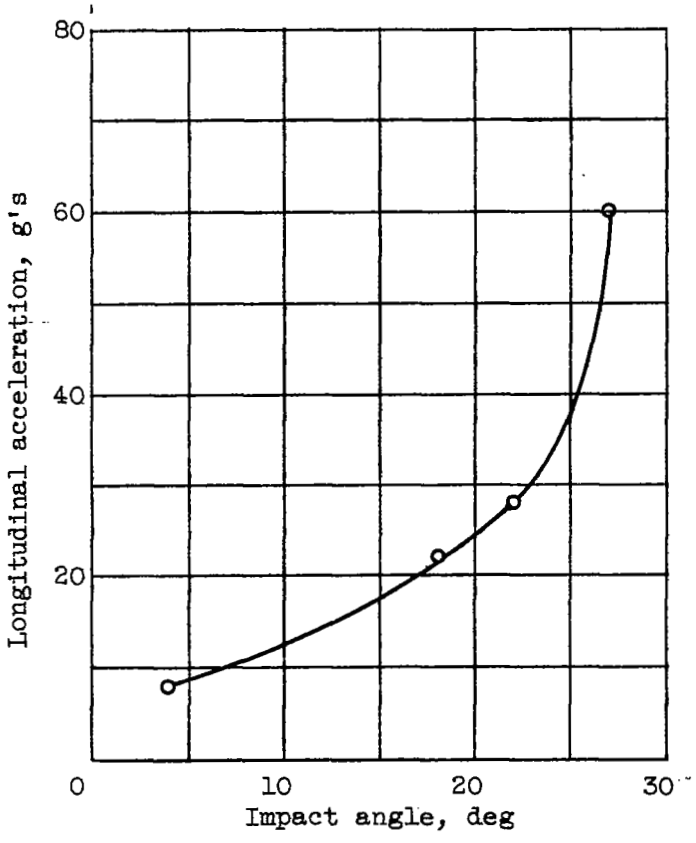


Figure 27. - Relation between maximum longitudinal acceleration of airplane at center of gravity and impact angle during crashes of fighter airplane.

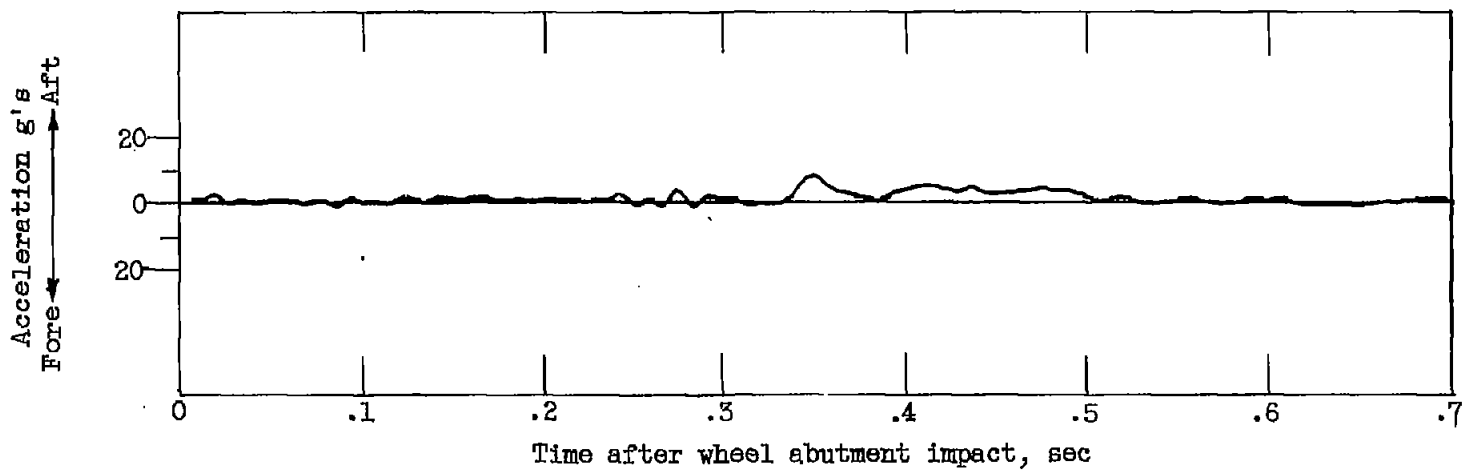


Figure 28.- Longitudinal acceleration of airplane center of gravity for initial impact during $4^{o}$ ground-loop crash.

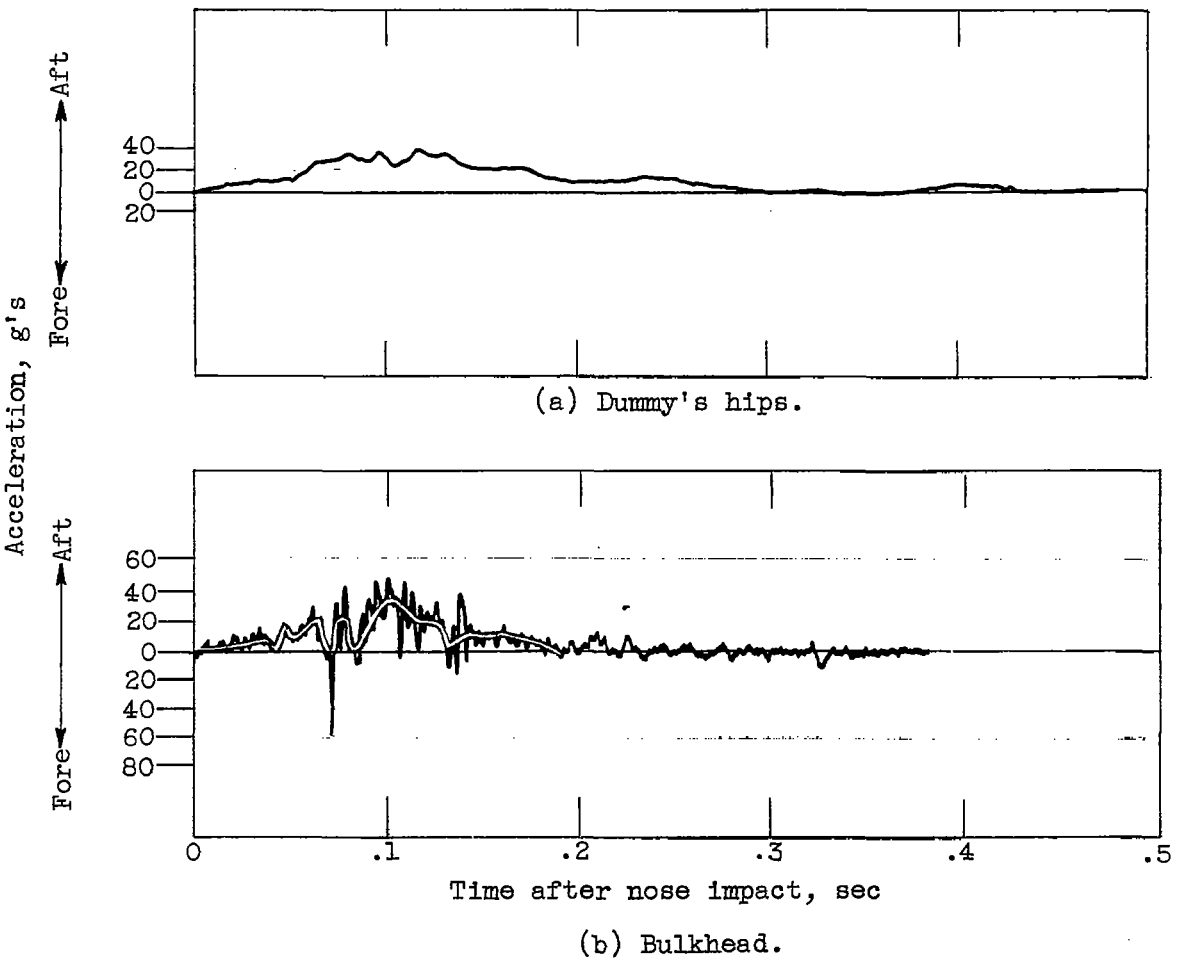


Figure 29. - Comparison of longitudinal acceleration of dummy's hips with that of bulkhead in 18° unflared landing crash of fighter airplane.

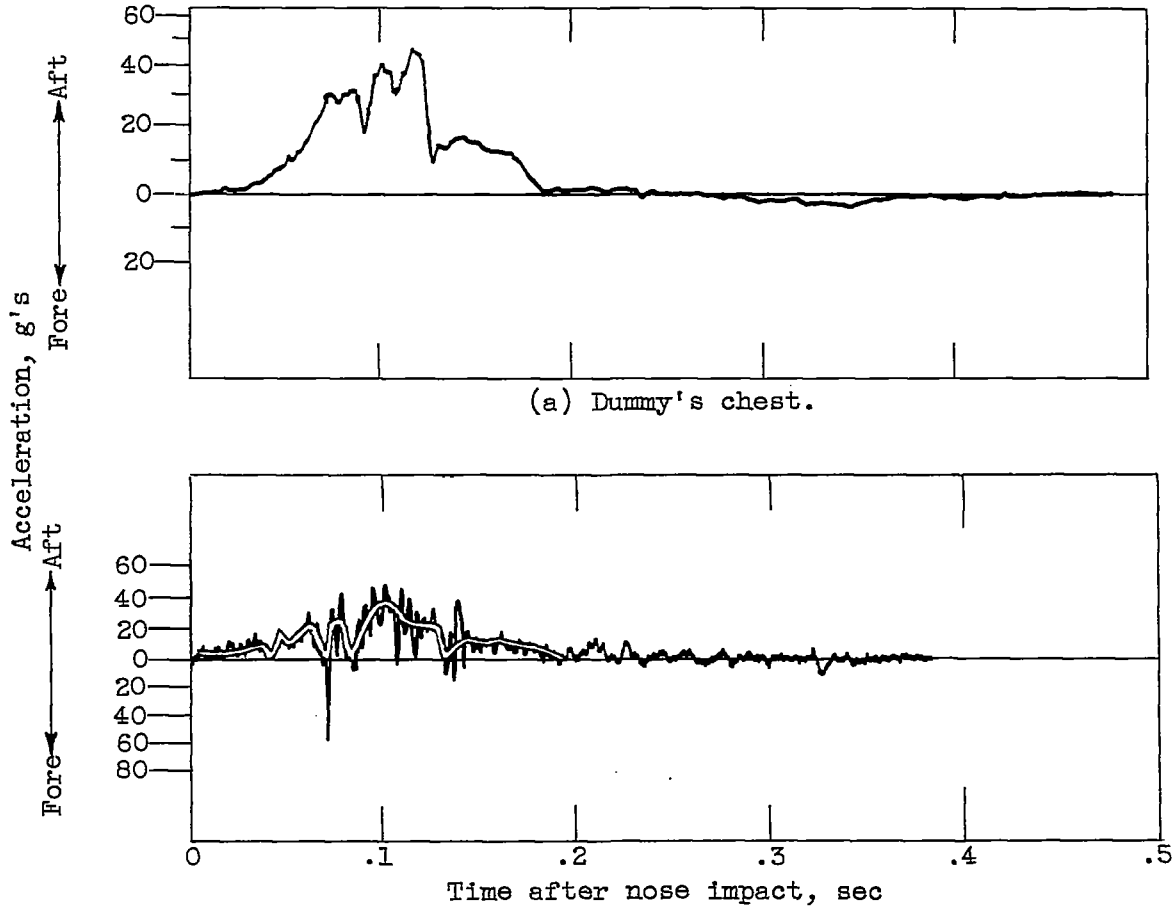


Figure 30. - Comparison of longitudinal acceleration of dummy's chest with that of bulkhead in 18° unflared landing crash of fighter airplane.

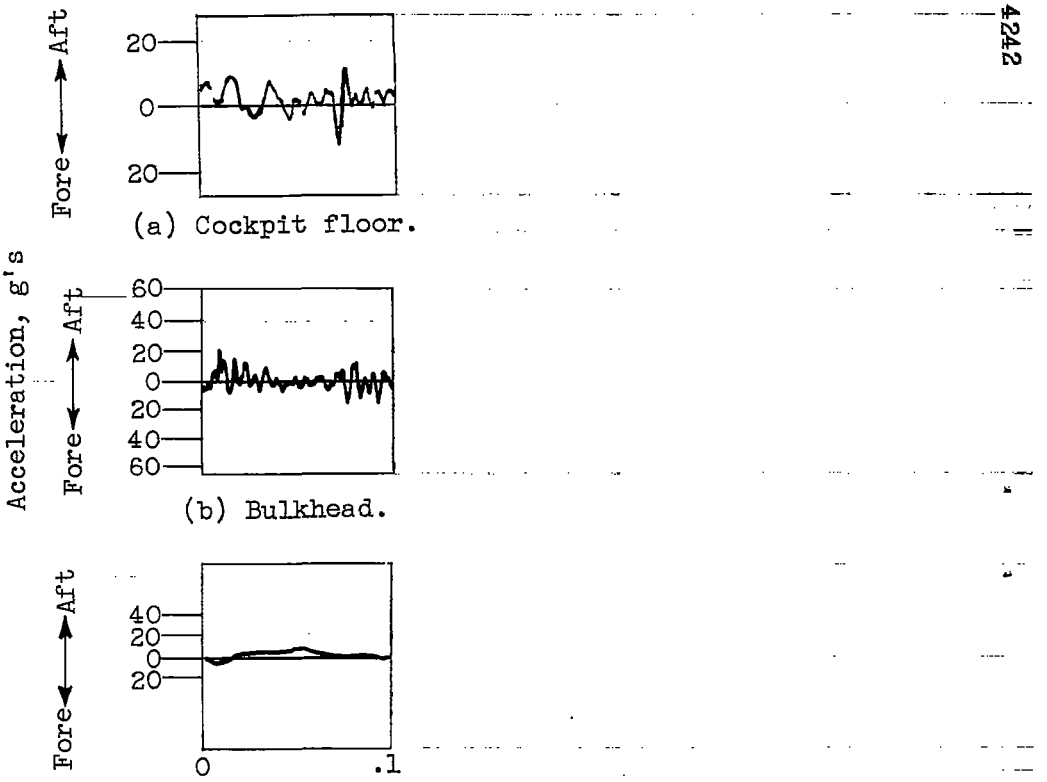


Figure 31. - Longitudinal acceleration of cockpit floor, bulkhead, and dummy's hips resulting from airplane landing-gear assemblies being torn out by wheel abutment.

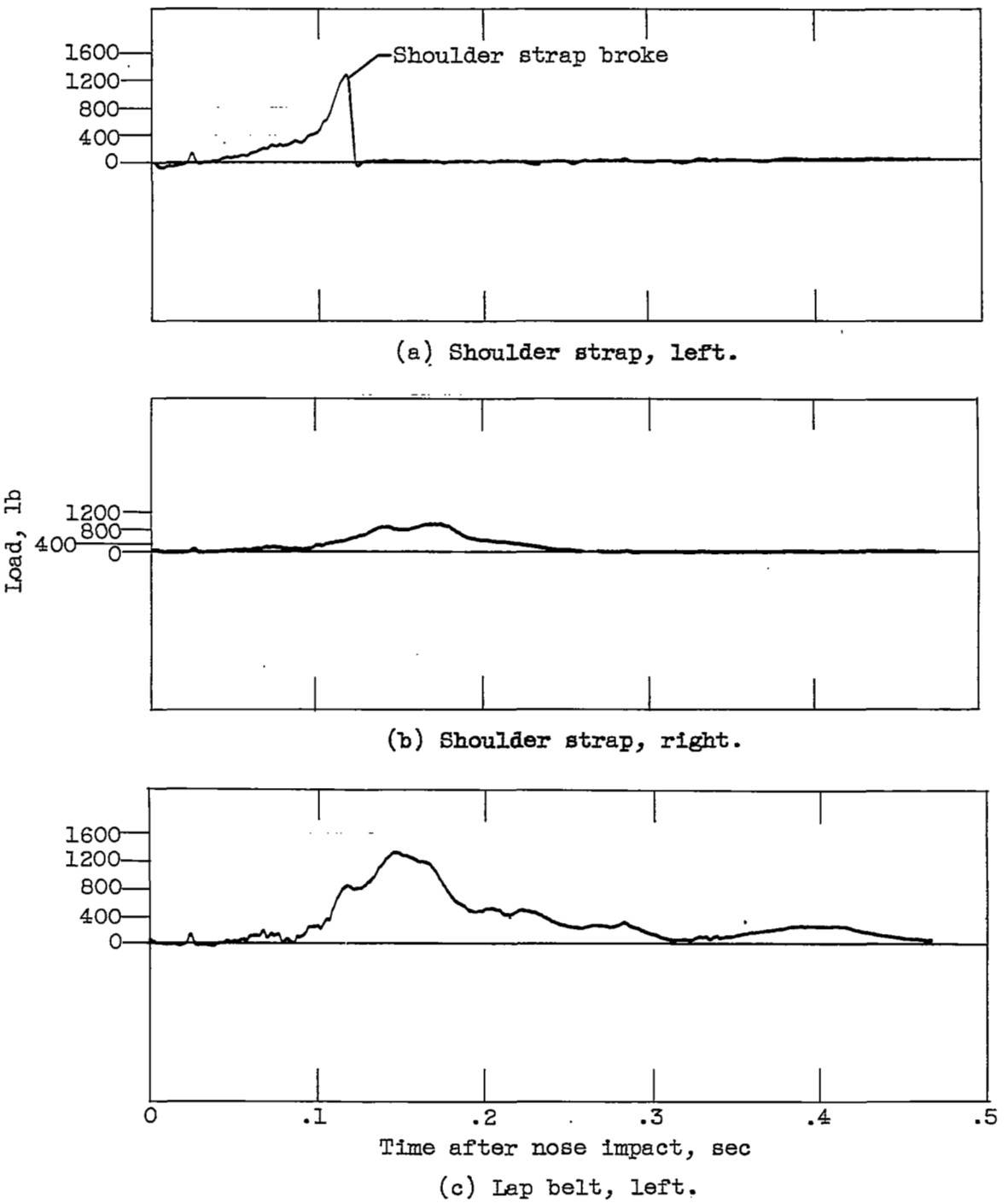


Figure 32. - Harness loads obtained during 18° unflared landing crash of fighter airplane.

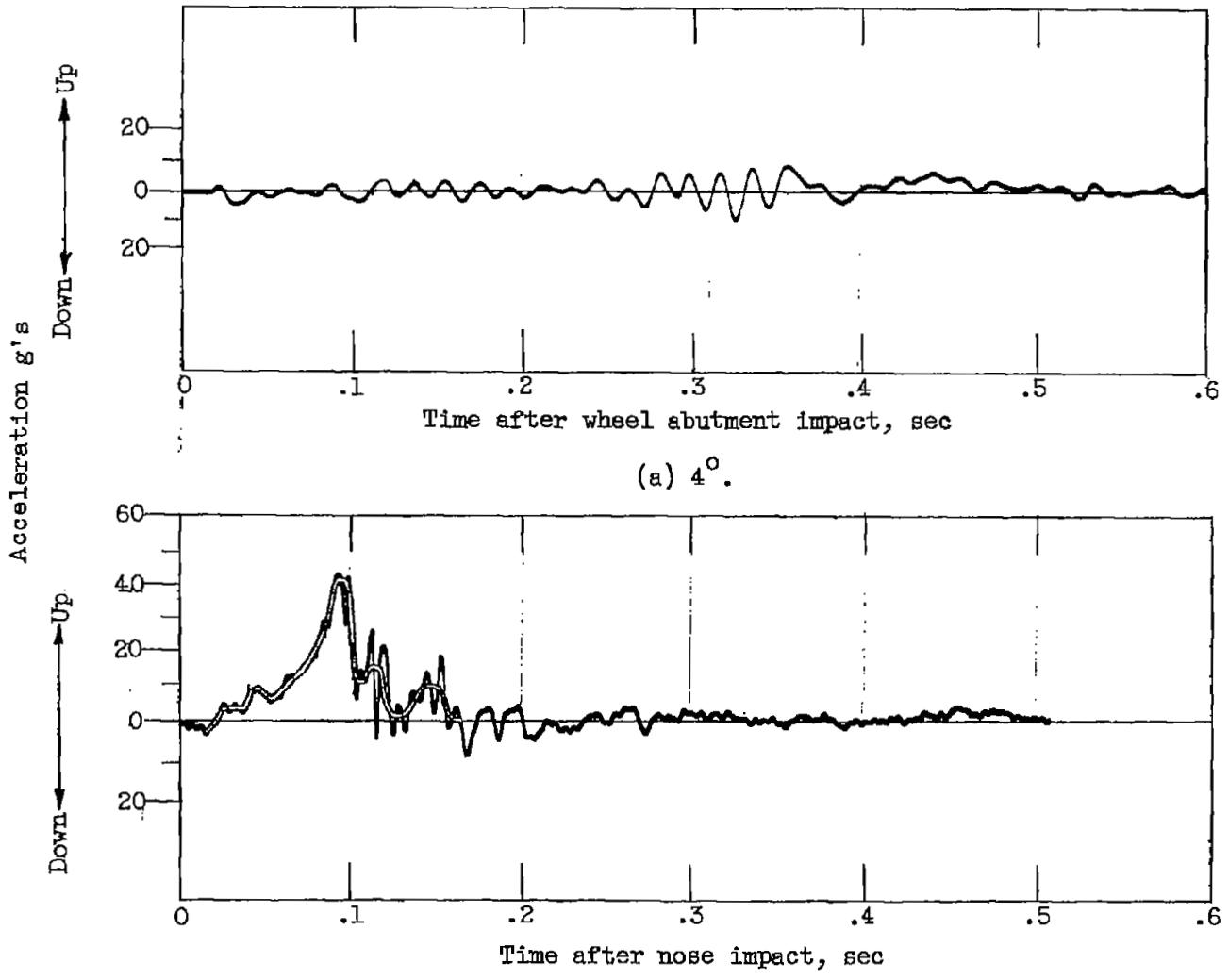


Figure 33.- Normal accelerations of airplane center of gravity for initial impact during 4° ground-loop crash and 22° unflared landing crash of fighter airplane.

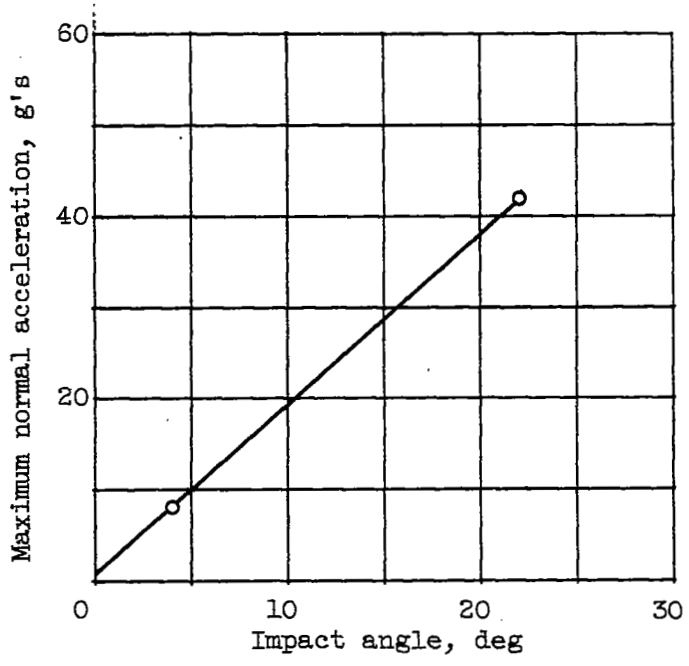


Figure 34. - Relation between maximum normal acceleration of airplane at center of gravity and impact angle for initial impact during crashes of fighter airplane.

2.246 2.286

2.324 2.370

2.406 2.442


2.488 2.526

(a) 2.246 to 2.526 seconds.

Figure 35. - Strip film from motion pictures of second impact in 22° unflared landing crash of fighter airplane.

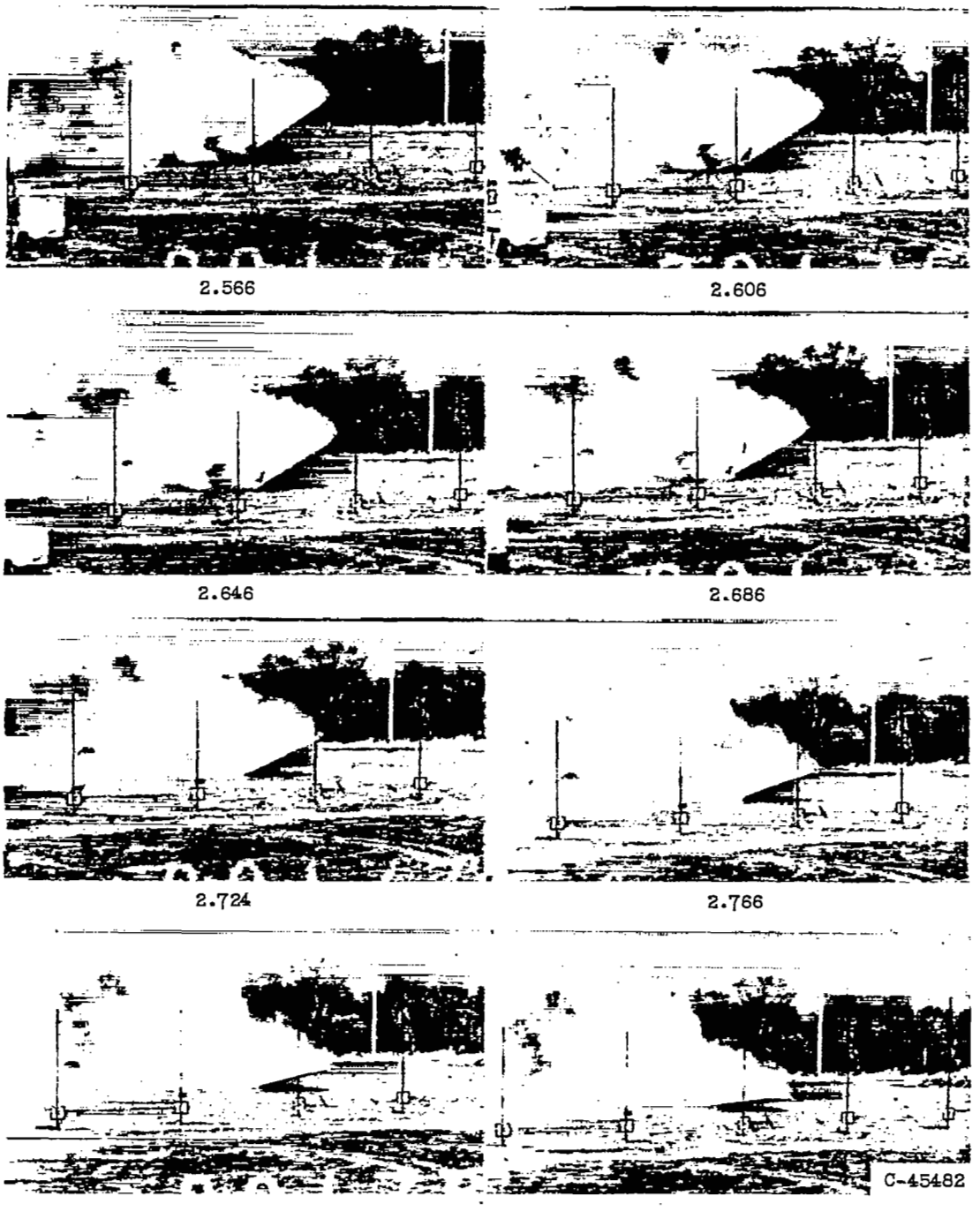


(b) 2.566 to 2.842 seconds.

Figure 35. - Concluded. Strip film from motion pictures of second impact in 22° unflared landing crash of fighter airplane.

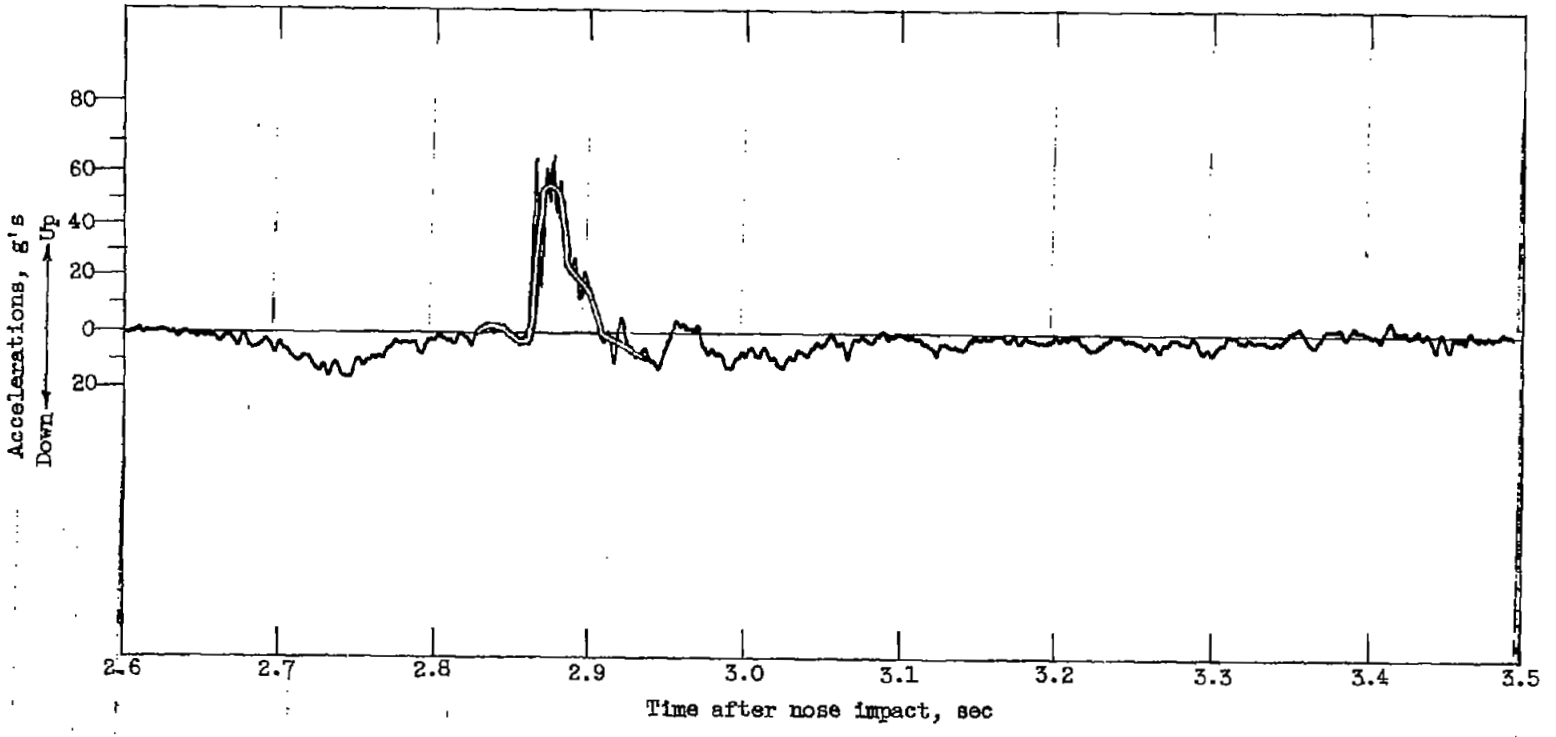


Figure 36. - Normal acceleration of cockpit floor during second impact in 22° unflared landing crash of fighter airplane.

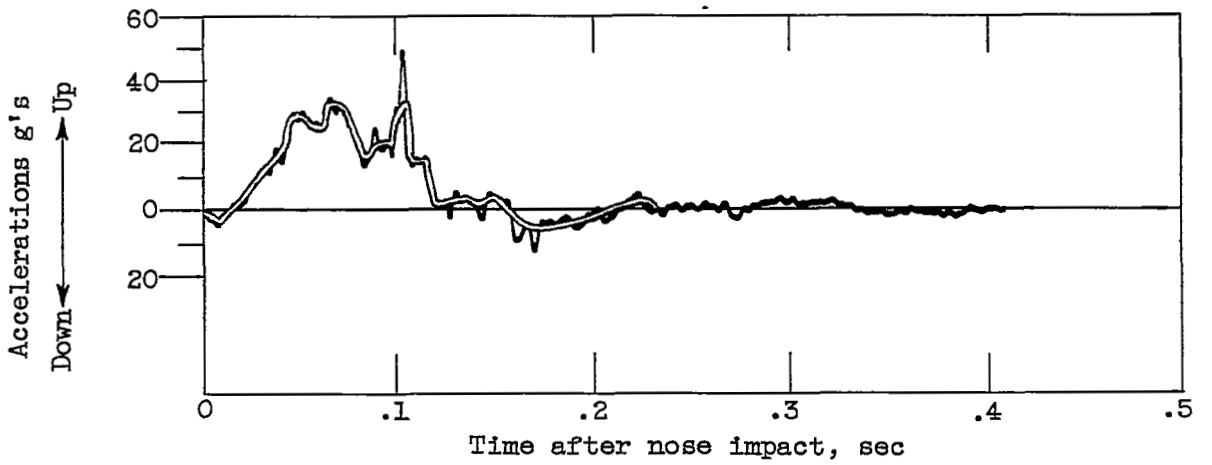


Figure 37. - Normal acceleration of cockpit floor during initial impact in 22° unflared landing crash of fighter airplane.

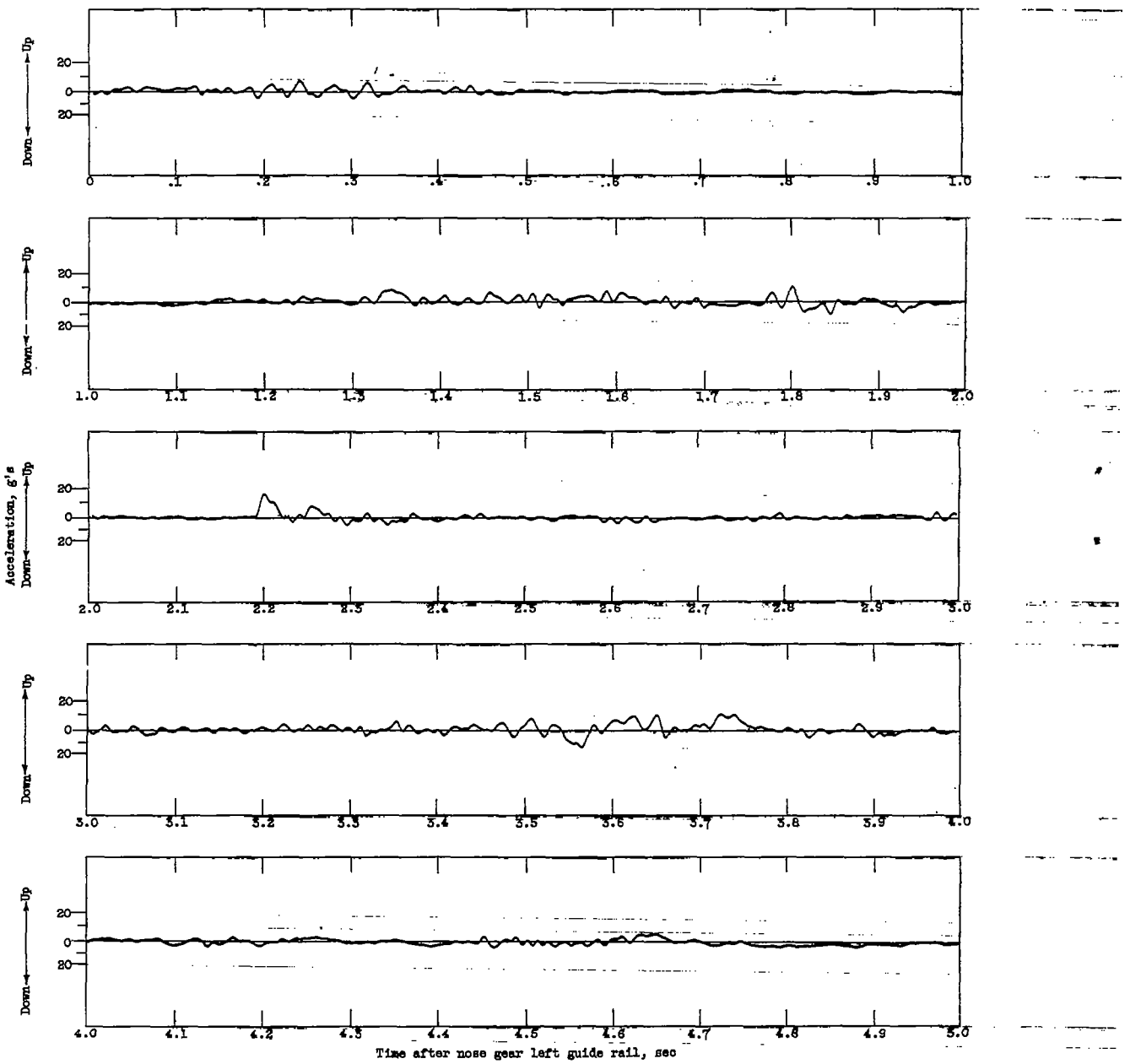


Figure 58. - Normal acceleration of cockpit floor during cart-wheel crash of fighter airplane.

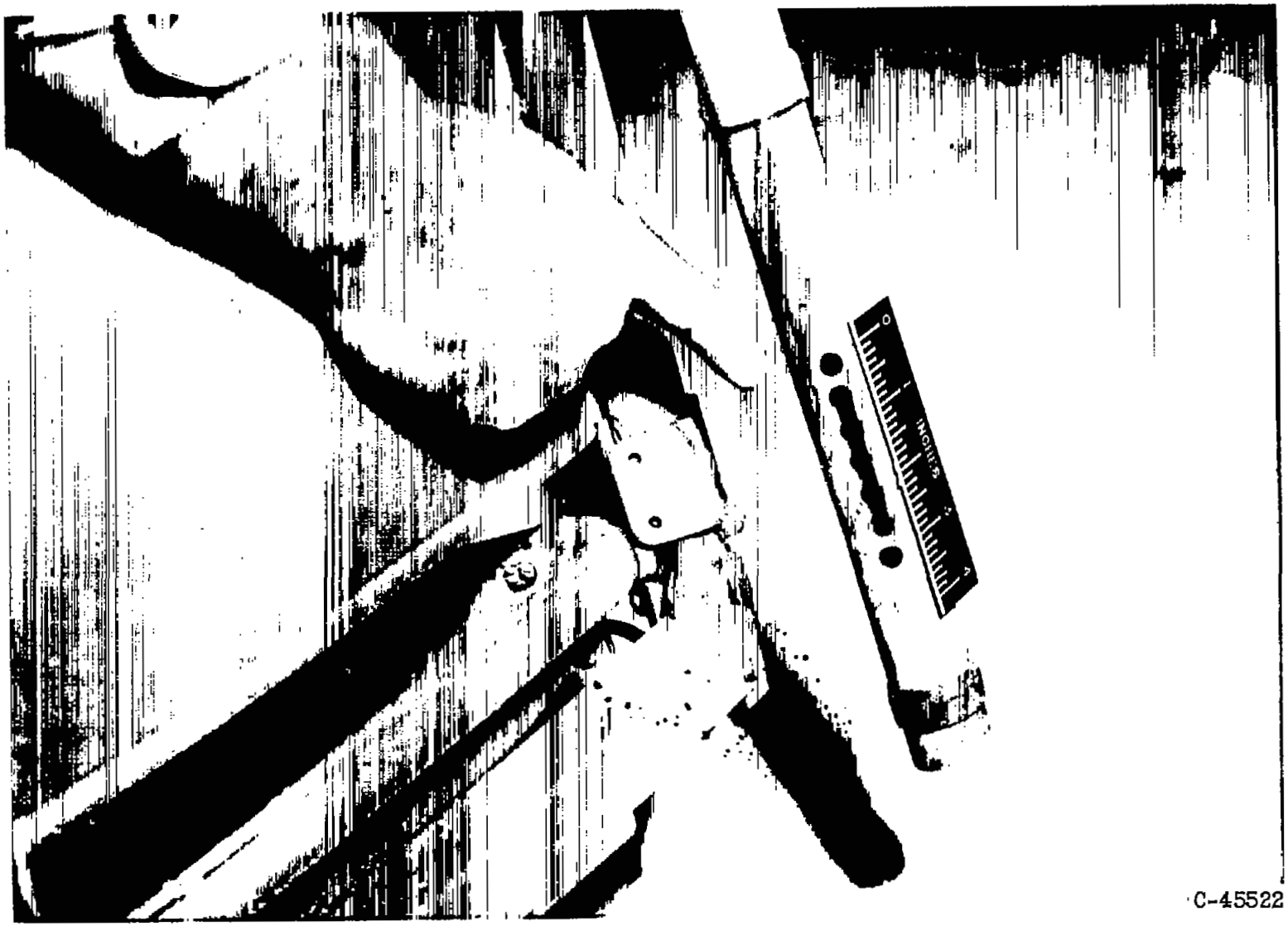


Figure 39. - Holes sheared in seat support tube during 22° unflared landing crash of fighter airplane.

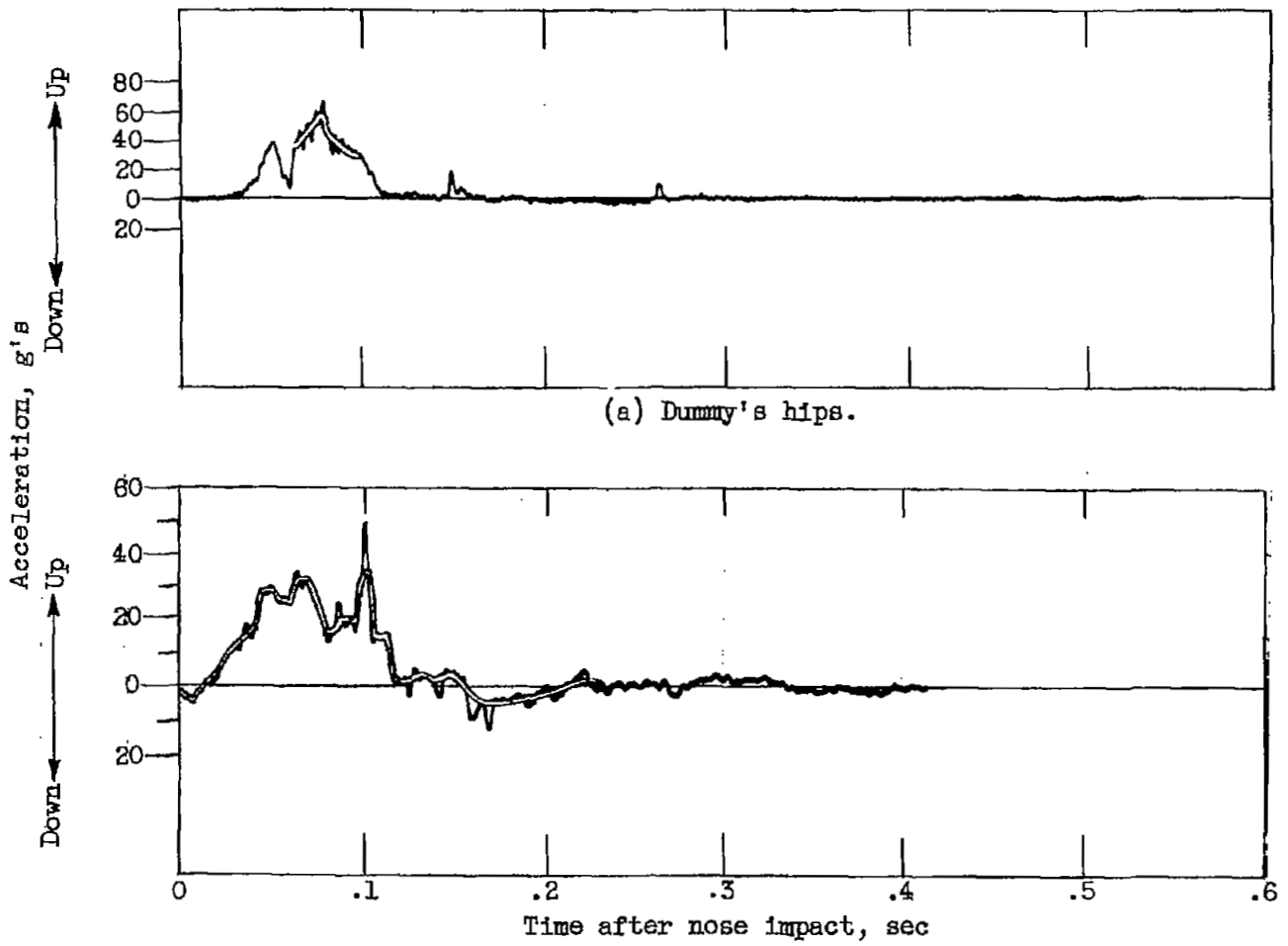


Figure 40. - Comparison of normal accelerations of dummy's hips with those on cockpit floor during nose impact in 22° unflared landing crash of fighter airplane.

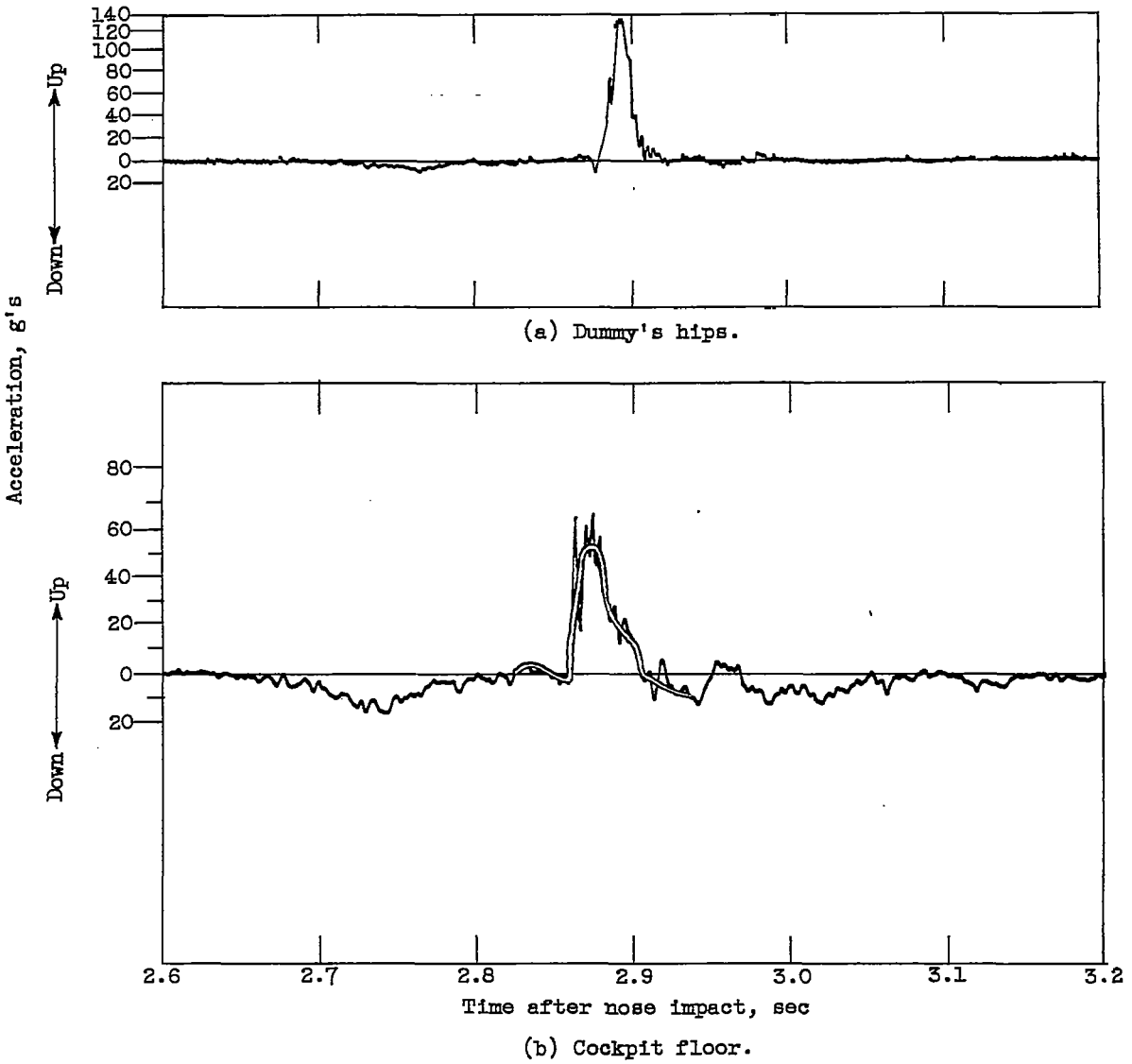


Figure 41. - Comparison of normal accelerations of cockpit floor with those on dummy's hips during second impact in 22° unflared landing crash of fighter airplane.

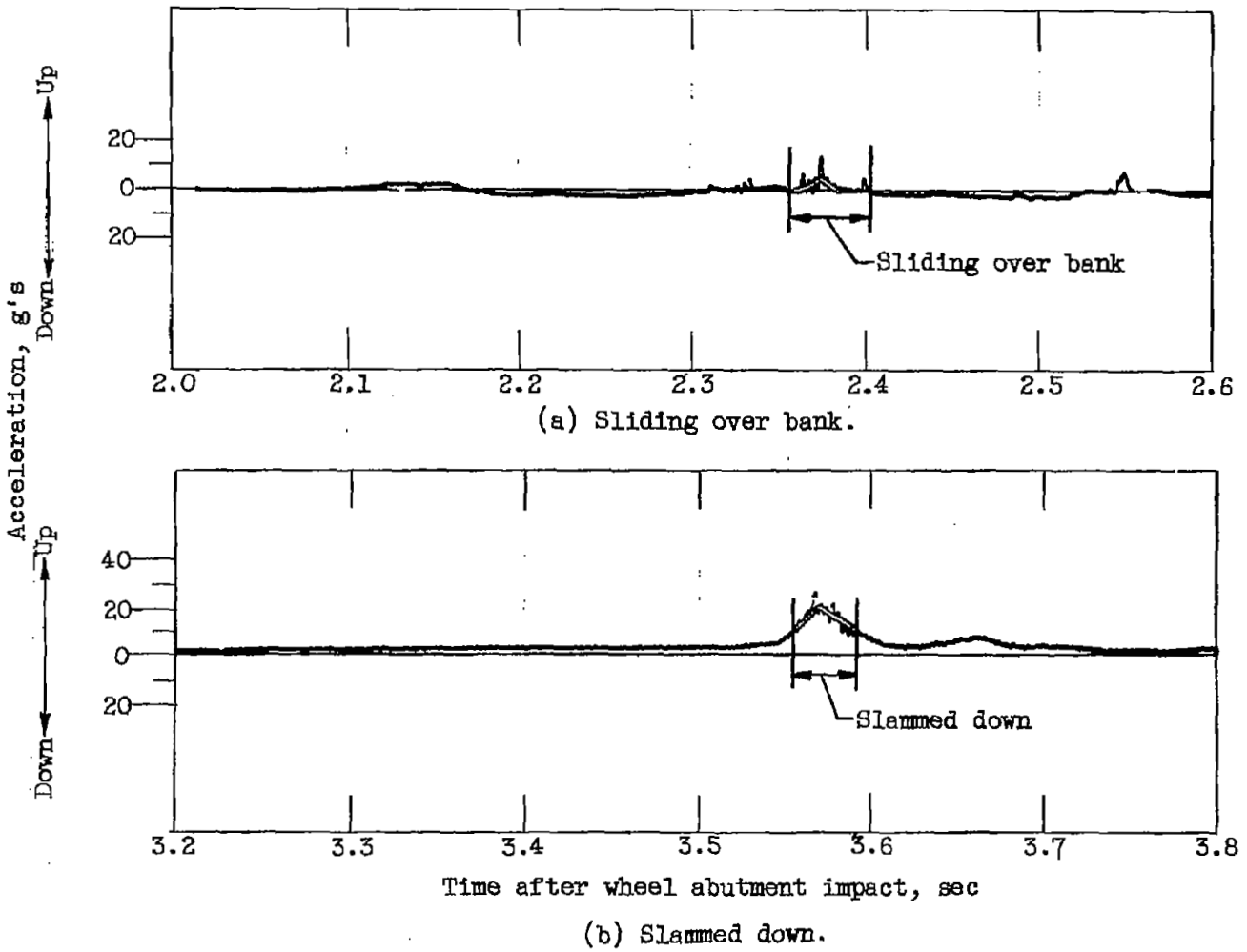


Figure 42. - Normal acceleration on dummy's hips as airplane slid over bank and slammed down during ground-loop crash of fighter airplane.